

WITHIN POND VARIATIONS OF GAS FLUXES AND THE SPATIO-TEMPORAL VARIATIONS OF BENTHIC  
ALGAE AND LIMNOLOGICAL CHARACTERISTICS IN SHALLOW PONDS LOCATED IN THE HUDSON BAY  
LOWLANDS (HBL), NEAR CHURCHILL, MANITOBA

RYAN RIMAS

A THESIS SUBMITTED TO THE FACULTY OF GRADUATE STUDIES IN PARTIAL FULFILLMENT OF THE  
REQUIREMENTS FOR THE DEGREE OF MASTER OF SCIENCE

GRADUATE PROGRAM IN GEOGRAPHY

YORK UNIVERSITY

TORONTO, ONTARIO

December 2019

© Ryan Rimas, 2019

## Abstract

The enhanced warming in the Subarctic is thawing the permafrost in the Hudson Bay Lowlands, making the peatlands carbon sources to the atmosphere. In the Hudson Bay Lowlands, studies have observed that the shallow aquatic systems are sequesters of carbon. In this study, we observed that temperature is a significant variable in determining respiration rates from extracted pond sediment cores that were manipulated in incubation experiments (Strange Pond:  $R^2= 0.90$ ; Left Pond:  $R^2= 0.81$ ). In the ponds that were studied, Strange Pond had an average sequestration or net ecosystem exchange (NEE) of  $-0.71 \mu\text{mol}/\text{m}^2/\text{s}$  and the average oxygen production was  $1.03 \mu\text{mol}/\text{m}^2/\text{s}$ . Biological activity (microbial activity) occurs as deep as 2 cm in the studied cores, indicating that photosynthesis, grazing, and decomposition occur within the top 2 cm of the sediment surface due to the availability of organic carbon. The ponds studied were benthically dominant, with low efficiency found in green pelagic algae, while cyanobacteria activity in the water column was undetectable. Benthic cyanobacteria are proportionally dominant, making up between 55.9 to 59.3% of the benthos. The concentration of chlorophyll *a* (chl *a*) of the three different types of pelagic algae are similar in the ponds studied ( $p < 0.05$ ). It was found that as the area of the pond becomes smaller, the spatial location of pond water and benthos sampling is of minor importance in characterizing the pond as a whole. However, even these shallow ponds are stratified, and sampling locations within the vertical water column needs to be specified. Limnological variables, and changes in benthic algae concentrations differ significantly on a temporal scale.

### Acknowledgements

Thanks to Churchill Northern Studies Centre for accommodating my needs of food and sleep, and York University and Northern Scientific Training Program for funding. I'd like to thank Katarina Sofos for being my support, Patrick Shuman, Coren Pulleyback, Olalekan Balugan, Tasnuva Rashid, Kimisha Ghunowa and most of all Dr. Bello for allowing me to work with him and checking off Churchill off of my bucket list. I'd also like to extend my gratitude to those who have supported me and edited this paper.

## Table of Contents

Abstract.....	ii
Acknowledgements.....	iii
Table of Contents.....	iv
List of Tables.....	vii
List of Figures.....	viii
Chapter 1.....	1
1.0.0 Chapter 1: Introduction and Climate change.....	1
1.1.0 Hudson Bay Lowlands.....	1
1.2.0 The study of shallow ponds in the Hudson Bay Lowlands: Objective and Hypothesis.....	3
1.3.0 Literature Review.....	4
1.3.1 The three pelagic and benthic algae classes observed in this study.....	4
1.3.2 Primary Production of benthic and pelagic algae.....	8
1.3.3 Sediment.....	10
1.3.4 Pond characteristics to be studied.....	12
1.4.0 Fate of carbon.....	14
Chapter 2.....	16
2.0.0 Chapter 2: Methodology.....	16
2.1.0 Field Research: 2013.....	18
2.1.1 Sampling protocol: Some Pond transect.....	18
2.2.0 Equipment.....	20
2.2.1 BenthosTorch.....	20
2.2.2 AquaPen.....	21
2.2.3 YSI 600 QS Probe.....	21
2.2.4 In situ weather data.....	22
2.3.0 Field Research: 2014.....	23
2.3.1 Spatial and temporal variation.....	24
2.3.2 Oxygen and carbon dioxide measurements and modelling.....	24
2.3.3 Chl <i>a</i> concentrations of pelagic algae measured using the BenthosTorch.....	26
2.3.4 Sediment characteristics.....	26

2.3.5 Sediment core respiration experiment .....	26
2.3.6 Benthos Assemblages.....	27
2.3.7 Photometry .....	28
2.4.0 Calculations.....	29
2.4.1 Attenuation coefficient of PPFD .....	29
2.4.2 Calculating NEE and oxygen production .....	30
2.4.2 Statistical analysis .....	31
Chapter 3.....	32
3.0.0 Chapter 3: Spatial and temporal variations in biogeochemical and limnological variations within the ponds studied.....	32
3.1.0 Results: Spatial and temporal variations .....	32
3.1.1 Photosynthetic Active Radiation.....	32
3.1.2 Temperature fluxes in the ponds in 2013 and 2014.....	36
3.1.3 Water level fluxes in Strange Pond in 2014 .....	35
3.1.4 Cumulative precipitation in the 2013 and 2014 field seasons.....	37
3.1.5 Wind velocity at the pond.....	38
3.1.6 Proportions of chlorophyll a concentrations .....	41
3.1.7 Spatial and temporal patterns of benthic algae of Some Pond in 2013 .....	41
3.1.8 Comparing spatial and temporal patterns of the benthic algae in Some Pond in 2013 and 2014....	43
3.1.9 Temporal and spatial patterns of benthic algae in Strange Pond and Left Pond 2014 .....	46
3.1.10 Temporal and spatial patterns of benthic algae in a desiccated Puddle Pond, 2014 .....	48
3.1.11 Quantum efficiency of green algae in the top and bottom of the water column in Some Pond in 2013 .....	50
3.1.12 Limnological properties of Some Pond 2013 and 2014 .....	51
3.1.13 Measured abiotic variables of the ponds .....	55
3.1.14 Assessing the quantum efficiency values and efficiency of the pelagic algae in the summer field season of 2014 .....	58
3.2.0 Chapter 3 Discussion of within pond variability of the measured limnological variables.....	62
3.2.1 How ambient atmospheric and weather conditions affect ponds .....	62
3.2.2 Benthic algae patterns in the shallow subarctic ponds .....	64
3.2.3 Benthic algae concentrations in Some Pond .....	65
3.2.4 Benthic algae concentrations in Strange Pond .....	66

3.2.5 Benthic summary .....	67
3.2.6 Benthic algae concentrations in Puddle Pond .....	67
3.2.7 Pelagic patterns of ponds in 2013 and 2014.....	68
3.2.8 pH patterns in the water column of the ponds .....	69
3.2.9 Dissolved oxygen patterns in the water column of the ponds .....	69
3.2.10 Quantum efficiency patterns of Some Pond in 2013.....	70
3.2.11 Quantum efficiencies of the studied ponds.....	70
3.2.12 Conclusion: Cyanobacteria dominance and where to collect samples .....	71
Chapter 4.....	73
4.0.0 Chapter 4: Benthic algae NEE and produced CO <sub>2</sub> , and sediment respiration .....	73
4.1.0 Results: Measuring Temperature and respiration of sediment cores for Left and Strange Pond.....	73
4.1.1 Modelling respiration flux of Strange Pond .....	74
4.1.2 Modelling respiration and benthic cumulative respiration of Some Pond.....	77
4.1.3 Dissolved oxygen concentrations in the benthic chamber .....	78
4.1.4 Gas fluxes within the benthic chamber .....	79
4.1.5 Active surface sediment of Strange Pond .....	81
4.1.6 Organic carbon in Strange Pond .....	82
4.1.7 Pelagic algae chlorophyll <i>a</i> concentrations and cell counts in pond water columns in 2014 .....	83
4.1.8 Comparing regional pelagic and benthic algae concentrations.....	86
4.1.9 Average algal distribution of the cores from Left Pond and Strange Pond .....	88
4.2.0 Chapter 4 Discussion of benthic productivity and characteristics at the bottom of the ponds.....	89
4.2.1 Temperature and respiration of sediment cores for Left Pond and Strange Pond .....	89
4.2.2 Benthic algae on the surface layer and the 2-4 cm layer.....	89
4.2.3 Critique of the BenthosTorch chlorophyll <i>a</i> measurements .....	91
4.2.4 Pond productivity in Strange Pond .....	92
4.2.5 Pelagic algae in the studied ponds.....	94
4.2.6 Organic carbon and the vertical distribution of the algae in the sediments .....	96
4.2.7 Implications from studying the net ecosystem flux of Strange Pond .....	97
4.2.8 Concluding remarks on shallow subarctic ponds in the Hudson Bay Lowlands .....	98
5.0.0 Concluding chapter .....	100
6.0.0 Bibliography .....	101

List of tables

Table 1	Collection of limnological variables of small freshwater bodies in various regions in the Arctic and Subarctic (Rautio et al., 2011).	4
Table 2	Chlorophyll <i>a</i> concentration of each benthic algae type measured with the BenthosTorch in the 2014 field season.	41
Table 3	The average limnological and biological characteristics of the water column at each sample location of Some Pond in 2013.	55
Table 4	The limnological and biological characteristics of the water column of each sample location in Strange Pond in the summer field season of 2014.	56
Table 5	The limnological and biological characteristics of the water column of each sample location in Left Pond in the summer field season of 2014.	56
Table 6	The limnological and biological characteristics of the water column of each sample location in Some Pond in the summer field season of 2014.	57
Table 7	<i>Sum of chl a in each layer of the sediment bottom in Strange Pond up to 10 cm in depth.</i>	82
Table 8	Comparison of the chlorophyll benthic and pelagic algae in the studied ponds measured using the BenthosTorch. Value for Strange Pond for the 1 mm slab was calculated using the linear equation model estimating chl <i>a</i> concentrations at 0.1 mm and summing the values to 1 mm.	85
Table 9	Sediment characteristics in Strange Pond from the extracted sediment cores.	85
Table 10	CO <sub>2</sub> sequestration rates of peatland type and features in the Hudson Bay Lowlands in Manitoba, Ontario and Quebec (McLaughlin et al., 2014).	94

List of figures

Figure 1	Satellite image of the coastal Hudson Bay Lowlands near Churchill Manitoba (satellite image from Google).	16
Figure 2	Strange Pond from the South Eastern shore showing the dock in the far left.	17
Figure 3	The eastern sample location of Left Pond. A highly active pond that features a benthos with a red hue.	17
Figure 4	Without a water column, Puddle Pond's benthic sediment is exposed to the air. Small drainage channels can be seen where the water follows as the pond is drying up.	18
Figure 5	The transect of Some Pond showing water depths at ten meter intervals with a vertical exaggeration of x100.	19
Figure 6	The different coloured LED lights that are part of the BenthosTorch detector used to excite the algae cells.	20
Figure 7	The Aqua Pen is a small hand held unit that quickly measures the quantum efficiency and optical density of the 2 mL water sample.	21
Figure 8	At the height of the tripod, an anemometer and LI-COR pyranometer are attached taking readings of wind velocity and incoming solar radiation. The devices are attached to a Campbell Scientific data logger that takes readings every 10 s and computes the observations to 15 min averages.	23
Figure 9	The YSI 600 QS probe used to instantaneously measure and record limnological characteristics of the pond water.	23
Figure 10	This set up shows the IRGA gas chamber tightly fits and sits onto the rim of which is supported 1 cm above the water. This image shows readings taken near 0°C with the ice bath.	27
Figure 11	A 2.0 cm slice of pond sediment extracted from the core that has already been sampled.	28
Figure 12	The incoming photosynthetic active radiation that reaches the top (A) and bottom (B) of the water column, and observed PAR reaching the sensor in the water column of Some Pond measured at an approximate depth varying between 10.0-15.0 cm in the field season.	33
Figure 13	Example of the distribution of PPFD over the 2014 field season showing peak times occurring between the hours of 12 (12:00 p.m.) and 14 (2:00 p.m.).	34
Figure 14	The fluctuation of water and air temperatures measured every 10 seconds and averaged every 15 minutes during the 2013 field season.	35
Figure 15	The temperature profile of the air, water column, and sediments measured every 10 seconds and averaged 15 minutes during the 2014 field season.	36
Figure 16	Recorded data of the average water level of Strange Pond, recorded every hour during the study period using data from a level water sensor	36
Figure 17	The daily and cumulative precipitation during the 2013 field season.	38
Figure 18	The daily and cumulative precipitation during the 2014 field season.	38
Figure 19	Wind velocity measured every 10 seconds and averaged every 15 minutes during the 2013 field season 1m.	39



Figure 20	The wind distribution of wind by direction during the 2013 summer field season.	40
Figure 21	The frequency of wind direction during the 2014 field season.	40
Figure 22	The average benthic algae concentrations in Some Pond for each sampling day.	42
Figure 23	The seasonal average of each sampling location in Some Pond.	42
Figure 24	The concentration of benthic green algae in Some Pond in 2013 and 2014, with the x-axis indicating the sampling location along the transect.	43
Figure 25	The concentration of benthic cyanobacteria in Some Pond in 2013 and 2014, with the x-axis indicating the sampling location along the transect.	44
Figure 26	The concentration of benthic diatoms in Some Pond in 2013 and 2014, with the x-axis indicating the sampling location along the transect.	44
Figure 27	The benthic algae concentration of each algae types in Some Pond in 2014.	45
Figure 28	The average benthic algae concentrations of the three taxa in Strange Pond at each sample location.	46
Figure 29	The average benthic algae concentrations of the three taxa in Strange Pond of each sampling day.	47
Figure 30	The average benthic algae concentrations of the three taxa in Left Pond at each sample location.	47
Figure 31	The average benthic algae concentrations of the three taxa in Left Pond of each sampling day.	48
Figure 32	The average benthic algae concentrations of the three taxa in Puddle Pond at each sample location.	49
Figure 33	The average benthic algae concentrations of the three taxa in Puddle Pond of each sampling day.	49
Figure 34	The temporal and spatial pattern of QY of the upper layer of the water column in Some Pond during the 2013, summer field season (n= 91). Each bar represents the sample location along the transect of Some Pond represented by the average depth at which the sample was taken of the top layer of the water column in cm. The error bars are the standard deviation of the average quantum efficiency measured.	50
Figure 35	The temporal and spatial pattern of QY of the upper layer of the water column in Some Pond during the 2013, summer field season (n= 81). Each bar represents the sample location along the transect of Some Pond represented by the average depth at which the sample was taken of the bottom layer of the water column in cm. It is important to note that sample location 1 is omitted and defined as an upper layer due to very shallow depths. The error bars are the standard deviation of the average quantum efficiency measured.	50
Figure 36	The seasonal average of pH of the upper (A) and bottom (B) layer of the water column in Some Pond during the 2013 summer field season. It is important to note that sample 1 is omitted and presented as the top layer of the water column only.	53
Figure 37	Spatial pattern of average pH of the top layer (A) and bottom layer (B) of the water column of each sampling location in Some Pond.	53
Figure 38	Temporal pattern of average pH of the top (A) and bottom (B) of the water column of each sampling location in Some Pond.	54
Figure 39	Spatial pattern of average DO concentrations of the top layer (A) and bottom layer (B) of the water column of each sampling location in Some Pond.	54
Figure 40	Temporal pattern of average DO concentrations of the top (A) and bottom (B) of the water column of each sampling location in Some Pond.	55
Figure 41	Temporal pattern of the quantum efficiency measured in Strange Pond in 2014.	58

Figure 42	Spatial pattern of the quantum efficiency in Strange Pond in 2014.	58
Figure 43	Temporal pattern of the quantum efficiency in Left Pond in 2014.	60
Figure 44	Spatial pattern of the quantum efficiency in Left Pond in 2014.	60
Figure 45	Temporal pattern of the measured quantum efficiency in Some Pond in 2014.	61
Figure 46	Spatial pattern of the quantum efficiency measured in Some Pond.	61
Figure 47	The exponential relationship and influence of temperature on the respiration flux of sediment cores from Left Pond (n= 24).	73
Figure 48	The exponential relationship and influence of temperature on the respiration flux of the sediment cores from Strange Pond (n= 140), with a standard error of 0.074.	74
Figure 49	Based on the exponential relationship found from the sediment core respiration flux with temperature, respiration flux in Strange Pond was estimated using both the water temperature and sediment temperature at 1 cm below the sediment surface.	75
Figure 50	A 3 day period of the estimate respiration flux. The various fluctuations indicate day time peaks and night time lows.	76
Figure 51	The cumulative benthic respiration from the beginning to the end of monitoring Strange Pond in the 2014 field season (June 27 to July 25, 2014).	76
Figure 52	Modelled respiration of Some Pond using the equation determined by the sediment respiration in lab experiments in 2014.	77
Figure 53	Modelled cumulative respiration of Some Pond during the 2013 field season from June 28 to July 25, 2013.	78
Figure 54	Observed DO concentrations on July 10, 2014, between the times of 2:30 p.m. and 6:10 p.m. This is a closer depiction of the fluctuations during each cycle, but also smaller fluxes occurring within the chamber. The highlighted areas discern the peaks of O <sub>2</sub> produced from algal photosynthesis during the chamber's closed circulation phase. The throughs of the graph indicate the equilibration of the gas chamber with ambient water within the pond during the chamber's open circulation phase.	78
Figure 55	DO concentration fluctuations on July 11, 2014 between 9:30 a.m. and 4:15 p.m. The observed DO fluxes are not as consistent as seen on July 10, 2014. The highlighted areas discern the peaks of O <sub>2</sub> produced from algal photosynthesis during the chamber's closed circulation phase. The throughs of the graph indicate the equilibration of the gas chamber with ambient water within the pond during the chamber's open circulation phase.	79
Figure 56	Net ecosystem flux of O <sub>2</sub> during the closed circulation of the benthic chamber (June 26, July 6, July 10, and July 11) regressed against PPF (A) and temperature (B). Production of oxygen was indicated as positive values, and consumption of O <sub>2</sub> in the system was indicated as negative values.	80
Figure 57	The modelled consumption of O <sub>2</sub> based on the temperature of the sediment at a depth of 1 cm. Increasingly negative values indicate higher consumption of O <sub>2</sub> .	80
Figure 58	Dependence of primary production of O <sub>2</sub> on a PPF (A) and temperature (B) during the closed circulation of the benthic chamber (for June 26, July 6, July 10, and July 11). Production of oxygen is indicated as negative values and consumption of O <sub>2</sub> in the system is indicated as positive values.	81
Figure 59	The average respiration flux of each of the 5 thicknesses of sediment cores.	82
Figure 60	Pelagic algae chlorophyll a concentrations of each algae type in Strange, Left, and Some Pond. Concentrations of chl <i>a</i> for each of the three algae types are significantly different from each of the three ponds ( $p < 0.05$ ).	83

Figure 61	Chlorophyll a measurements taken with the BenthosTorch @ 2.0 cm increments. The linear equation of each chl <i>a</i> concentration can then be used to estimate the concentrations in a per mm increment or the entire core. The linear regression for total concentration for 0-4 cm ( $y = -34.582x + 65.503$ , $R^2 = 0.97$ ) and for 4-10.0 cm ( $y = -4.6213x + 11.872$ , $R^2 = 0.97$ ). For cyanobacteria the linear regression for 0-4 cm ( $y = -26.764x + 25.559$ , $R^2 = 0.9825$ ) and for 4-10.0 cm ( $y = -9.3403 + 11.353$ , $R^2 = 0.99$ ). The linear regression for green algae at 0-4 cm is ( $y = 6.0233x - 2.6619$ , $R^2 = 0.0031$ ) and for 4-10.0 cm ( $y = -8.2711x + 10.003$ , $R^2 = 0.97$ ). The linear regression for diatoms is ( $y = 93351x - 14.242$ , $R^2 = 0.95$ ).	84
Figure 62	Comparison of the Churchill pelagic algae concentrations to Subarctic and Arctic freshwater ecosystems listed in Rautio et al. (2011).	86
Figure 63	Comparison of the Churchill ponds to the different pelagic algae concentrations studied in Rautio et al. (2011). The modelled concentrations are from Strange Pond cores, and the in-situ sediment surface measurements are from the survey of surface chl <i>a</i> on the 4 ponds studied.	86
Figure 64	The average algal concentration or available labile carbon found in the sediment at surface of each sediment slab measured in 2.0 cm increment depths.	88
Figure 65	The biological zone (highlighted in red), establishing the same zonal thickness despite the different depths of the sediment cores that would be extracted from Left Pond and Strange Pond.	90

### 1.0.0 Chapter 1: Introduction

Freshwater ecosystems are important components of the global carbon budget, with previous studies focusing only on large aquatic systems, with smaller systems being relatively ignored. There has been an increased emphasis on studying shallow lakes and ponds as they are seen to process carbon at a higher rate than larger systems (Downing et al., 2008). Anthropogenic induced climate change will impose significant changes on the pelagic and benthic algae communities in marine and freshwater ecosystems. Approximately one quarter of all lakes and shallow ponds on Earth are found in the northern high latitudes and are sensitive to climatic changes. The Arctic and Subarctic water bodies are experiencing an accelerated change caused by anthropological activity, at a magnitude that has never been witnessed. This new geological era is dubbed the *Anthropocene* (Taranu et al., 2015). The shallow freshwater ecosystems within the Subarctic region are very important, acting as a window for understanding how the rapid changes are affecting the carbon dynamics, CO<sub>2</sub> budget and primary productivity of these systems. The changing climate has prompted changes in the biogeochemical and geomorphological characteristics of small and large ponds in the Subarctic and Arctic regions (Rautio et al., 2011).

Thermokarst ponds in the Subarctic and Arctic regions started forming during the Pleistocene-Holocene transition (Hinkel et al., 2012). These lakes and ponds have been observed to be significant sources of CO<sub>2</sub> and CH<sub>4</sub>. Hobbie et al. (1980), Kling et al. (1992) and Rouse et al. (1997; 2005) have done intensive short-term studies sampling many ponds and lakes but have not conducted meticulous studies of singular ponds looking at the spatial and temporal variability. Photosynthesis from pelagic and benthic algae during sunlight hours is responsible for the uptake of carbon dioxide, whilst respiration from the algae and sediments are responsible the emission of carbon dioxide into the atmosphere. With Subarctic regions characteristically experiencing amplified changes due to climate change, it will be informative to see how variable the effects are on the biogeochemical and geomorphological pond characteristics especially in ponds found in significant Subarctic regions such as the Hudson Bay Lowlands.

### 1.1.0 Hudson Bay Lowlands

The Hudson Bay Lowlands (HBL) near Churchill, Manitoba is a unique region in which three different ecosystems converge within the area. These ecosystems are the boreal forest, tundra and the

marine system (Rouse and Bello, 2002). There are approximately 450,000 km<sup>2</sup> of peatlands globally, and the Hudson Bay Lowlands has the second largest global peatland, acting as a substantial carbon sink. The Hudson Bay Lowlands near Churchill, Manitoba is covered by approximately 25% of shallow freshwater ponds. The permafrost in this region is mostly continuous, in which the ponds occupy depressions in the landscape (Wolfe et al., 2011). The combination of the vegetation, freshwater systems, and continuous and discontinuous permafrost are significant in the biogeochemical processes that control the carbon cycle in the Subarctic.

Climate change in the Hudson Bay Lowlands will induce changes in biological processes and regional environmental change. The changes in the limnology and morphology of the ponds are attributed to temperature change. Increasing temperatures can alter the circulation patterns, air masses and winds in the Churchill region. Temperatures have a direct influence on biochemical reactions, while infrared wavelengths directly influence the production of cells (Guðmundsdóttir, 2012). The growing season for pelagic and benthic algae has the potential to lengthen with the correspondence of increasing water temperature, creating a unique system for adaptive algae to grow productively (Rouse et al., 1997) and becoming a carbon dioxide sink (Zona et al., 2010). Counterintuitively, the ponds have the potential to desiccate and disappear as permafrost melting accelerates drainage, being replaced by terrestrial vegetation, causing a change in the carbon dioxide flux of the pond bottom becoming an active carbon source (Zona et al., 2010).

In the Subarctic regions such as the Hudson Bay Lowlands, phytoplankton experience photo-inhibition in clear water, diminishing the efficiency of photosynthesis. In combination with the low concentrations of nutrients within the water column, the ponds are considered to be oligotrophic. Clear water allows, benthic algae to receive a substantial amount of incoming radiation from the surface, allowing for the benthic algae to dominate the primary productivity of the shallow ponds (Rautio et al., 2011). However, the benthic algae are also exposed to ultraviolet radiation which governs the type of species that dominate the benthos.

As a result of warming, the hydrological pathways and landscape of the Subarctic ecosystems will also transform. In Alaska, lake drainage is triggered by lateral breaching when the banks on the shore lose the integrity of their structure (Jones et al., 2011). Warmer temperatures increases mineralization of organic carbon in freshwater ecosystems. The cold freshwater ponds and lakes have been hypothesized to emit CO<sub>2</sub> when they are warmed up due to climate change. For example, in the northern Québec region, Subarctic ponds have become precipitation driven due to climate change.

Precipitation in this region fills the ponds with allochthonous dissolved organic carbon from the runoff. In turn, allochthonous derived dissolved organic carbon (DOC) becomes a driver in the processes that govern the production and consumption of carbon. These changes in the limnological characteristics of the ponds will also change the composition and behaviour of existing algae and the biogeochemical processes on the sediment interface.

Climate change affects the integrity of the permafrost, alongside the ponds in the Hudson Bay Lowlands. Melting permafrost exposes the peat that was once frozen which promotes decomposition, emitting greenhouse gases such as CH<sub>4</sub> and CO<sub>2</sub> that contribute to the positive feedback of global warming. With significant environmental change in the Subarctic, understanding pond characteristics and variables that affect the local CO<sub>2</sub> budget will allow us to forecast the fate of the ponds. Ponds have the potential to help compensate for the terrestrial changes in the Subarctic carbon budget by sequestering CO<sub>2</sub> due the productivity of primary producers or conversely suffer the fate of disappearing and succumbing to the increased temperatures.

### 1.2.0 The study of shallow ponds in the Hudson Bay Lowlands: objectives and hypotheses

The shallow ponds in the Hudson Bay Lowlands, near Churchill Manitoba have the potential to offset emissions from melting permafrost in the peatlands. These aquatic systems vary in depth and area. Therefore, they potentially differ in their capacity to act as carbon sinks. This study investigates the importance of sampling time and location on the ability to characterize the carbon dynamics using commonly obtained limnological variables and algal chl *a* concentrations. By determining if primary production and respiration results in a positive net primary production then the ponds are a potential net CO<sub>2</sub> sink.

I hypothesize that due to the shallow depths of the ponds, the biogeochemical and limnological characteristics of the ponds will vary temporally. Conversely shallow depths and small pond areas limit within-pond spatial variability but have the potential to enhance between-pond variability. All these factors have sampling implications.

Secondly, I hypothesize that benthic primary production of the ponds in the Hudson Bay Lowlands is responsible for the processing of autochthonous carbon in keeping with measurements taken in some other Arctic locations (Rautio et al., 2011). In comparison to other northern regions, studies of benthic algae near Churchill, Manitoba are minimal, as seen in Figure 1 and therefore this

research will potentially fill in a portion of the knowledge gap that has been identified by Rautio et al. (2011).

Table 1: Collection of limnological variables small of freshwater bodies in various Arctic and subarctic regions (Rautio et al., 2011).

Region	Water										Benthos	
	pH	Cond. $\mu\text{S}\cdot\text{cm}^{-1}$	DOC $\text{mg}\cdot\text{L}^{-1}$	TP $\mu\text{g}\cdot\text{L}^{-1}$	TN $\mu\text{g}\cdot\text{L}^{-1}$	SRP $\mu\text{g}\cdot\text{L}^{-1}$	$\text{NO}_3^-$ $\mu\text{g N}\cdot\text{L}^{-1}$	Chl- $\alpha$ $\mu\text{g}\cdot\text{L}^{-1}$	PP ( $P_{\text{max}}$ ) $\mu\text{g C}\cdot\text{L}^{-1}\cdot\text{h}^{-1}$	BP $\mu\text{g C}\cdot\text{L}^{-1}\cdot\text{h}^{-1}$	Chl- $\alpha$ $\text{mg}\cdot\text{m}^{-2}$	PP ( $P_{\text{max}}$ ) $\text{mg C}\cdot\text{m}^{-2}\cdot\text{h}^{-1}$
Barrow	7.3	160	12.5	13	800	1.2	6.5	0.4	0.6	na	na	13
Toolik	7.8 $\pm$ 0.8	124 $\pm$ 105	9.2 $\pm$ 2.6	8 $\pm$ 6	225 $\pm$ 189	2.8 $\pm$ 2.2	4.0 $\pm$ 0.8	0.8 $\pm$ 0.4	3.2 $\pm$ 1.1	0.7 $\pm$ 0.3	105 $\pm$ 105	60 $\pm$ 28
Mackenzie	8.4 $\pm$ 0.3	691 $\pm$ 560	29.4 $\pm$ 5.9	14 $\pm$ 2	< 100 $\pm$ 0	2.0 $\pm$ 0.2	< 2 $\pm$ 0	1.3 $\pm$ 0.8	8.3 $\pm$ 5.1	0.3 $\pm$ 0.1	na	151 $\pm$ 37
Resolute	8.5 $\pm$ 0.1	323 $\pm$ 176	2.1 $\pm$ 0.5	5 $\pm$ 0.5	185 $\pm$ 34	1.3 $\pm$ 0.5	1.3 $\pm$ 10.5	1.2 $\pm$ 1.1	0.6 $\pm$ 0.3	na	85 $\pm$ 46	9 $\pm$ 8
Ward Hunt	8.5	100	4.4	3 $\pm$ 2	120	< 2 $\pm$ 0	30.0	0.3 $\pm$ 0.3	na	na	88 $\pm$ 24	9
Hazen	8.3 $\pm$ 0.5	440 $\pm$ 400	15.7 $\pm$ 15.1	35 $\pm$ 14	1110 $\pm$ 1350	1.6 $\pm$ 0.1	na	1.4 $\pm$ 1.5	na	na	121 $\pm$ 88	na
Bylot	8.4 $\pm$ 1.0	83 $\pm$ 42	12.1 $\pm$ 6.5	35 $\pm$ 46	191 $\pm$ 352	2.0 $\pm$ 2.1	102 $\pm$ 154	2.7 $\pm$ 3.7	na	18 $\pm$ 12	na	na
Churchill	8.1 $\pm$ 0.1	582 $\pm$ 93	12.0 $\pm$ 1.0	12 $\pm$ 1.0	600 $\pm$ 50	4.0 $\pm$ 0.5	54.4 $\pm$ 5.0	na	na	na	na	na
Boniface	5.4 $\pm$ 0.6	18 $\pm$ 3	13.4 $\pm$ 4.7	28 $\pm$ 21	na	4.1 $\pm$ 0.5	na	3.2 $\pm$ 3.4	na	na	na	na
BRG site	7.0 $\pm$ 0.6	65 $\pm$ 76	4.9 $\pm$ 3.0	97 $\pm$ 94	375	2.3 $\pm$ 0.6	51.1 $\pm$ 42.6	2.2 $\pm$ 2.3	na	1.4 $\pm$ 1.2	na	na
Kuujuarapik	7.0 $\pm$ 0.7	84 $\pm$ 71	10.0 $\pm$ 4.0	14 $\pm$ 11	550 $\pm$ 215	1.2 $\pm$ 0.5	3.4 $\pm$ 0.9	2.9 $\pm$ 1.9	5.8 $\pm$ 5.1	na	229 $\pm$ 157	23 $\pm$ 19
KWAK site	6.8 $\pm$ 0.5	361 $\pm$ 556	7.9 $\pm$ 2.2	60 $\pm$ 24	282 $\pm$ 62	4.8 $\pm$ 5.6	51.9 $\pm$ 33.6	5.6 $\pm$ 4.7	32.9 $\pm$ 10.3	0.89 $\pm$ 0.34	na	na
Disko	7.7 $\pm$ 1.0	135 $\pm$ 156	na	32 $\pm$ 59	na	na	na	1.4 $\pm$ 1.0	na	na	na	na
Kangerlussuaq	8.2 $\pm$ 0.5	298 $\pm$ 165	na	15 $\pm$ 6	858 $\pm$ 269	10.0 $\pm$ 3	< 5	1.4 $\pm$ 1	na	na	na	na
Zackenbergl	6.8 $\pm$ 0.4	23 $\pm$ 17	9.4 $\pm$ 4.6	10 $\pm$ 7	363 $\pm$ 219	na	na	1.7 $\pm$ 1.3	2.3 $\pm$ 1.3	na	11.3 $\pm$ 8.5	19 $\pm$ 16
Svalbard	7.7 $\pm$ 0.5	257 $\pm$ 100	1.2 $\pm$ 0.7	33 $\pm$ 38	760 $\pm$ 594	19 $\pm$ 16	na	2.7 $\pm$ 1.2	13 $\pm$ 9	14 $\pm$ 6	na	na
Kilpisjärvi	6.8 $\pm$ 0.9	22 $\pm$ 18	4.7 $\pm$ 5.3	8 $\pm$ 6	295 $\pm$ 218	na	na	1.4 $\pm$ 0.9	3.0 $\pm$ 2.9	0.1 $\pm$ 0	10 $\pm$ 12	22 $\pm$ 19

### 1.3.0 Literature Review

#### 1.3.1 The three pelagic and benthic algae classes observed in this study

The freshwater algae assemblages of the shallow Subarctic ponds in Churchill Manitoba, are important as indicators of the climate of the region. In the Subarctic and Arctic regions, the dominant type of algae found in the shallow freshwater ecosystems are either green algae, cyanobacteria, or diatoms. In many freshwater lakes and ponds, diatom species are the main sources of primary production in either the water column or the benthos (Rühland et al., 2015). In the northern latitudes algal assemblages are not evenly divided amongst the three algae classes, and are usually dominated by one photosynthetic organism. Shallow ponds and lakes in Bylot Island, have a composition comprised of 77.3% of cyanobacteria, 16.6% diatoms, and 4.9% of green algae (Vézina & Vincent, 1996). However, there are aquatic systems in the Arctic such as the ones in southern Baffin Island that are dominated by diatoms (63%), followed by green algae (20%) (Moore, 1974). Dominance by cyanobacteria and diatoms are due to their similar tolerance (Low-Décarie et al., 2011), and the proportions of their benthic dominance are determined by the climate and ecosystem conditions.

Diatoms are a unique type of microalgae. There are 3 distinct groups of diatoms and are either automictic or apomictic (self-fertilizing) (Edlund et al., 1997). Diatoms are able to uptake CO<sub>2</sub> through photosynthesis. The diatom structure is composed of a silica wall which enables the species to thrive in harsh conditions. Diatom species are powerful environmental indicators that allow scientists to understand environmental conditions in the past (Michelutti et al., 2003). Diatoms are primarily abundant in waters that range from a pH of 5.0 to 7.7 and prefer a temperature of 9.3 to 15.0°C (Weckström, 1997). In a study that looks at periphyton community structure in cold environments, it has been found that the average pH for optimal productivity for diatoms is 6.7 pH with temperatures of 3.15-6.90°C (Maltais & Vincent, 1996). Diatoms are less likely to be abundant within the water column since diatom species are heavy and prefer to inhabit the sediment of a pond or lake. It has also been found that variability in diatom species and biomass amongst lakes and ponds in the high Arctic, on Victoria Island, is due to the underlying substrate diatoms are on (silt, sand, rocks, etc.). Diatom species diversity is inversely related to the latitude of the pond or lake (Michelutti et al., 2003).

Diatoms were dominant prior to the 1880s in shallow lakes (Jeppesen et al., 2005, Wolfe et al., 2013). Temperature changes have caused biomass and cyanobacteria abundance to increase on a continental scale, accelerating since the mid-1940s (Taranu et al., 2015), as measured by chlorophyll a and carotenoids (McGowan et al., 2012). Within the past 15 to 30 years, significant increases have been observed, especially in the rise in air and sea temperature. Taxonomic shifts have now been observed in the Hudson Bay Lowlands by Smol et al. (2005), and Rühland et al. (2003). It has been postulated that the decrease in sea ice may play a factor in the increase in species diversity and complexity of the benthic diatom communities found in the Hudson Bay Lowlands in a region where diatoms did not exist for a millennia due to persistent ice cover (Antoniades et al., 2007). Unlike cyanobacteria, and green algae, diatoms exhibit a weaker response to the increase of CO<sub>2</sub> concentrations in the water column (Low-Décarie, 2011). An increase in CO<sub>2</sub> concentrations and decrease in pH will result in diatom concentration or biomass to increase.

Diatom diversity is correlated with the diameter of the pond or lake, with the larger the area, the higher the diversity of species of diatom (Antoniades et al., 2004). After 1880, there has been a decrease in species composition and concentration, and changes in the diatom assemblages, with accelerated change from 1950 to 1970 (Wolfe et al., 2013). This change in diatom behavior is related to the increase in atmospheric and aquatic temperatures, and changes to the concentrations of atmospheric CO<sub>2</sub>, leading to a rise in cyanobacteria. A study in the Northwest Territories, Canada, found



that there has been shift from benthic diatom to planktonic diatoms over time due to climate change. Shorter growing seasons would favour both benthic and pelagic diatoms (Rühland & Smol, 2005) and increases in temperature will affect diatoms in circumpolar and temperate regions, decreasing the abundance of diatoms (Rühland et al., 2015).

Cyanobacteria are pioneer colonizers (Lin and Wu, 2014), photosynthetic prokaryotes that are ancestors of eukaryotic algae and higher plants (Boulay et al., 2008). The most common cyanobacteria found in northern latitudes are *Oscillatoriales*, *Nostocales* and *Chroococcus* (Bonilla, 2003), and are psychrotolerant rather than psychrophobic (Kosek et al., 2016). Cyanobacteria are well suited for an environment with long exposures of ultraviolet radiation throughout an 18-hour average summer long day. Cyanobacteria have survival mechanisms that help the species to adapt to the harsh conditions in the shallow ponds. Cyanobacteria represent 50% of the biomass in many aquatic systems, that serve a major food source and fertilizer as nitrogen fixers (Häder, 2007). Cyanobacteria concentrations have been increasing since the 1800s and have increased at a more significant rate since 1995. When N is limiting, cyanobacteria will produce an enzyme known as nitrogenase that enables them to fix atmospheric nitrogen ( $N_2$ ) (Singh et al., 2010). In South America and Europe, Kosten et al. (2012) found that cyanobacteria populations have been increasing due the warming of ecosystems in the respective regions.

Adaptability is integral in providing self-sufficient primary productivity in stressful conditions. For cyanobacteria in the Subarctic and Arctic, their optimal temperature growth is higher than their ecosystem growth ranging from 5.0 to 40.0°C depending on the species (Tang et al., 1994). Increases in temperature up to the optimum temperature is correlated with increases in light utilization efficiency, photosynthetic capacity and irradiance. Cyanobacteria have the ability to adjust the photosynthetic apparatus depending on the climatic conditions, mainly temperature and irradiance. In colder conditions, chlorophyll concentration and light harvesting pigments decrease inside the apparatus and the activity of RuBisCO (ribulose 1, 5-bisphosphate carboxylase oxygenase) increases substituting the photosynthetic process.

In a study by Beaulieu et al. (2013) it was observed that either total nitrogen or water temperature are the best variables to provide a model that estimates the cyanobacterial biomass in a water body but only explains 25% of the variance. Fully formed mats in the shallow freshwater ecosystem are capable of preventing erosion, deposition and deformation of lake and pond banks (Singh et al., 2010). In a study done by Griffiths et al. (1987), it found that a diurnal pattern existed with oxygen

availability and temperature. Cultures of cyanobacteria were observed to photosynthesize more efficiently in warmer temperatures. Furthermore, the study showed that the cyanobacteria will respire at the same rate as the cells photosynthesize.

Some species of cyanobacteria can exist in ecosystems with high UV radiation exposure due to their mobility. Motile cyanobacteria can move to the lower depths of the water column. The ability to photosynthesize under oxidative stress allows the cyanobacteria to be productive under the harshest of conditions, altering their cell wall structure using carotenoids and other compounds to protect itself from UV radiation (Lin and Wu, 2014; Singh et al., 2010). Under stressful and anoxic conditions, cyanobacteria are able to photosynthesize by using bicarbonate instead of CO<sub>2</sub>. *Cyanobacterium scynechocystus* PCC 680 is able to survive in high UV radiation condition because it is able to dissipate energy absorbed by the phycobilisome (Boulay et al., 2008). Studies have shown that cyanobacteria are most productive under mid-level CO<sub>2</sub> concentrations, and yet can become productive in low concentrations of CO<sub>2</sub> due to the low photosynthetic compensation point (Low-Décarie, 2011). Cyanobacteria are the dominant type of algae in waters above a pH of 8.0 (Schlichting, 1974). Planktonic cyanobacteria in the water column are able to control their buoyancy to position themselves at more stable depths. Their buoyancy is controlled by gas vesicles in the water and lose buoyancy at high irradiance and accumulates carbohydrates because photosynthesis cannot occur. The cell regains its buoyancy once low irradiance occurs, thus allowing the carbohydrates to be consumed (Wastly et al., 2005).

Species of green algae are less common in comparison to diatoms and cyanobacteria in the Arctic and Subarctic. Unlike cyanobacteria, green algae lack mechanisms to sustain productivity under stressful light conditions. Green algae are efficient in photosynthesis when the concentrations of CO<sub>2</sub> in the water column are relatively high (Low-Décarie, 2011) and are often dominant in waters that have a low pH (Schlichting, 1974). With high pH levels in the Hudson Bay Lowlands, it is expected to see low concentrations of green algae in an environment dominated by cyanobacteria or diatoms.

### 1.3.2 Primary Production of benthic and pelagic algae

It has been suggested that shallow lakes in the Arctic will become more productive as the climate warms (Smol et al., 2005). However, seasonal productivity is difficult to measure and model. There is incomplete knowledge of interactions that produce net CO<sub>2</sub> exchange with the atmosphere in

the Subarctic and Arctic (Quinones-Rivera, 2015). Correlations and relationships of different environmental variables can change from year to year. The high variability of seasonal primary production is thought to be caused by other local effects. Environmental variables can be poor predictors of areal daily primary productivity (Cobelas & Rojo, 1994).

Carbon is a compulsory component in the photosynthetic process of algae and a product of algal respiration. Carbon dioxide can also act as a constituent to inhibit or limit algal processes. Elevated carbon dioxide concentrations cause the down regulation of the carbon concentration mechanism (CCM) activity (Pierangelini et al., 2014). The increase of CO<sub>2</sub> concentration inhibits and alters the algal cells ability to use the harvested light. The adaptability to stressful conditions is characterized by the algae and its components such as the photosystem II used to regulate state transitions. Many recent studies have observed evasion of CO<sub>2</sub> from inland waters (Perga et al., 2016). The study concluded that nutrient concentration is a primary control for lake surface CO<sub>2</sub>, but these systems are converting to a temperature driven system with the rise of temperature.

Carbon exists in many forms in freshwater ecosystems only inorganic C is controlled by buffers. Carbon exists as CO<sub>2</sub> in the atmosphere and many types of organic carbon (org C). The lithosphere is composed of 80% of CaCO<sub>3</sub> (Calcium carbonate) and 20% org C, and as CO<sub>2</sub>, HCO<sub>3</sub><sup>-</sup> (bicarbonate) and as CO<sub>3</sub><sup>2-</sup> (carbonate) in the hydrosphere (Schneider & Le Campion-Alsumard, 2010) along with dissolved organic carbon (DOC). Photosynthesis affects the pH of the water column ( $2\text{H}_2\text{O} + \text{CO}_2 + 8 \text{ photons} \rightarrow \text{O}_2 + \text{H}_2\text{O} + \text{CH}_2\text{O}$ ). The higher the concentration of HCO<sub>3</sub><sup>-</sup> and OH<sup>-</sup>, the more alkaline the water column is. A system that is supersaturated with CO<sub>2</sub> is more acidic with a lower pH.

Both oxygen and carbon dioxide assimilation, electron transport of photosynthesis and respiration are enzymatically controlled, and therefore affected by temperature (Fujita et al., 2014). Dissolved oxygen is a fundamental parameter in freshwater limnology, governed by temperature, respiration, atmospheric and hydraulic pressure. Dissolved oxygen is well mixed in the epilimnion during the summer. In the summer, large freshwater systems are typically stratified. The top layer or the epilimnion, is highly oxygenated versus the hypolimnion which is often anoxic during the summer months (Canadian Council of Ministers of the Environment, 1999). A study done in shallow ponds in subarctic Quebec, has found that stratification did occur despite the shallow depths for most of the season with a hypoxic or anoxic hypolimnion. These systems are also considered to be heterotrophic, containing large concentrations of CO<sub>2</sub> and CH<sub>4</sub> (Laurion et al., 2013).

Studies in different aquatic ecosystems of the Hudson Bay Lowlands around the perimeter of the Hudson Bay and James Bay, have measured and modelled CO<sub>2</sub> respiration. In bogs of Ontario the carbon sequestration is -1.7 to 0.5 g C /m<sup>2</sup>/d (Roulet et al., 1992) (negative values indicate that the ecosystem is a CO<sub>2</sub> sink, and positive values indicate the system as a CO<sub>2</sub> source), and in the bogs of northern Quebec is -0.2 g C /m<sup>2</sup>/d (McEnroe et al., 2009). In the fens of northern Ontario CO<sub>2</sub> sequestration is -1.0 to -0.4 g C /m<sup>2</sup>/d (Roulet et al., 1992, 1994; Bubier, 1995), in northern Quebec it is -0.6 to 0.2 g C /m<sup>2</sup>/d (Moore et al., 1994; Pelletier et al., 2007), and in Manitoba the sequestration rate is 0.9 to 0.7 g C /m<sup>2</sup>/d (Boubier et al., 1995; Joiner et al., 1999). In thermokarst ponds found in Manitoba the sequestration rate is 0.54 g C /m<sup>2</sup>/d (Bellisario et al., 1999). In the shallow ponds in the Hudson Bay Lowlands, the sequestration rate is 3.0 to 3.1 g C /m<sup>2</sup>/d (Roulet et al., 1994), in Quebec it is 0.22 g C /m<sup>2</sup>/d (McEnroe et al., 2009), and in Churchill, Manitoba it is 1.1 to 4.5 g C /m<sup>2</sup>/d (Macrae et al., 2004).

Ponds and lakes that are located in the peatlands of Mer Bleu, Ottawa, Canada are supersaturated with CO<sub>2</sub> and CH<sub>4</sub>. The water bodies in Mer Bleu have an emission flux between 0.0072-0.086 mg C/m<sup>2</sup>/s (Billett & Moore, 2008), and an average of 0.04 ±0.0007 mg C/m<sup>2</sup>/s (Dinsmore et al., 2009). These values indicate that the lakes and ponds in Mer Blue are a hotspot of carbon dioxide and methane emissions. The studies determined that there is a linear relationship with the increase of carbon dioxide emissions from the water bodies in Mer Bleu and increasing temperature. Winter fluxes found in other systems by Yang et al. (2015) show an average flux of 37.3 mg/m<sup>2</sup>/h and 24.9 mg/m<sup>2</sup>/h in the autumn. Uptake of CO<sub>2</sub> from a study by Tang & Kristensen, 2007 ranged from 2.0-5.0 μmol/m<sup>2</sup>/h and with the onset of darkness a release of CO<sub>2</sub> was 1.5-3.5 μmol/m<sup>2</sup>/h.

Streams and rivers are responsible for approximately 1.8<sup>9</sup>mg/yr while lakes and reservoirs account for approximately 0.32<sup>10</sup>mg/yr of carbon stored in the sediments (Raymond et al., 2013). Warming of Subarctic and Arctic taigas and tundra will result in them transforming into strong emitters of CO<sub>2</sub> and CH<sub>4</sub> (Humburg et al., 2010). Shallow subarctic ponds that are predominantly thermokarst formations are more susceptible to the changes in temperature (Bowden, 2010) near Churchill, Manitoba (58°440N, 94°490W). The shallow ponds and lakes contribute to the carbon fluxes, energy balance and biodiversity of the region. The loss of pond surface area and depth are attributed to the intensifying temperatures causing increased evaporation and permafrost degradation (Taranu et al., 2015), creating more pathways for loss of water.

### 1.3.3 Sediment effects on the benthos

In Subarctic and Arctic ecosystems, 19% of the photosynthesis is due to benthic primary production (Larsen et al., 2007). Benthic algae concentrations and productivity are more pronounced than the pelagic algae due to the ability to use nutrients in the sediments, making the benthic algae a control for the nutrient flux that occurs in the sediment and the water column (Pasternak et al., 2009). In regions studied in the high Arctic, the benthic algae is 1.5 times more productive than the pelagic algae (Glud et al., 2009).

Sediment at the bottom of a lake or pond is an important substrate that contains biological processes that produce and consume carbon. Sediments act as a sponge that have the potential to be a source or storage of biological carbon. Sediment respiration tends to be lower than epilimnetic respiration (Raymond et al., 2013). In hypoxic and anoxic conditions, microbial activity and the inferring biodegradation and decomposition form sediment layers. Within these layers the availability of electron acceptors regulates carbon degradation pathways (Bellido et al., 2011). The granular size of the sediment on the surface can determine the makeup of the benthic community. The sediment surface is home to benthic algae that process carbon into oxygen, and benthic grazers that respire carbon dioxide. The sediment layers contains temporal information of past limnological characteristics of the pond and its organisms based on the composition of the sediment and diatoms that have been buried by sedimentation.

Through paleo-studies of sediments, shallow ponds in Subarctic Québec have been found to have their physio-chemical dynamics change over time due to climate change (Bouchard et al., 2011). The composition of sediments and diatoms can be extracted using coring techniques and analyzed to reconstruct characteristics such as *in situ* pH and nutrient concentrations in the water column, and climatic conditions in the atmosphere. The analysis showed that there is an increasing trend in the concentration of allochthonous organic matter in the sediment layers and that there has been a decrease in the bottom oxygen concentration in the ponds (Bouchard et al., 2011). This affects the biological activity and is an indication of increased respiration relative to oxygen supply.

In a study done by Stanley (1976), benthic algae were in the first 2 cm of the sediment. This is important to note because wind mixing in the shallow ponds can affect sedimentation and benthic algae growth in ponds. Most of the biological activity in the sediment occurs within the first 2 cm of the benthic sediment due to factors such as the availability of light and oxygen within the first 2 cm of the

sediment, and anoxic in the layers below (Cantonati & Lowe, 2013). Studies have determined that 97% of benthic algae production can be lost by grazing and burial where wind mixed depth is shallow enough to affect the benthos (Stanley, 1976; Moss 1977). Furthermore, the top 4 cm of the sediment is susceptible to grazer organisms where up to 15.1% of the algal biomass can be lost without the effects of wind mixed loss (Stanley, 1976). When strong enough winds do occur, epipsammic freshwater algae that are attached to grains, and epipelagic algae that live freely on sediment are both buried by the wind and eaten by grazers. Respiration occurs in combination with the algae and microorganisms in the water, therefore grazer organisms need to be accounted for in tundra Alaska Ponds. However, epipsammic algae are able to photosynthesize when buried for 7 days on average until succumbing to grazers (Moss, 1977).

In the Arctic foothills of Alaska, the microphytobenthos accounts for 77% of the algal biomass in the freshwater system. The oxygen production is spatially controlled by nutrient availability (Whalen et al., 2013). Although photosynthesis can occur between 0 to 2 mm in the sediment, O<sub>2</sub> availability and penetration can occur as deep as 14 mm (Whalen et al., 2013). A study that measured oxygen using an oxygen electrode in 0, 2, and 4 mm of the sediment, determined that thick mats experienced very little photoinhibition, dominating the layers 2 and 4 mm below the sediment surface. Cyanobacteria are found to dominate the sediment up to 4 mm deep. In the upper 0 to 20 mm of the sediment, it has been found that there is a low DO concentration approximately < 40% making the zone anoxic (Coulombe et al., 2016). Lentic periphyton or benthic algae are prone to photoinhibition when oxygen levels in the water column are high. Furthermore, photosynthesis and photoinhibition are affected by temperature and nutrient concentration (Dodds et al., 1999). The sediment photic zone is established to approximately 0.5 mm in fine sediment grains, and 3.5 mm with coarse sediment grains (Masini et al., 2001). Light is strongly attenuated through the vertical profile of polar microbial mats that are dominated by cyanobacteria (de los Rios et al., 2015). A photosynthetic marker of chl *a* can potentially be found representing diatoms in resting stages, which are known to form at the end of a bloom during mass sinking (Overnell et al., 1995).

In stratified lakes, the net ecosystem exchange is governed by the processes in the water column and any sediment above the thermocline. Products from processes that occur below the thermocline have very little chance of interacting with the surface-atmosphere boundary (Algesten et al., 2005). The low-lying vegetation in the Churchill region allows for the wind to maintain velocity over a larger landscape uninhibited by tall vegetation. Wind velocity, air temperature, and long and shortwave

radiation are important variables in determining the local water temperature and thermal stability of the water column which affect both the pelagic and benthic diatom and algal communities (Hadley et al., 2014; Rühland et al., 2015). In shallow systems that are strongly mixed, nutrient limitation to pelagic algae biomass in the water column is weak. However, in studies done in 2012, the shallow ponds experience mixing to the bottom even with a limited fetch (Rimas, 2012, unpublished BSc thesis).

#### 1.3.4 Identifying pond characteristics to be studied

The study of the diurnal and daily patterns of ponds and lakes are important in understanding the role of shallow freshwater ponds in carbon processing and the mechanisms responsible for them. As well, the processes responsible for the annual patterns should be understood as well. In a two-year study done in the large shallow Lake Vertsjav, Estonia, it has been determined that there were annual differences in the overall behaviour of processing carbon. In 2009, the pelagic algae in the large shallow lakes water column represented storage of carbon, and in the follow year, 2010, observed that the lake was a source of carbon dioxide (Rõõm et al., 2014). The annual difference in CO<sub>2</sub> emission and sequestration is moderated by sediment temperature, oxygen concentration and water column depth. The increase in sediment temperature has a positive linear correlation with the production and emission of carbon dioxide. Furthermore, increase in oxygen concentration and in water column depth has a negative linear correlation with the production and emission of carbon dioxide (Rõõm et al., 2014).

Many studies have found that temperature is a significant factor that affects the biological processes of photosynthesis and respiration in the water column and the sediment bottom. In a study done by Stanley (1976), 74-95% of the variation in photosynthetic fluxes are due to temperature. Temperature is an important variable to measure because it influences the growth rate, photosynthetic and respiration rates of the pelagic and benthic algae. For benthic algae and sediment respiration, temperature does have a direct effect on the metabolism of the microbes (Hornbach et al., 2017). Thus, the temperature directly affects the amount of CO<sub>2</sub> respired from the sediment layer of the ponds. Due to variations amongst components of ecosystems, each pond may have a variable that is more prominent in affecting the biological processes, such as allochthonous dissolved organic carbon and nutrient concentration. Temperature is important variable because increasing temperature promotes the development of benthic algae mats that are dominated by cyanobacteria (Taranu et al., 2015) and in the longer term, increasing temperature affects the depth, and surface area of the ponds through

changes that affect both precipitation and evaporation (Riordan et al., 2006, Plug et al., 2009, Rautio et al., 2011). Temperature also affects the solubility of O<sub>2</sub> and CO<sub>2</sub> with lower solubility occurring when the water column is warmer (Yang et al., 2015).

In shallow water columns, the water layer is small enough to allow PAR and UV to penetrate all the way to the bottom of the ponds, while deeper water columns absorb solar radiation and have less PAR and UV penetrate to the benthic algae (Plug et al., 2009). Temperature extremes are larger when water is shallower. A deeper water column benefits the benthic algae because it produces a less stressful, more stable environment for the benthic algae. Shallow water columns may allow for aqueous gas exchange to occur more efficiently between the atmosphere and the benthos but also limits the reservoir of dissolved gases like CO<sub>2</sub> needed for photosynthesis.

The combination of long durations of high PAR, and low coloured DOC, would effectively stress the phytoplankton in the water column, and benthic algae on the surface of the pond sediments (Sabbe et al., 2004). Due to the shallow depths of the water column, the wind effectively mixes the water and resuspends sediment which affects the extinction of PAR (Einem & Granéli, 2010 Rimas 2012). In shallow Arctic Lakes, the attenuation coefficient is between 1.17 and 2.07 mm<sup>-1</sup> which is an indication of clear water columns. In high UVB regions such as the Subarctic and Arctic, with a range of coefficients of 1.17 and 2.07 mm<sup>-1</sup> (Whalen et al., 2013), high UVB regions, diatoms can experience a photoinhibition of 40%, whereas cyanobacteria can experience a decrease in photosynthetic efficiency of 50 -100% (Vinebrooke & Leavitt, 1999).

UV-A radiation ranges from 315 to 400 nm, and UV-B radiation from 280 to 315 nm (Pessoa, 2012). In the Arctic and Subarctic, the susceptibility of algae to ultraviolet radiation is more pronounced due to the depleted ozone layer (Saulnier-Talbot et al., 2003) Ultraviolet radiation is able to penetrate the water column to significant depths, forcing algae and microorganisms to adapt using photoprotection strategies such as pigments (Häder et al., 2007). An abundance of ultraviolet radiation induces oxidative stress and lipid peroxidation (Moon et al., 2012). UV-B radiation significantly changes the algal assemblage of a shallow pond. UV-A radiation has the potential to inhibit the productivity of diatoms by 40%, allowing taxa that adapt better in high radiation ecosystems to be dominant, where relative to diatoms and green algae, cyanobacteria have the potential to increase productivity by 50% (Häder et al., 2007).



The depth of the wind mixed depth is dependent on the extent of the surface of the water body (fetch) and wind velocity. The larger the fetch or surface area of the pond is, the deeper the mixing depth of the water column will be (Fee et al., 1996). The highest biomass of pelagic algae is found in the most turbulent water columns. Mixing intensity and water column depth are two crucial variables that affect phytoplankton production due to redistribution of nutrients. Deep water columns will produce minimal sediment mixing and experience low light availability, and highly turbulent water columns will support high rate of downward mixing of pelagic algae to light limiting depths. In order to maintain a population of pelagic algae that are adapted to sinking, shallow water depth and a minimal turbulence is required to counter the sinking loss. As a result, a depth of 0.40 m must be maintained in the freshwater pond or lake to support a non-motile pelagic community (Jäger et al., 2010). Physical disturbance from waves will affect and disturb the sediment surface, causing the burial of benthic algae by having the underlying sediment mix and settle on top of the benthic algae and further affecting the primary productivity and vertical distribution of active algae in the sediment availability (Whalen et al., 2013).

Quantum efficiency ( $Q_y$ ) is a measure that evaluates photoinhibition or primary productivity of a cell (Figueroa et al., 2003). In stressful conditions, quantum efficiency decreases, indicating the inability for the algae to photosynthesize productively. Quantum efficiency is the ratio between the number of electron produced and the photons absorbed by the photosystem II of the algae (Lasik et al., 2014; Sakshaug et al., 1997). Quantum efficiencies in the high Arctic in lakes on Cornwallis Island and Little Cornwallis Island (73-75°N, 92- 95°W) are less than 10 mmol C/mol/quanta (Markager et al., 1999). In southern Spain (36°13'N 5°27'W), the quantum efficiency in estuaries are between 40-45% in green pelagic algae (compared to a theoretical maximum of 79%), indicating that there is photoinhibition in parts of the world below the Arctic Circle where moderate intensities of PAR occur.

#### 1.4.0 Fate of carbon

Pond area and depth may be significant variables in determining the rate at which shallow freshwater ponds emit CO<sub>2</sub> and store carbon. However, there are many postulations to how Arctic ponds will respond to climate change. It has been hypothesized that there will be an increase in lake and pond area where water depths increase as permafrost melts, according to Jones et al. (2011). Plug et al. (2008) suggest that lakes and ponds will both grow in area or shrink and disappear depending on the water budget. Finally, minimal to no changes are hypothesized to occur, according to Riordan et al.

(2006). Furthermore, climate change effects may lag in the Hudson Bay Lowlands due to the interior ice cover in the Hudson Bay versus the high Arctic, which cools the region longer than central subarctic systems in Canada (Rühland et al., 2015). This may cause a delayed shift in the assemblages of the benthic and pelagic algal taxa (Rühland et al., 2013). Alternatively, this theorized delay in climatic and local changes in the Hudson Bay Lowlands is countered in a study of observed and projected changes. In the Hudson Bay Lowlands near Churchill, Manitoba, between 1943 and 2009 there has been increased pond surface fluxes, earlier ice break ups, increased open water duration, and increased rainfall. However, with the enhanced climatic conditions, several studies also show decreases in pond water surfaces (Macrae et al., 2014). The year to year variability can make primary production of the benthos in the Hudson Bay Lowlands difficult to ascertain due to the inter-annual variability in the regional ecosystems.

## 2.0.0 Chapter 2: Methodology

For this study extending over two summer field seasons, four ponds of varying size and depth were selected from a group of ponds near Churchill, Manitoba previously studied by Macrae et al. (2004). *Some Pond* (all names unofficial) was selected as the large pond during the preliminary field season in 2013, focusing on within-pond temporal and spatial changes in the algal assemblages and limnological variables. In 2014, along with *Some Pond*, 3 more ponds were added to the study. *Strange Pond* (Figure 2) represented medium sized ponds, *Left Pond* (Figure 3) represented small ponds, and *Puddle Pond* (Figure 4) was selected as the ephemeral desiccated pond. In the summer field season of 2013, *Some Pond* was the focus of the study. The goal of the study was to observe the extent of within-pond spatial and temporal variability along an east to west transect.

In the 2014 summer field season, *Strange Pond* was selected as the main experimental pond for study. In *Strange Pond*, primary productivity and respiration rates were evaluated using measurements of dissolved oxygen (DO), temperature, and benthic algae concentration as indicators. Spatial and temporal changes in limnology and algal concentrations in *Some Pond*, *Left Pond* and *Puddle Pond* were also observed.

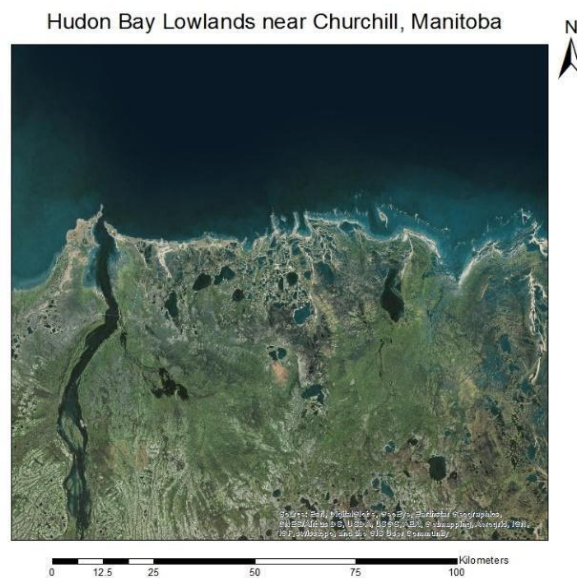


Figure 1: Satellite image of the coastal Hudson Bay Lowlands near Churchill Manitoba (image from Google).



*Figure 2: Strange Pond from the South Eastern shore showing the dock in the far right.*



*Figure 3: Close up figure of the eastern sample location of Left Pond. A highly active pond that features a benthic mat with a red hue.*



*Figure 4: Without a water column, Puddle Pond's benthic sediment is exposed to the air. Small drainage channels can be seen where the water follows during rain events as the pond is drying up.*

### 2.1.0 Field research: 2013

Field work occurred during June and July in 2013. During the field season, the Hudson Bay Lowlands experienced a summer drought, with many of the smaller and shallower ponds drying up. Some Pond was selected to monitor and observe the spatial and temporal variations due to its accessibility from the Churchill Northern Science Centre (CNSC), and its depth allowed for a 12 ft. aluminum boat to be used for sampling without obstructing instruments or disturbing sediments.

#### 2.1.1 Sampling Protocol: Some Pond transect

A 100 m long transect was set up in a east-west direction across the midline of the pond. Sample locations at 10 m intervals were indicated by rebar driven into the bottom sediments (Figure 5). At each sample location, the boat was tethered to the rebar and allowed to rotate around the rebar into the prevailing wind direction until stable. Triplicate readings using a BenthosTorch were obtained by submerging the sensor until the foam pad contacted the sediments to measure the concentration ( $\text{mg}/\text{cm}^2$ ) and cell count of benthic algae. The BenthosTorch requires 10 s to complete a single measurement.

Limnological variables, benthic and pelagic algae and reflectance readings were taken from the side of the boat. The water column was divided into a top layer and a bottom layer. The mid-point of the

water column was determined, and then the water samples and measurements were taken at the midpoint of the top layer, and the mid-point of the bottom layer.

Water was extracted at the two midpoints using a triple-rinsed syringe with 60 cm long tubing. Extracted water was dispensed into a triple rinsed Nalgene sampling bottle to collect water samples for the analysis by the YSI 600QS probe. The water sub-sample for chlorophyll fluorescence was directly dispensed from the syringe into a 2 mL acrylic cuvette, which was filled to the top, and capped. Water samples in the cuvettes were stored in an insulated pouch and taken back to the lab for later analysis to measure the quantum yield (or efficiency,  $Q_y$ ) and optical depth of the pelagic algae in the water using an AquaPen (Photosystems Inc.).

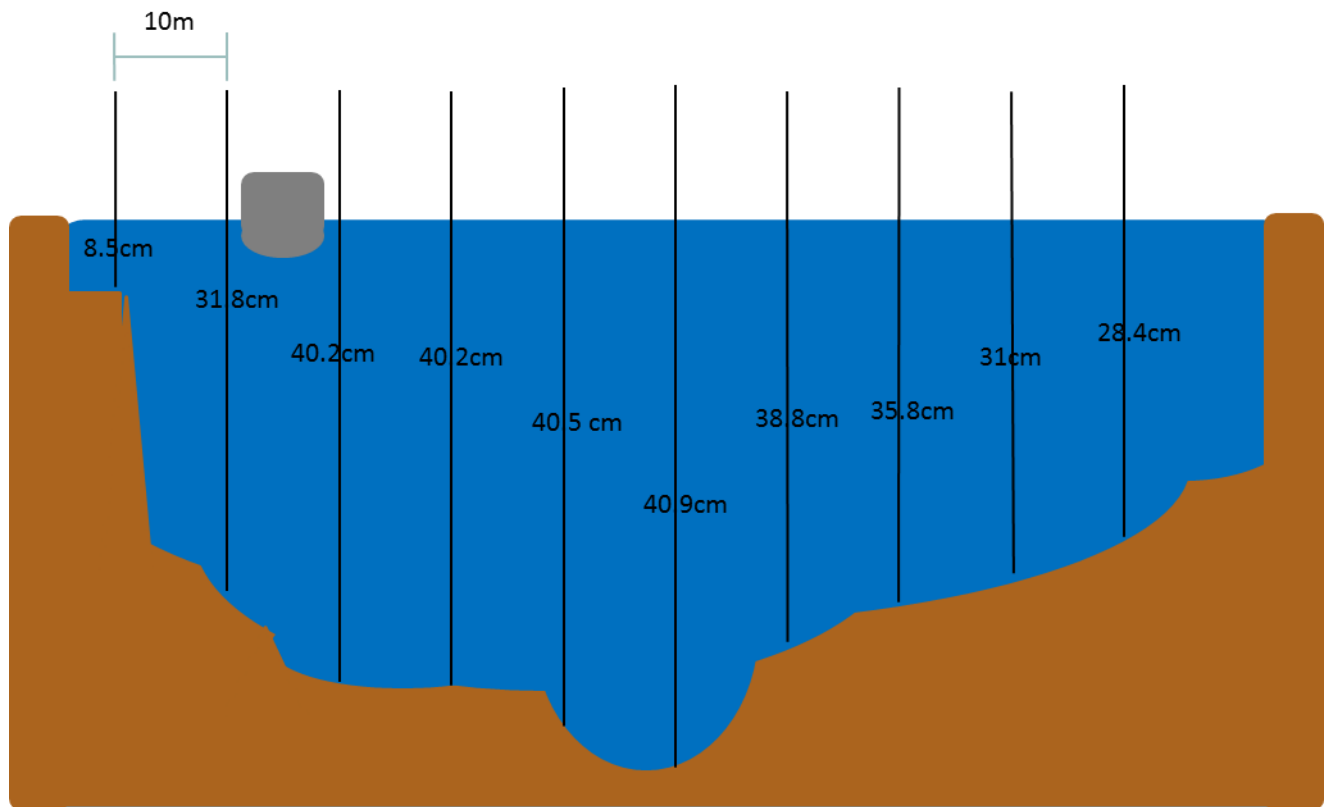


Figure 5: The transect of Some Pond showing water depths at ten meter intervals with a vertical exaggeration of x100.

## 2.2.0 Equipment

### 2.2.1 BenthosTorch

The BenthosTorch (bbe-Moldaenke) is a chlorophyll fluorometer that measures the concentration of chlorophyll *a* of the three major algae taxa: cyanobacteria, diatoms, and green algae. Its primary use was to measure benthic algae concentrations at the bottom of the four ponds being studied. The BenthosTorch has seven LEDs that excite chlorophyll *a* molecules by pulsing three different wavelengths of light at 470 nm, 525 nm, and 610 nm (Figure 6). An eighth LED pulses a wavelength of light at 700 nm which compensates for background reflection. The unit internally measured the intensity of light emitted by the excitation of chlorophyll *a* molecules and converts the readings into algal concentration and cell count for each taxon. Each taxon contained different pigments that react or are excited by different wavelengths and transfers energy to chlorophyll *a*. The BenthosTorch measured the distinct wavelengths that are re-emitted from the algae and assigns chlorophyll *a* concentration for each taxon (Low-Décarie et al., 2011). The chlorophyll reemitting radiation are confined to the surface layer of a few mm absorbing excitation radiation. The detector end of the 40 cm long sensor was lowered vertically to make physical contact with the bottom sediments and then manually triggered by the operator. Replicates of three readings were taken at each sample location.



*Figure 6: The different coloured LED lights that are part of the BenthosTorch detector used to excite the algae cells.*

### 2.2.2 AquaPen

The AquaPen-C AP-C 100 (Figure 7) is a portable fluorometer that uses fluorescence to measure quantum yield ( $Q_Y$ ), and optical density (OD) of the water column. The quantum yield of the pelagic algae in the water is measured by emissions at 450 nm and 620 nm. The 455 nm wavelength excited the chlorophyll of the pelagic algae. The 620 nm wavelength excites the phycobilin and was used to measure the quantum efficiency of cyanobacteria. Optical density was measured using 680 nm and 720 nm pulses. Measurements for  $Q_Y$  and OD were taken three times for each water sample. Prior to each reading, the water sample was vigorously shaken for a minimum of 10 s to suspend sediment material and organics in the water.

Water samples were collected in situ using a 2.0 mL square clear acrylic cuvette. The cuvette was rinsed away from the sampling area with the pond water then dipped below the water surface of the sampling area, and then capped, dried and stored in a dark holding container. The quantum efficiency and optical density of the algae in the water column was measured in lab daily, typically in the evening.



*Figure 7: The Aqua Pen is a small hand-held unit that quickly measures the quantum efficiency and optical density of the 2 mL water sample.*

### 2.2.3 YSI 600 QS Probe

The YSI 600 QS Probe was a multiparameter probe allowing the measurement and recording of the limnological characteristics of the pond water. Readings include pH, DO, ORP, temperature, and electrical conductance. The YSI probe was submerged vertically into the water column to collect



readings at the pre-determined depths in the ponds. If the water column was too shallow for the entire unit to be submerged, measurement of the variables were still possible as long as the probe sensors were fully submerged without being in contact with the sediment. To maintain the accuracy of the YSI, the sensors on the probe were calibrated every 3 to 4 days using standard operating procedures.

#### 2.2.4 In situ weather data

A weather station was set up on the western side of Some Pond (Figure 8). Ambient weather and environmental conditions were measured every ten seconds and recorded using CR 1000 and CR 3000 Campbell Scientific data loggers. Data was averaged and stored every ten minutes. Incoming photosynthetically active radiation PAR was measured with a LI-COR quantum sensor over land at a height of 1.0 m, and an aquatic photosynthetically active radiation sensor (LI-COR) was submerged 10.0 cm above the bottom sediments. Wind velocity and direction were measured at a height of 1.0 m using a Davis vane and anemometer system. Air and water temperatures were measured using custom copper-constantan thermocouples with the sensor tips painted white to minimize solar heating. The thermocouple measuring air temperature was placed close to the PAR sensor at 1.0 m. The thermocouple measuring water temperature was wrapped around the aquatic PAR sensor. The sensors were attached to a tripod with cross arms. The underwater PAR sensor and thermocouple were attached to a LI-COR 2009S lowering frame made from anodized aluminum (designed specifically for LI-COR underwater Pyranometer) that was immovable when water turbulence increased.



*Figure 8: At the height of the tripod, an anemometer and LI-COR pyranometer are attached taking readings of wind velocity and incoming solar radiation. The devices are attached to a Campbell Scientific data logger that takes readings every 10s and computes the observations to 15 min averages.*



*Figure 9: The YSI 600 QS probe used to instantaneously measure and record limnological characteristics of the pond water.*

### 2.3.0 Field research: 2014

The field season of 2014 functioned primarily as a means to measure and monitor pond and benthic photosynthesis and respiration. Strange Pond was selected to measure pond productivity over a 30-day period. Complementary to the field work in the summer of 2014, four ponds were selected to study the temporal and spatial variation of the benthic and pelagic algae, and limnological

characteristics of the pond water. These ponds were Some Pond (large), Strange Pond (medium), Left Pond (small), and Puddle Pond (desiccated).

### 2.3.1 Spatial and temporal Variation

Measuring the temporal and spatial variations of Some Pond followed a similar protocol to 2013, however rather than taking measurements at ten different sample locations across the length of the pond, measurements were reduced to 5, ending near the deepest location at the midpoint of the pond with the assumption that one half of the pond is similar to the other. Measurements were taken at the 10 cm depth instead of dividing the water column.

Left Pond was subject to in situ measurements of the benthic algae and limnological characteristics using the BenthoTorch and the YSI 600 QS probe. Temporal measurements were taken over the summer, and in north, east, south and west quadrants proximal to the shore line. Depth measurements were carefully taken using a meter stick with minimal disturbance of the benthos and sediment surface. Water samples were collected directly into sterilized 2.0 mL cuvettes, which were then capped, dried, and stored to be analyzed in the lab using the Aqua Pen. BenthoTorch readings were taken in triplicates at each sample location. The YSI 600 QS probe measured water characteristics at a depth when the sensors located at the head of the probe were fully submerged in the water.

Strange Pond was also subject to in situ measurements following the same protocol as Left Pond. Strange Pond, being a larger pond, required 8 sample locations, in the attempt to sample around the circumference of the pond. The very shallow, most northern end of the pond was inaccessible, being unable to leave the sediments undisturbed and therefore the northern location was omitted. Sample locations included the north-eastern, eastern, south-eastern, southern, south-western, western, and north-western ends of Strange Pond. Later in the field season, Puddle Pond was chosen to monitor the changes of the sediment of a dried-up pond. Benthic algae readings using the BenthoTorch were taken at 4 sample locations covering the northern, eastern, southern, and western quadrants of the pond.

### 2.3.2 Oxygen and carbon dioxide measurements

Strange Pond included an intensive study of temporal variations and characteristics affecting the CO<sub>2</sub> budget of the pond. Equipment which included the CR 3000 data logger, batteries that powered the

water pumps and solar panels were stored on an L-shaped dock which extended approximately 3.0 m from shore. At the end of the dock an acrylic benthic chamber was submerged and anchored deep into the sediment bottom. The benthic chamber is 0.60 m x 0.60 m x 0.60 m  $\frac{1}{4}$ " acrylic, with an approximate volume of 27.75 L. It transmits approximately 92% of ambient photosynthetically active radiation. The average depth of the benthic chamber was 8.0 cm. One corner of the benthic chamber was submerged deeper into the sediment. The small tilt allowed any methane gas bubbles to flow towards the elevated corner to allow their exit via a small tube. This prevented gas from building up in the chamber and prevented the lid of the chamber from being accidentally dislodged, preventing external water to leak into the chamber while measurements were being taken. The lid could be manually removed to periodically clean the apparatus to prevent bio-fouling. This benthic chamber was attached to a small enclosure, encasing a silicone dissolved gas diffuser (SDGD). The SDGD was a network of silicone tubing allowing the diffusion of CO<sub>2</sub> in the pond water through the tube walls while preventing the passage of water. The tubing of the SDGD was attached to the LI-COR 8100 Infrared gas analyzer that measures CO<sub>2</sub> concentration. The enclosure of the SDGD also contained an YSI 600 QS probe that was attached to a battery, simultaneously recording dissolved oxygen, pH, and temperature of pond water within the chamber at 1-minute intervals.

Water circulation was controlled by the two large aquarium pumps. These water pumps were attached to the side of the dock for water intake, and a pump was located within the SDGD chamber to mix and expel water. Water from the pond circulated freely into the benthic chamber, for 15 minutes to allow chamber water to equilibrate with ambient pond water. Then valves were closed for 15 minutes while water was only recirculated within the chamber. During this time, the rate of change in concentration of oxygen and carbon dioxide were monitored and converted into an equivalent gas exchange flux ( $\mu\text{mol}/\text{m}^2/\text{s}$ ) with the bottom sediments. Unfortunately, the SDGD set up contained some leaks which would have compromised the integrity of the LI-COR infrared gas analyser (IRGA). As a result, rather than measuring CO<sub>2</sub> flux directly, it was calculated based on the fluctuations of the DO in the cycled water which were measured four times per hour and then modelled from the sediment core experiment.

### 2.3.3 Chl *a* concentrations of pelagic algae measured using the BenthosTorch

To assess whether the ponds were benthically or pelagically driven, a comparison of primary producers was needed. The concentration of pelagic chl *a* was measured using the BenthosTorch. For each pond, three litres of water was collected using a 200 mL Nalgene bottle submerged below the water surface. In the lab, water was shaken thoroughly to homogenize the contents in the water container before being filtered. 200 mL of water was hand pumped through a 1.2µm GF/E filter. As the filter was left on the Buchner funnel, the BenthosTorch was carefully placed onto the surface of the filter. Measurements of the chl *a* concentrations were collected in triplicates, and the values are converted to µg/L using the formula:

$$\frac{\mu\text{g}}{\text{L}} = C \times A_f / V \quad (1)$$

Where C is the concentration of chl *a* in µg/cm<sup>2</sup>, and A<sub>f</sub> was the area of filtered water. V was the volume of water filtered multiplied by 5.

### 2.3.4 Sediment characteristics

Sub samples of the extracted cores were taken to determine the bulk density, organic fraction, and carbon content in 2.0 cm increments. The wet weight and dry weight were taken to determine the bulk density of the sediment. The sediment samples were dried at a temperature of 60°C over a 24-hour period. A subsample of the dried sediment was then weighed and placed in crucibles for loss on ignition (LOI) at 550°C for 2-hours to determine the organic fraction, and carbon content of the sediments.

### 2.3.5 Sediment core respiration experiment

In order to understand the effects of temperature on primary production and respiration of the pond sediments, an experiment was set up to determine the respiration rate from five sediment cores of varying thickness extracted from the pond bottoms. All cores preserved the surface benthos and in total were 2, 4, 6, 8, and 10.0 cm thick (Dodds et al., 1999). The cores were extracted in situ using 10.0 cm diameter corers made from PVC piping. Each corer was 2.0 cm longer than the corresponding depth of the sample. Each corer was slowly pushed into the sediment until the sediment inside the corer reached the 2.0 cm mark. A plastic lid then pushed slowly into the sediments, capping the bottom of the

corer. The capped corer was then lifted slowly, making sure that water and sediments would not spill out of the corer. For transport, a second lid was placed on the top of the corer.

In the lab, each of the five cores was placed in a water bath to regulate temperatures while CO<sub>2</sub> respiration rates were measured (Figure 10). Respiration was measured at 7 different temperatures, in 5°C increments (0, 5, 10, 15, 20, 25, 30°C) following a study done by Rae and Vincent (1998) that used similar increments of temperature. Measurements start at room temperature (20°C). The water bath was cooled by adding ice, down to 0°C. At each temperature interval, respiration flux for the 5 sediment cores were measured in triplicate using the LI-COR 8100 IRGA.

The 10 cm survey chamber of the LI-COR 8100 was slowly lowered onto the top of the core to ensure an air-tight fit while CO<sub>2</sub> was recirculated through the closed system for 3 minutes. CO<sub>2</sub> concentration was then measured for 3 minutes at 1 s intervals by the IRGA with all light excluded. Once the measurement was complete, the survey chamber was slowly taken off, and then placed on the next core. The best-fit exponential slope of the concentration increase at ambient CO<sub>2</sub> levels was then converted to a flux ( $\mu\text{mol}/\text{m}^2/\text{s}$ ) using LI-COR *Fileviewer* software.



Figure 10: This set up shows the IRGA gas chamber tightly fits and sits onto the rim of which is supported 1.0 cm above the water. This image shows readings taken near 0°C with the ice bath.

### 2.3.6 Benthos assemblages

In order to assess the living algal assemblage within the sediment cores, chlorophyll fluorescence measurements were taken at 2.0 cm intervals with the Benthos in the lab. Each core was sliced using a pallet knife at 2.0 cm intervals in. This process was done in a dimly-lit room to minimize any photo-inhibition of the algae. Measurements were taken at each 2.0 cm interface, in

triplicate, including the sediment surface (Figure 11). A piston pushed out 2.0 cm of the core with gentle force, and the layer was carefully removed. The following layer was then subjected to BenthosTorch measurements, and this protocol occurred until each layer of the core was measured. Layers were stored in labelled Ziploc bags, and refrigerated for later bulk density and carbon content analysis.



*Figure 11: A 2.0 cm slice of pond sediment extracted from the core that has already been sampled.*

### 2.3.7 Photometry

The photosynthetic active radiation that was used by the algae was measured by using pyranometers developed (LI-COR Biosciences). Ambient or air photosynthetic active radiation was measured using a LI-COR LI-190SA Quantum Sensor. The detector of the LI-190SA is a high stability silicon photovoltaic detector. The detector was able to measure photosynthetic active radiation in the 400-700nm range, as a photosynthetic photon flux density ( $\mu\text{mol}/\text{u}^2/\text{s}$ ). The light penetrating the surface of the water was measured using the LI-COR LI-192SA Under Water Quantum Sensor. The unit had a high stability silicon photovoltaic detector, able to measure under water photosynthetic photon flux density (PPFD).

## 2.4.0 Calculations and statistics

### 2.4.1 Attenuation coefficient

The attenuation coefficient was important in order to determine the amount of ambient solar radiation or photosynthetic photon flux density (PPFD) that reached the sampling depths and the monitoring depth of the benthic chamber in Strange Pond. The attenuation coefficient was calculated by first determining the proportion of ambient solar radiation entering the water surface as a function of the solar time at which solar radiation was measured:

$$\text{Solar Time} = \text{CST} + 4(L - 90)/60 \quad (2)$$

where  $90^\circ$  was the longitude of the standard meridian for the Central time zone, CST is the central Standard Time, and L, the approximate longitude of the pond location. The solar declination,  $\delta$  was determined from:

$$\delta = -23.45 \times \cos((360(284 + \text{DOY})/365)) \quad (3)$$

where DOY is the Julian day of measurement. The solar zenith angle,  $z$  was determined from:

$$\cos(z) = \sin(\phi) \times \sin(\delta) + \cos(\phi) \times \cos(\delta) \times \cos(h) \quad (4)$$

where  $\phi$  was latitude and  $h$  was the hour angle of the sun given by:

$$h = 15 \times (12 - \text{Solar Time}) \quad (5)$$

Since the refractive index of water is 1.33, the angle of incidence of the direct beam solar radiation in the water,  $\theta$  is given by:

$$\sin(\theta) = \sin(z)/1.33 \quad (6)$$

So the path length,  $\ell$  through the water of depth,  $d$  is given by:

$$\ell = d/\cos(\theta) \quad (7)$$

The attenuation coefficient  $a$ , is then given by the Beers-Lambert law as:

$$\text{PPFD}_d = \text{PPFD}_0 \exp[-a \ell] \quad (8)$$

where the photosynthetically active radiation at the water surface,  $\text{PPFD}_0$  is related to the measured ambient radiation,  $\text{PPFD}_A$  by:



$$PPFD_0 = PPFD_A (1-\alpha_s) \quad (9)$$

where  $\alpha_s$  is the surface reflectivity, which for a plane water surface is given as:

$$\alpha_s = 0.5 \left( \frac{\sin^2(Z-1.33)}{\sin^2(Z+1.33)} + \frac{\tan^2(Z-1.33)}{\tan^2(Z+1.33)} \right) \quad (10)$$

Noon hour solar zenith angles between June 25 and July 28 vary between  $35.1^\circ$  and  $39.6^\circ$ , and path lengths vary between 1.108d and 1.138d, respectively.

#### 2.4.2 Calculating the NEE and oxygen production

Multiple variables were required to determine the benthic algae gas flux and the net ecosystem exchange gas flux. To determine the net  $CO_2$  gas flux or net ecosystem exchange, the DO flux in the benthic chamber was calculated using the formula:

$$DO_2 \text{ (mg/L/min)} = (\Delta O_2 / \Delta t) \quad (11)$$

where  $\Delta O_2$  was the recorded change of concentration of dissolved oxygen from when the chamber was first closed to when it becomes open to the surrounding pond system.  $\Delta t$  was the time interval while the chamber was fully closed in recirculation mode, and in this case was 15 mins. To calculate the net ecosystem exchange of the pond system, the oxygen flux,  $F_{O_2}$ , from the change in concentration  $DO_2$ , was first converted from volume to a per unit area basis using the formula:

$$F_{O_2} \text{ (mg/m}^2 \text{ /min)} = DO_2 \text{ (mg/L/min)} / v' \quad (12)$$

where  $v'$  is the specific volume of the benthic chamber ( $132 \text{ L/m}^2$ ).  $F_{O_2}$  gas flux was then converted from mass to molarity using the formula:

$$F_{O_2} \text{ (mmol/m}^2 \text{ /min)} = F_{O_2} \text{ (mg/m}^2 \text{ /min)} \times 32 \quad (13)$$

where 32 is the molarity of  $O_2$ . The  $F_{O_2}$  gas flux can be converted to  $F_{CO_2}$ , by utilizing the molarity of the carbon molecule, which was done by:

$$F_{CO_2} \text{ (mmol/m}^2 \text{ /min)} = F_{O_2} \text{ (mg/m}^2 \text{ /min)} \times 44 \quad (14)$$

using the assumption of a photosynthetic efficiency of 1.0. (i.e. the evolution of each oxygen molecule requires the assimilation of one carbon dioxide molecule). Using the net ecosystem exchange flux (NEE)(equation 13) derived from the change in concentration of dissolved O<sub>2</sub> in the benthic chamber, assimilation of CO<sub>2</sub> by the benthic algae, A, can be calculation from:

$$A = NEE - R \quad (15)$$

where A is the photosynthesis or assimilation of CO<sub>2</sub> by the benthic algae and R, the benthic respiration modelled from the sediment core experiments using measured temperature.

#### 2.4.3. Statistical analysis

The data set for this project included limnological variables measured at different sampling days and locations amongst 4 shallow ponds. Before applying statistical tests to analyze if significant spatial and temporal patterns exist, the data sets must be determined to be normally distributed. In the instance that the data collected are normally distributed than an Analysis of Variance (ANOVA) is used for determining significance of a single variable differs within multiple independent variables and a T-test is used when comparing two dependent variables is applied. Using a Bartlett test in tandem with an ANOVA was done to test for homogeneity in the data set. Alternative analyses were used when the data set is not normally distributed. Kruskal-Wallis test (H-test) was used instead of an ANOVA. And a Wilcoxon test was used instead of a T-test. Variables that were assessed for temporal and spatial variability include photon flux density, temperature, dissolved oxygen, pH, quantum yield, and chl *a* concentrations.

### 3.0.0 Chapter 3: Spatial and temporal variations in biogeochemical and limnological variations within the ponds studied

#### 3.1.0 Results: Spatial and temporal variations

This chapter presents an analysis of the spatial and temporal variability of biotic and abiotic limnological variables in the water columns and sediments of the study ponds in the Hudson Bay Lowlands. The results of the 2013 and 2014 field season are compiled to illustrate different aspects of the pond characteristics found in the four ponds. Interactions of ambient weather conditions and limnological variables in the water column and pond bottom will be illustrated in this chapter. These variations will be examined both horizontally (transect and perimeter sampling) and vertically (water column and sediment).

#### 3.1.1 Photosynthetic active radiation

Incoming PAR measured above the surface of the water and in the water column of two ponds were similar in both 2013 and 2014 ( $p > 0.05$ ). The water columns are somewhat similar in clarity as the calculated average attenuation coefficient for Strange Pond is  $0.12 \text{ cm}^{-1}$  and for Some Pond is  $0.07 \text{ cm}^{-1}$ . PAR during the 2013 field season is illustrated in Figure 12a. The average incoming  $\text{PPFD}_A$  prior to entering the water column was  $466 \mu\text{mol}/\text{m}^2/\text{s}$ . The average incoming  $\text{PPFD}_0$  entering the water was  $366 \mu\text{mol}/\text{m}^2/\text{s}$  with a maximum incoming  $\text{PPFD}_0$  of  $1596 \mu\text{mol}/\text{m}^2/\text{s}$ .

The average amount of PAR that reached the surface of the water column in the 2014 summer field season in Strange Pond was  $399 \mu\text{mol}/\text{m}^2/\text{s}$  (Figure 12b). The maximum measured  $\text{PPFD}_0$  that was readily available was  $1796 \mu\text{mol}/\text{m}^2/\text{s}$ . When comparing the PPFD levels in the 2013 and the 2014 field seasons, the maximum, minimum and average levels of PAR are similar. Days with low incoming radiation indicate days of extended overcast conditions and/or precipitation. Peak times for  $\text{PPFD}_A$  occurred between the times of 12h to 14h (Figure 13).

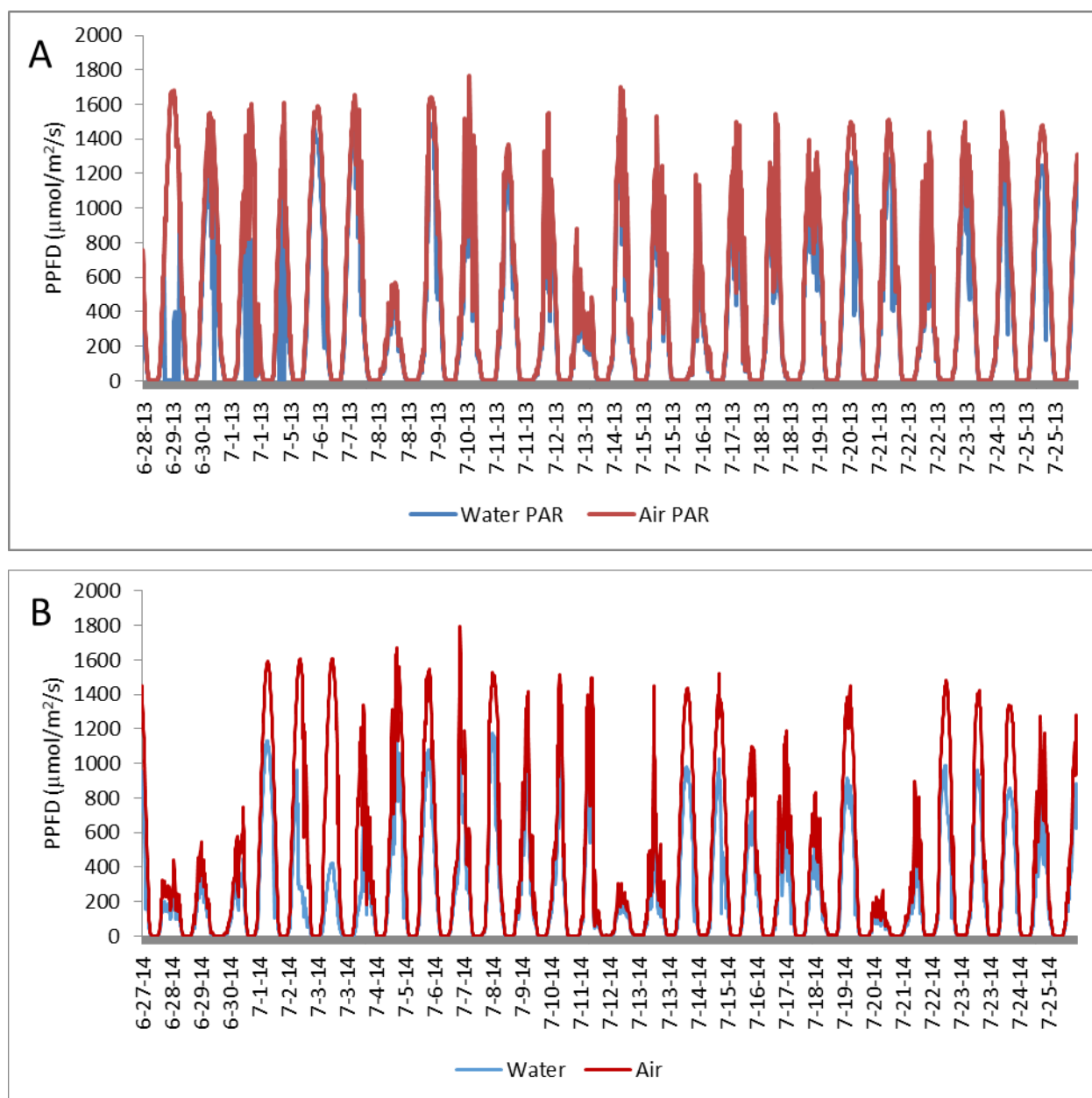


Figure 12: The incoming photosynthetic active radiation that reaches the top of the water column, and observed PAR reaching the sensor below the surface of Some Pond measured at an approximate depth varying between 10-15.0 cm in the 2013 (A) and 2014 (B) field season.

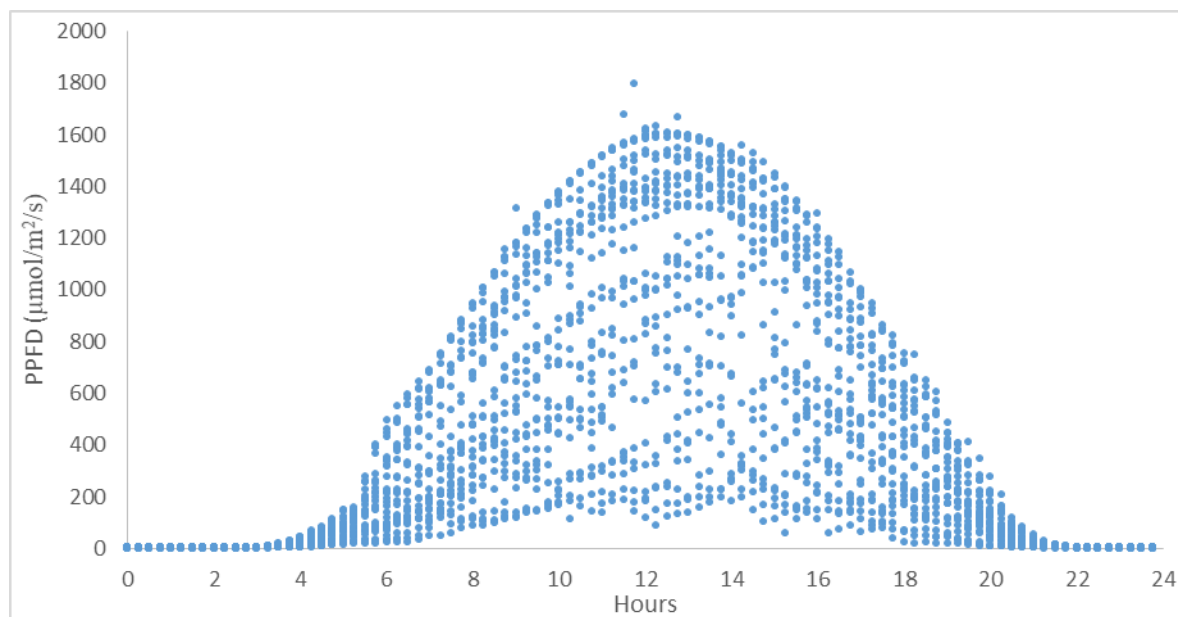


Figure 13: Example of the distribution of PPFD over the 2014 field season showing peak times occurring between the hours of 12 (12:00 p.m.) and 14 (2:00 p.m.).

### 3.1.2 Temperature patterns in the ponds in 2013 and 2014

The temperature of the ambient air and water column followed similar fluctuations at Some Pond (Figure 14) on a temporal scale. The closely related fluctuations are also observed in Strange Pond (Figure 15), where the air and water temperatures were shown to further impact the sediment temperature, following the same peaks and valleys but with a smaller magnitude. This will be important to note as air or water temperatures has the potential to be used to model respiration rates of the benthic algae.

In the 2013 field season, air temperatures near Some Pond fluctuated between 5.11°C and 31.50°C with an average of 13.40°C  $\pm$  4.78°C. The average temperature of the water in Some Pond was 16.00°C  $\pm$  3.07°C with a range of 8.95°C-23.69°C. The high heat capacity of the water delays the temperature fluxes of the air. Therefore, air temperature experiences fluctuations prior to the water column. Deviation of temperature within the water column is also smaller in comparison the measured air temperature indicating the stability water provides to the biota in the aquatic system, though they are shallow.

The 2014 field season provided an in-depth look at the temperature profile of Strange Pond. This included temperatures of the air, water, and sediment at 5 depths within the sediment in 2.0 cm

increments starting at 1.0 cm was plotted in Figure 15. The ambient air above the pond experienced larger changes in temperature in comparison to the water column and the sediment. The air had an average of  $13.06^{\circ}\text{C} \pm 5.35^{\circ}\text{C}$  with a range between  $3.42^{\circ}\text{C}$  and  $31.5^{\circ}\text{C}$ . The water had a higher average temperature of  $16.33^{\circ}\text{C} \pm 4.27^{\circ}\text{C}$  than that of the air. Due to the high heat capacity of water, the water column experienced a smaller range and deviation in temperature at  $5.52$  and  $28.26^{\circ}\text{C}$ . The water column serves to protect benthic algae, mitigating both PAR and air temperature fluctuations in the Hudson Bay Lowlands.

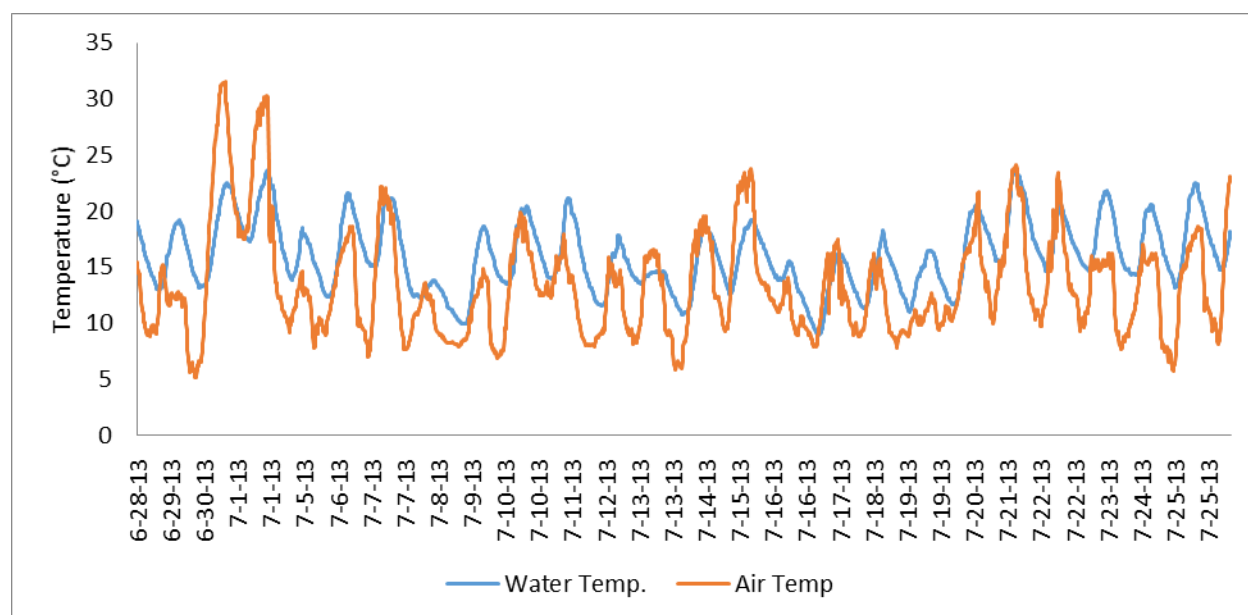


Figure 14: The fluctuation of water and air temperatures measured every 10 seconds and averaged every 15 minutes during the 2013 field season.

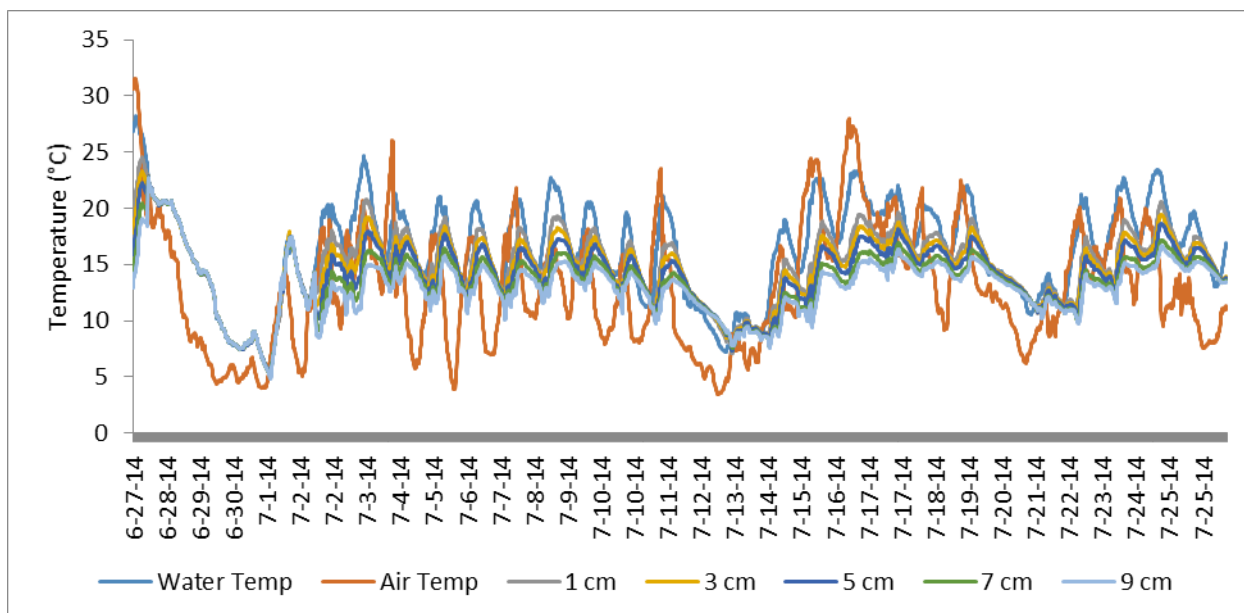


Figure 15: The temperature profile of the air, water column, and sediments measured every 10 seconds and averaged 15 minutes during the 2014 field season.

### 3.1.3 Water level fluxes in Strange Pond in 2014

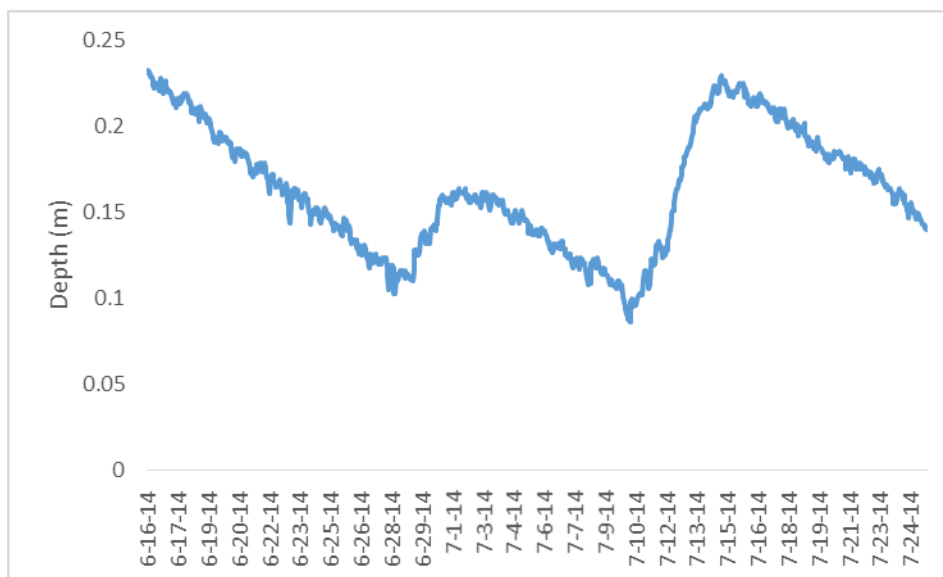


Figure 16: Recorded data of the average water level of Strange Pond, recorded every hour during the study period using data from a water level sensor.

Strange Pond water levels were measured over the 2014 field season. Figure 16 shows that Strange Pond experienced two major rainfall events from June 29 to July 1, and July 10 to July 14. The water depth at the beginning of the season was indicative of the snowmelt in late May and early June.

At this time the pond may be ephemerally connected to the surrounding catchment by shallow surface overland flow. The ponds in the HBL have the potential to desiccate as the inputs of water are limited to precipitation events. During the main growing season there were no inlets or outlets for the pond and it was essentially disconnected from the catchment except for potential groundwater connectivity.

The maximum average depth of Strange Pond is 22.3 cm, and the minimum average depth of Strange Pond during the study period is 8.6 cm. The small diurnal fluctuations exist due to daytime evaporative losses of water in Strange Pond with partial groundwater recovery overnight. Extended rain free periods are responsible for the major evaporative drawdowns in pond level.

#### 3.1.4 Cumulative precipitation in the 2013 and 2014 field seasons

Both field seasons saw infrequent precipitation events. Wet events are considered to be precipitation > 5.0 mm, and drought events are any day that has < 5.0 mm of precipitation (Macrae et al., 2004). Figure 17 illustrates the days of precipitation and the cumulative precipitation over the field season in 2013. The average daily precipitation was 0.20 mm indicating a very dry field season. The maximum rain event during the field season was 19.6 mm. The cumulative rainfall over the field duration was 363.30 mm. Major rain events on July 12, 2013 and July 15, 2013 helped saturate the environment for a short duration.

In comparison Figure 18 illustrates the cumulative rainfall in the 2014 field season with a cumulative rainfall of more than 600 mm. Major rain events occurred on June 30 and July 12, 2014. Rain events coincided with significant increases in the average water depth in Strange Pond. On June 30, the rainfall collected was 127 mm, and on July 12, significant rainfall up to 340 mm was observed. When comparing field seasons, the 2013 field season had more frequent wet days, but precipitation was heavier in the 2014 field season.



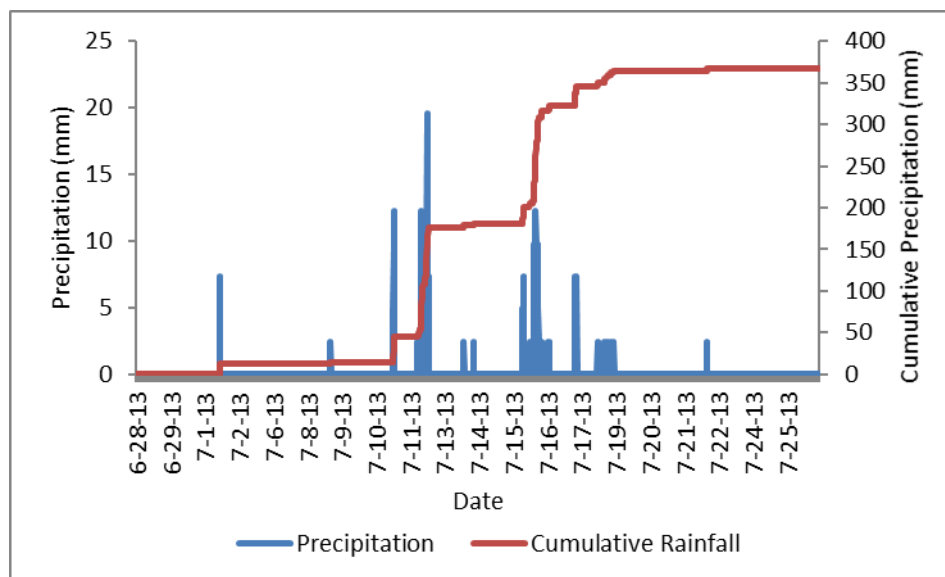


Figure 17: The daily and cumulative precipitation during the 2013 field season.

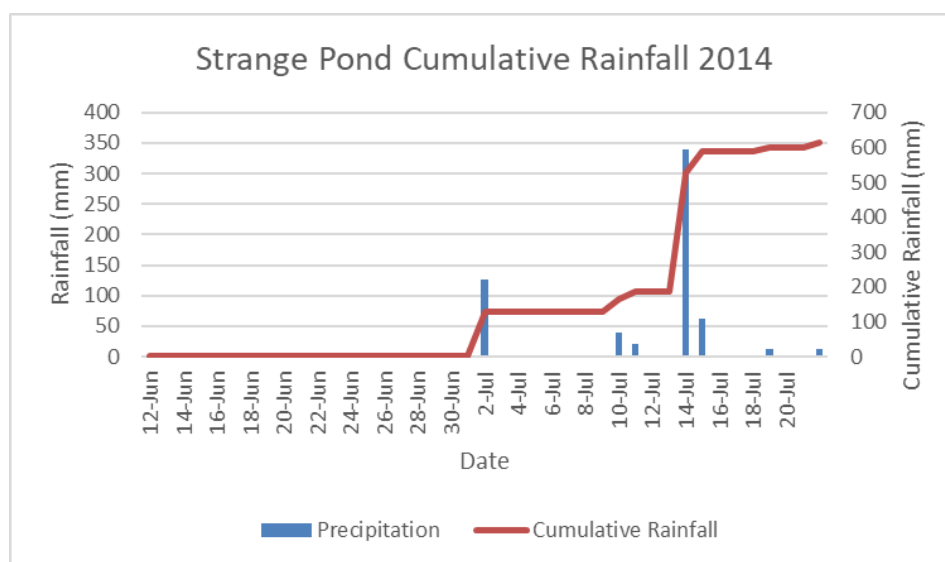


Figure 18: The daily and cumulative precipitation during the 2014 field season.

### 3.1.5 Wind velocity

Wind velocity throughout the 2013 field season is illustrated in Figure 19. The average wind speed during the field season was 3.11 m/s. The maximum wind speed was 9.27 m/s, and the lowest was 0.20 m/s (anemometer stall speed). The wind velocity was important in determining whether the shallow ponds are stratified or well mixed. Wind distribution has possible effects to the spatial patterns

of mixing in shallow ponds, as it affects fetch and therefore the spatial distribution of pelagic algae in the pond, as well as entrainment, deposition and burial of algae in the sediment in specific locations. The most frequent directions during the field season were northerly winds and westerly winds. There was very little influence from southerly winds as indicated in Figure 20.

Figure 21 illustrates the prominent wind direction during the 2014 field season. The most prominent wind directions during the 2014 field season were northerly and south-easterly. Corresponding to the locations of the ponds studied, northerly winds originate from the Hudson Bay, and the south-easterly winds originated from inland. In both field seasons, the most prominent wind direction was from the north. Some Pond was unprotected on the western side as opposed to Strange Pond. Some Pond is out in the open, whilst Strange Pond is heavily protected on its eastern shore by white spruce.

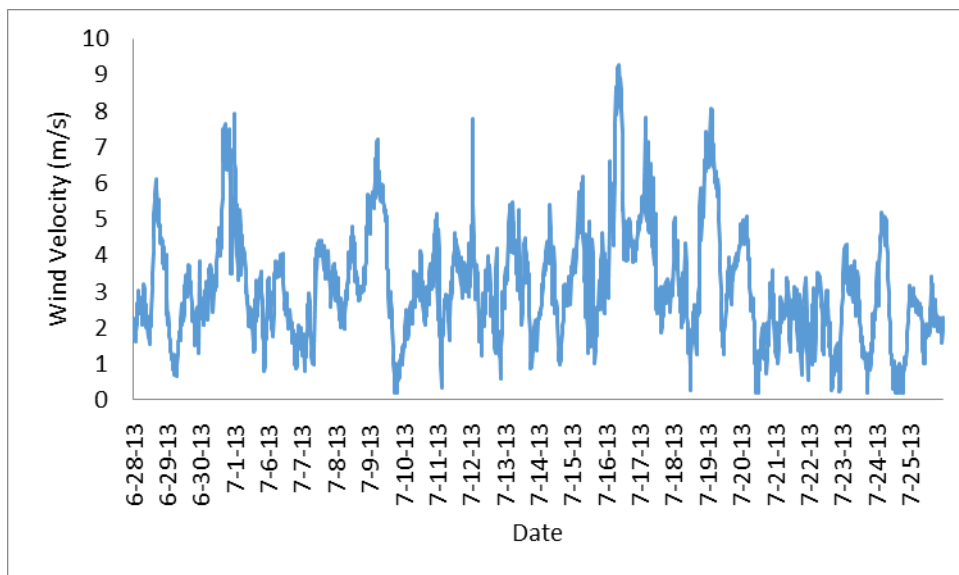


Figure 19: Wind velocity measured every 10 seconds and averaged every 15 minutes during the 2013 field season at 1 m.

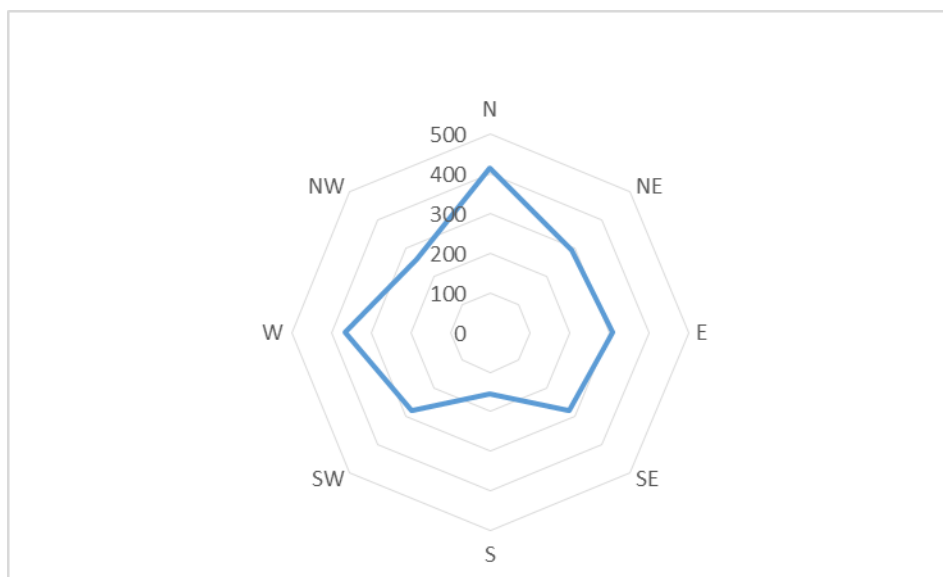


Figure 20: The wind distribution of wind by direction during the 2013 summer field season.



Figure 21: The frequency of wind direction during the 2014 field season.

### 3.1.6 Proportions of chlorophyll *a* concentrations

Table 2: Chlorophyll *a* concentration of each benthic algae type measured with the BenthosTorch in the 2014 field season.

	Cyanobacteria	Green Algae	Diatoms
Some Pond	63-73%	13-16%	11-23%
Strange Pond	48-58%	26-43%	21-43%
Left Pond	56-59%	31-37%	4-12%
Puddle Pond	39-48%	31-37%	14-30%

Regardless of whether the chlorophyll *a* concentrations were measured around the perimeter of the ponds or across a transect, there was one clear taxa that dominated, cyanobacteria. Chlorophyll *a* concentrations of Some Pond were collected across the pond in a transect in 10 m increments. Table 2 suggests that cyanobacteria dominated over both green algae and diatoms in all of the ponds. Cyanobacteria was particularly dominant in Some Pond. There were instances during the collection period in 2013 where diatoms experienced a small bloom dominating over green algae. Through statistical analysis using ANOVA, it was determined that the proportions of the average pond concentrations of cyanobacteria, green algae, and diatoms do not differ throughout the field season at a confidence level of  $p > 0.05$ . However, the average proportions at each sample location for all three taxa of algae were significantly different ( $p < 0.05$ ).

### 3.1.7 Spatial and temporal patterns of benthic algae of Some Pond in 2013

In Some Pond, using a Kruskal-Wallis test, it had been determined that benthic algae concentrations do not significantly change over time ( $p > 0.05$ ). However, by the change in depth over the length of the transect, it has been determined that benthic algae concentrations of cyanobacteria, green algae, and diatoms significantly differ from location to location ( $p < 0.05$ ). A large diatom increase was observed at sample location 8 on the west side of the pond (Figure 23). This event remains unexplained.

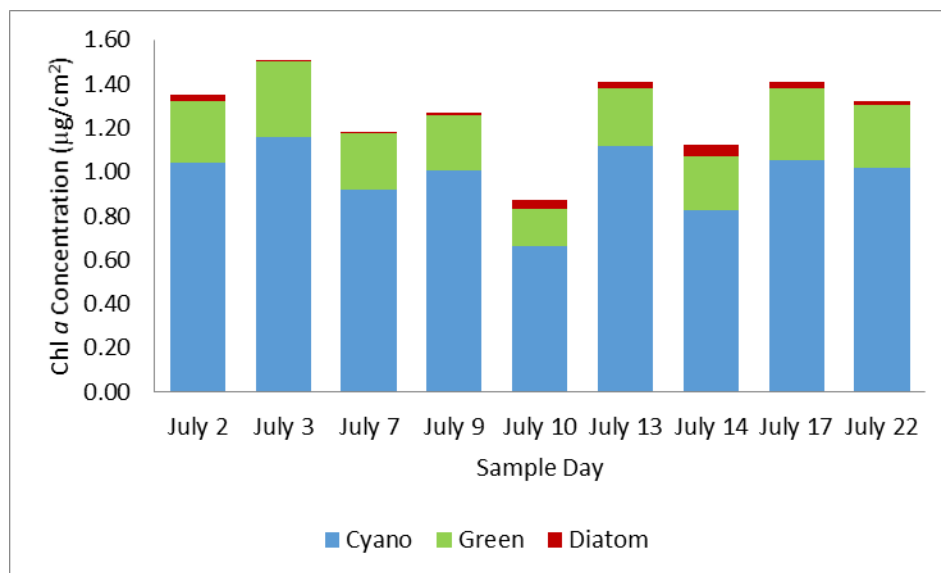


Figure 22: The average benthic algae concentrations in Some Pond for each sampling day.

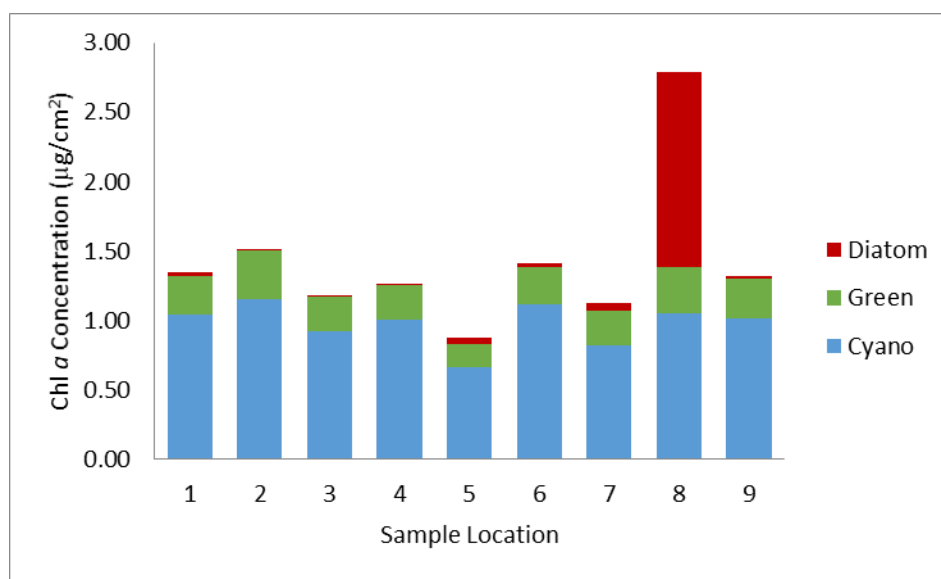


Figure 23: The seasonal average of each sampling location in Some Pond.

### 3.1.8 Comparing spatial and temporal patterns of the benthic algae in Some Pond in 2013 and 2014

The average chlorophyll *a* concentrations measured for each of the three taxa in Some Pond in 2013 and 2014 were similar. Collected in similar locations on the transect, it was found that the concentration of cyanobacteria (Figure 24), green algae (Figure 25), and diatoms (Figure 26) do not differ between the two years ( $p > 0.05$ ).

On June 30, Some Pond had the lowest average concentrations of all three benthic algae species (Figure 27). Through Kruskal-Wallis testing, the cyanobacteria and diatom temporal concentrations show no significant difference amongst sampling days ( $p > 0.05$ ). Green algae concentrations are significantly different among sampling days. When comparing the algal concentration of each sample location, there is no significant difference amongst the sampling locations ( $p > 0.05$ ). Cyanobacteria had a concentration of  $0.88 \mu\text{g}/\text{cm}^2$ , green algae has a concentration of  $0.70 \mu\text{g}/\text{cm}^2$  and diatoms had a concentration of  $0.14 \mu\text{g}/\text{cm}^2$ . On the last day of sampling in Some Pond, July 18 had the highest concentration of all three major taxa. Cyanobacteria had a concentration of  $1.28 \mu\text{g}/\text{cm}^2$ , green algae had concentration of  $0.29 \mu\text{g}/\text{cm}^2$ , and diatoms had a concentration of  $0.28 \mu\text{g}/\text{cm}^2$ .

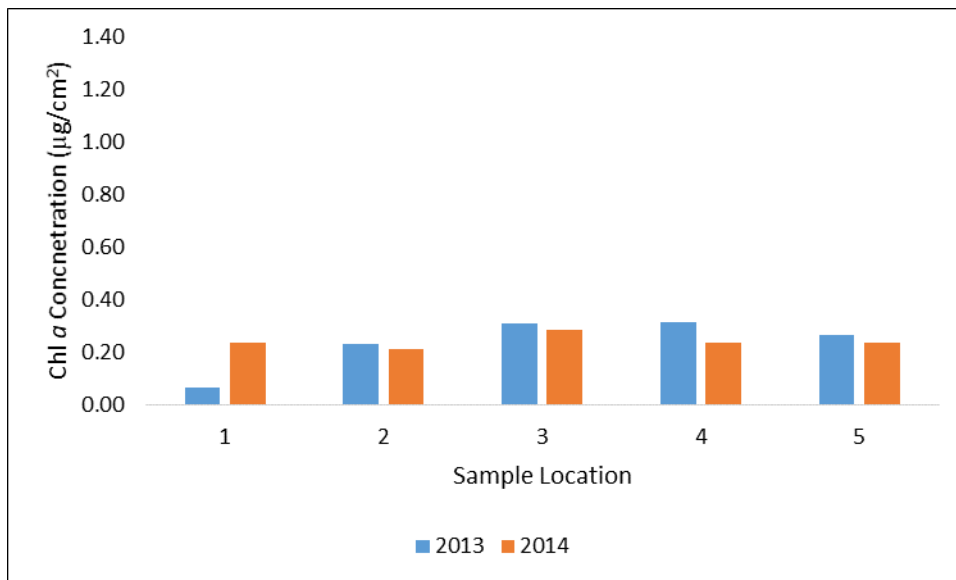


Figure 24: The concentration of benthic green algae in Some Pond in 2013 and 2014, with the x-axis indicating the sampling location along the transect.

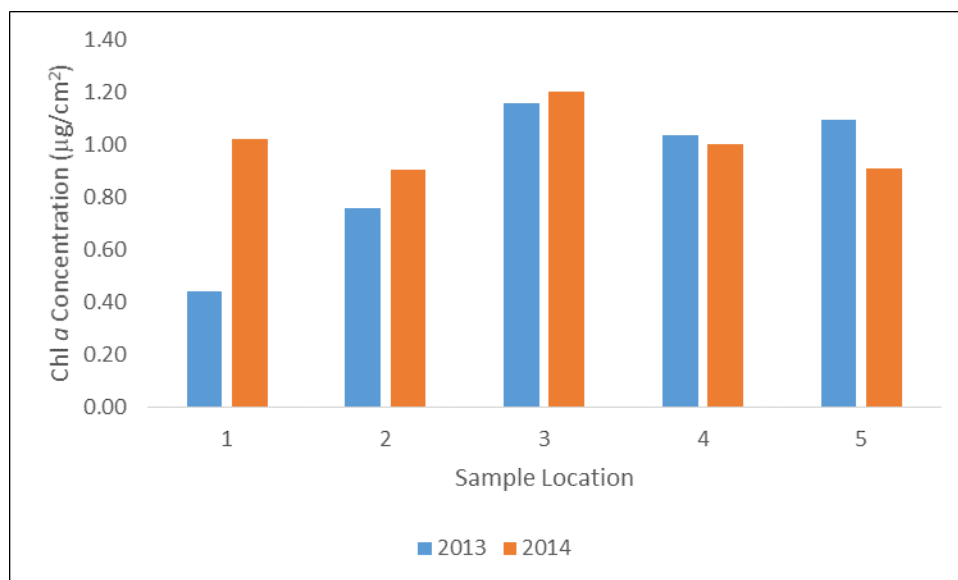


Figure 25: The concentration of benthic cyanobacteria in Some Pond in 2013 and 2014, with the x-axis indicating the sampling location along the transect.

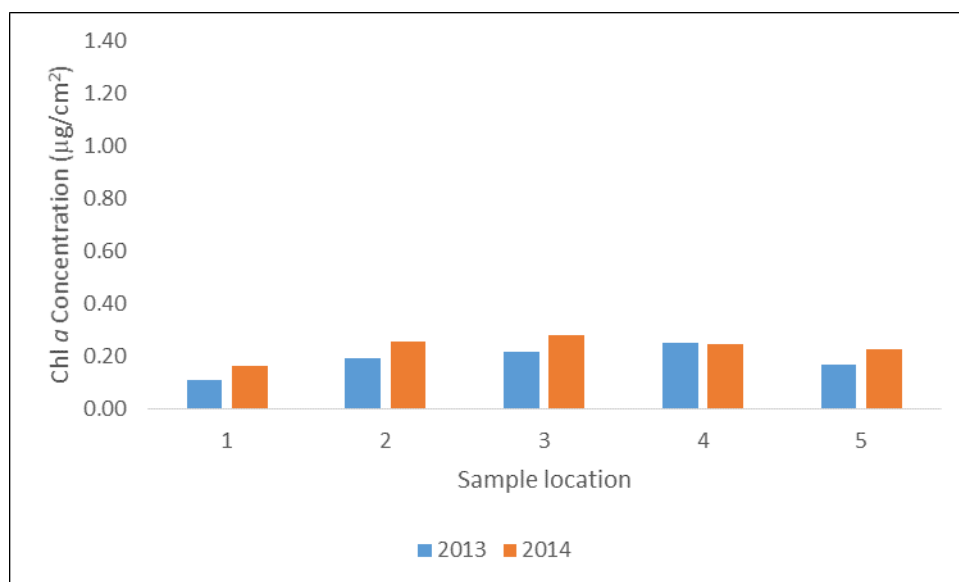


Figure 26: The concentration of benthic diatoms in Some Pond in 2013 and 2014, with the x-axis indicating the sampling location along the transect.

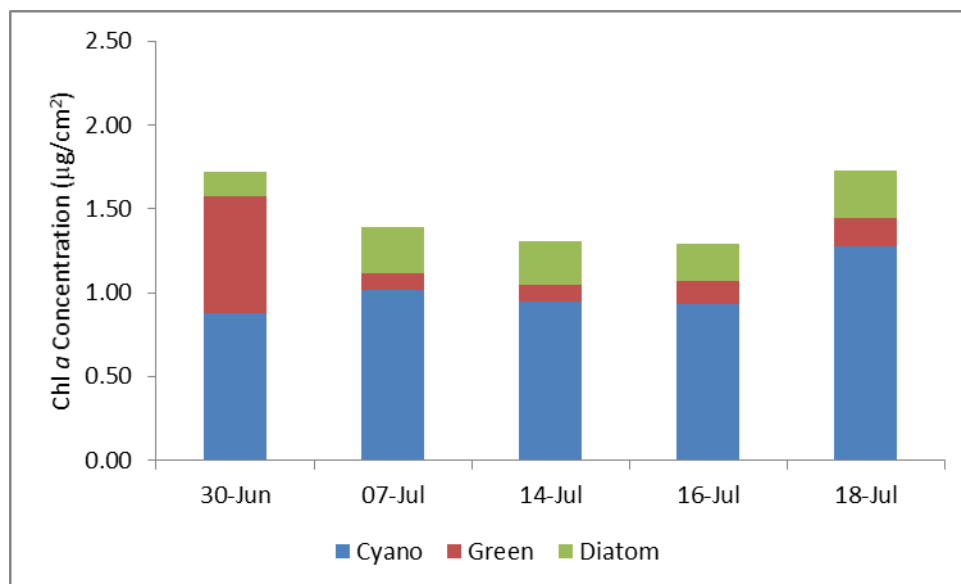


Figure 27: The benthic algae concentration of each algae type in Some Pond in 2014.

### 3.1.9 Temporal and spatial patterns of benthic algae in Strange Pond and Left Pond 2014

Spatial variability within the pond exists along the perimeter of the pond, but chlorophyll *a* concentrations for the three taxa do differ on a temporal scale. This pattern can be found for both Strange Pond and Left Pond when looking at cyanobacteria. As an established taxa on the sediment, changes may not occur within this specific taxa due to their dominance in the system. Figure 28 illustrated the benthic algae proportions of the seasonal averages in Strange Pond. Through Kruskal-Wallis testing, cyanobacteria and green algae show no significant difference amongst sampling days ( $p > 0.05$ ) and diatoms have a significant difference ( $p < 0.05$ ). Figure 29 illustrates the average benthic algae concentration on each sampling day. Statistically, average concentrations of green algae and diatoms within Strange Pond were significantly different when comparing concentrations of each type at each sampling location ( $p < 0.05$ ). For both Strange Pond diatoms concentrations varied on both a temporal and spatial scale, while the dominant cyanobacteria did not vary at all. For Left Pond, temporal variability existed for cyanobacteria. This may suggest that biotic processes that feed within the benthos, such as the growth of the algae, and decomposition are minimal or balance each other out depending on the taxa. Variability existed in different sampling locations for diatoms, even as a small pond like Left Pond. The spatial variability may exist due to a variety of reasons that will be further discussed.



When comparing cyanobacteria and green algae at each sample location in Left Pond (Figure 30), the concentrations of chl *a* show no significant difference amongst the sampling locations ( $p > 0.05$ ). The lack of spatial variability in the taxa may be influenced by the small size of Left Pond in comparison to Some Pond and Strange Pond. Diatom concentrations were significantly different ( $p < 0.05$ ), indicating that a blooming event during the sampling day. The average concentrations of cyanobacteria of each sampling day in Left Pond were significantly different ( $p < 0.05$ ), whilst changes in the green algae and diatom communities were insignificant ( $p > 0.05$ ). June 23 had the lowest concentrations of both cyanobacteria and green algae while June 16 had the lowest concentration of diatoms. July 9 had the highest concentration of both cyanobacteria and green algae with concentrations of  $1.18 \mu\text{g}/\text{cm}^2$  and  $0.54 \mu\text{g}/\text{cm}^2$  respectively, while in July 13, the highest concentration of diatoms with a concentration of  $0.19 \mu\text{g}/\text{cm}^2$ .

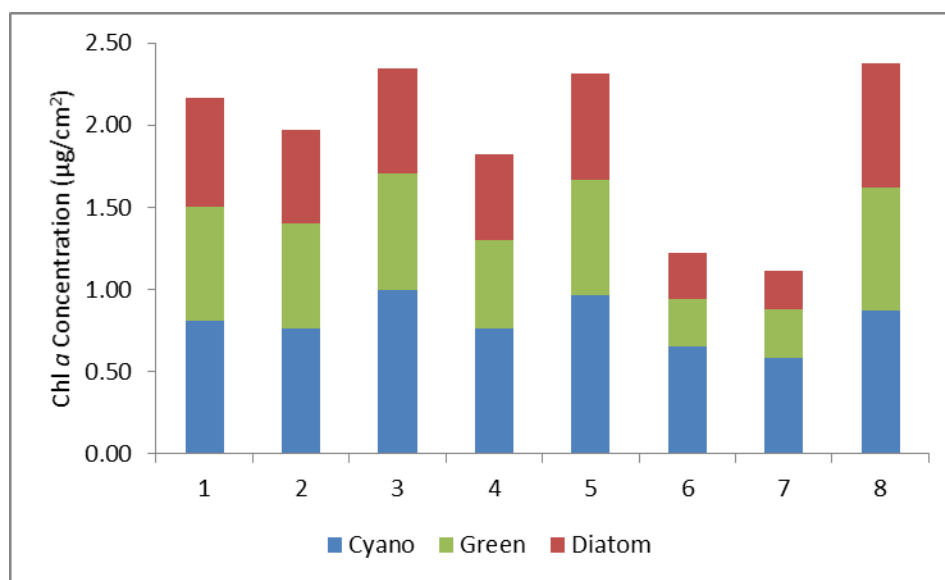


Figure 28: The average benthic algae concentrations of the three taxa in Strange Pond at each sample location.

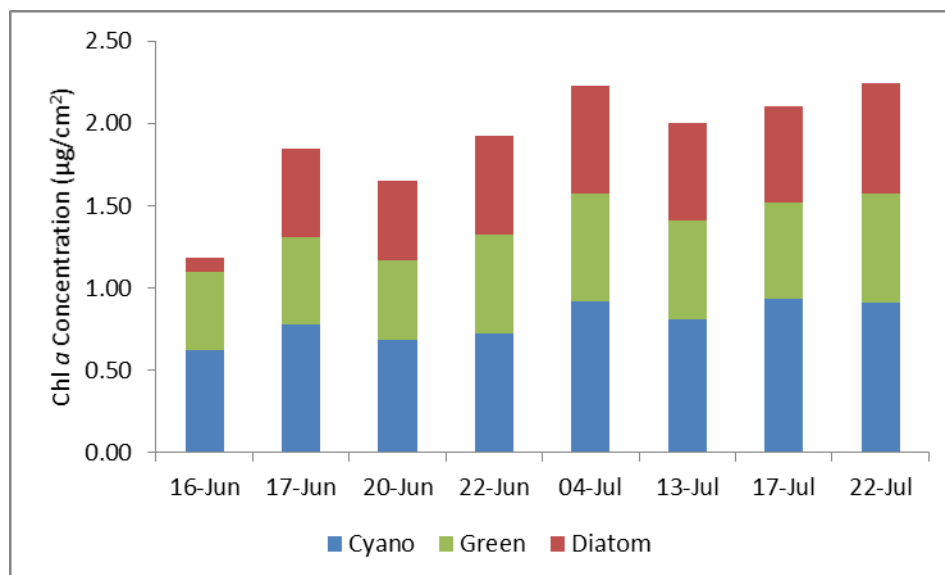


Figure 29: The average benthic algae concentrations of the three taxa in Strange Pond of each sampling day.

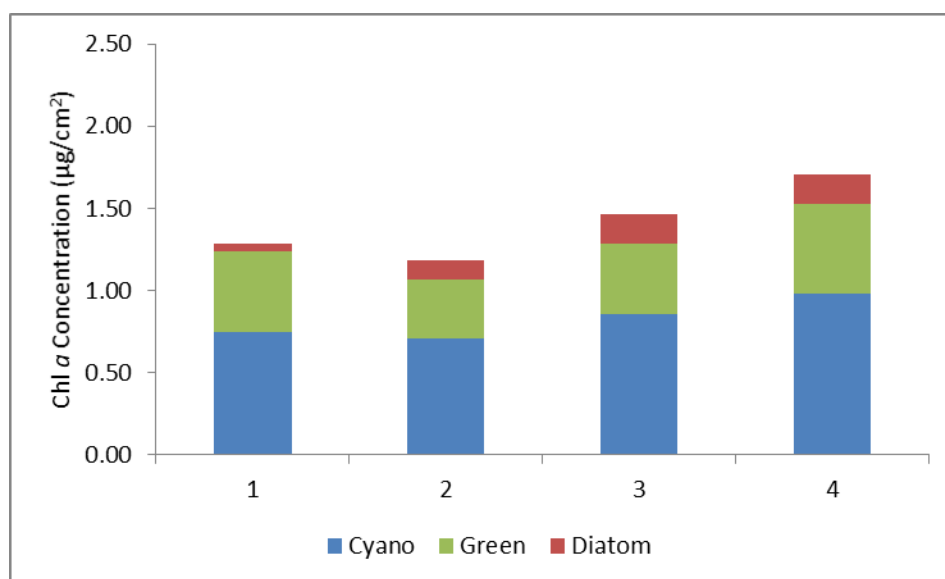


Figure 30: The average benthic algae concentrations of the three taxa in Left Pond at each sample location.

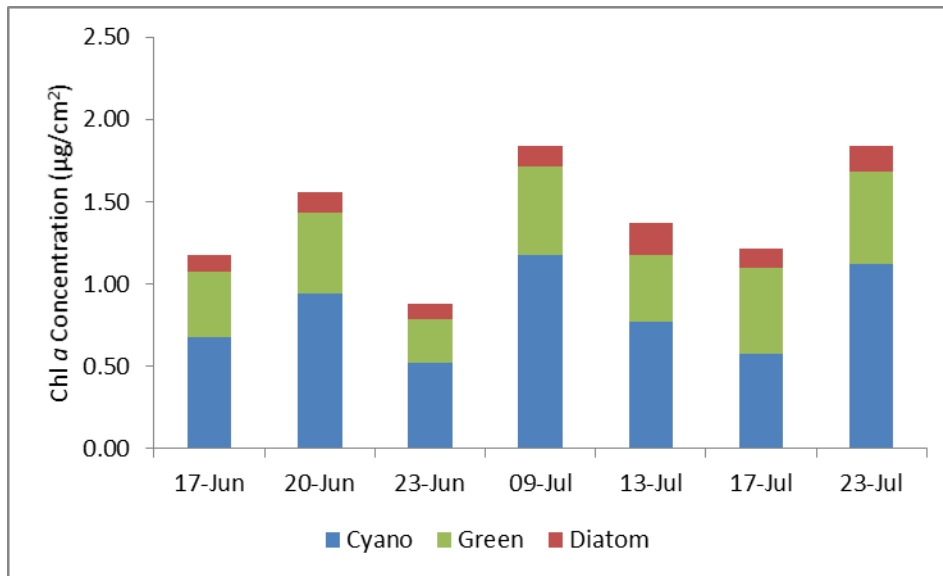


Figure 31: The average benthic algae concentrations of the three taxa in Left Pond of each sampling day.

### 3.1.10 Temporal and spatial patterns of benthic algae in a desiccated Puddle Pond 2014

In desiccated Puddle Pond, cyanobacteria was the dominant benthic taxa, exhibiting similar average concentrations amongst the sampling locations (Figure 33) ( $p < 0.05$ ). There was a significant difference when comparing the temporal average concentration of benthic cyanobacteria and green algae each sampling day (Figure 32) ( $p < 0.05$ ). The diatom concentration on the surface of the Puddle Pond insignificantly changed temporally ( $p > 0.05$ ) throughout the entire field season. However, the changes in chlorophyll *a* concentrations for cyanobacteria and green algae may indicate additional pressure of grazing from terrestrial invertebrates in the system. The changes in the taxa and the proportions may also indicate a transition from an aquatic phase to a drying phase.

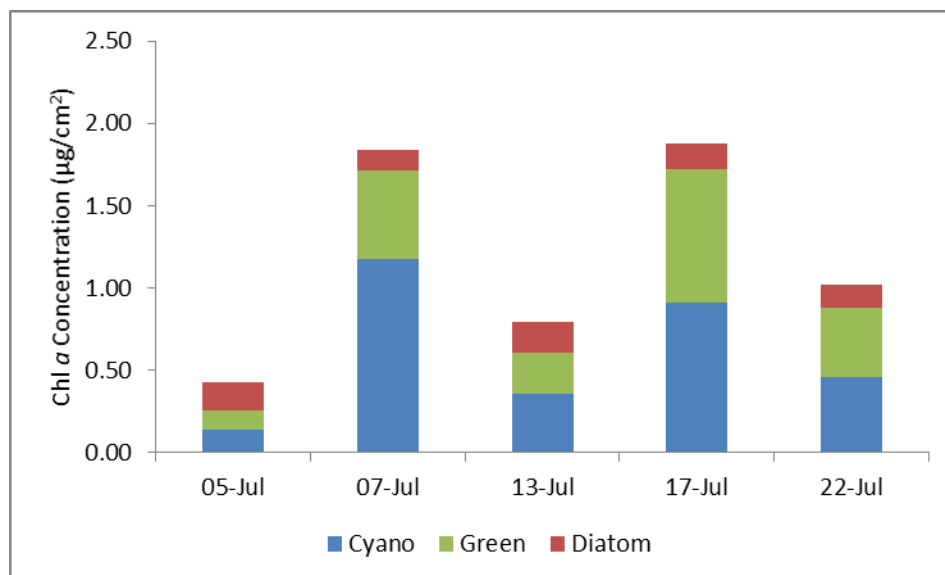


Figure 32: The average benthic algae concentrations of the three taxa in Puddle Pond at each sample location.

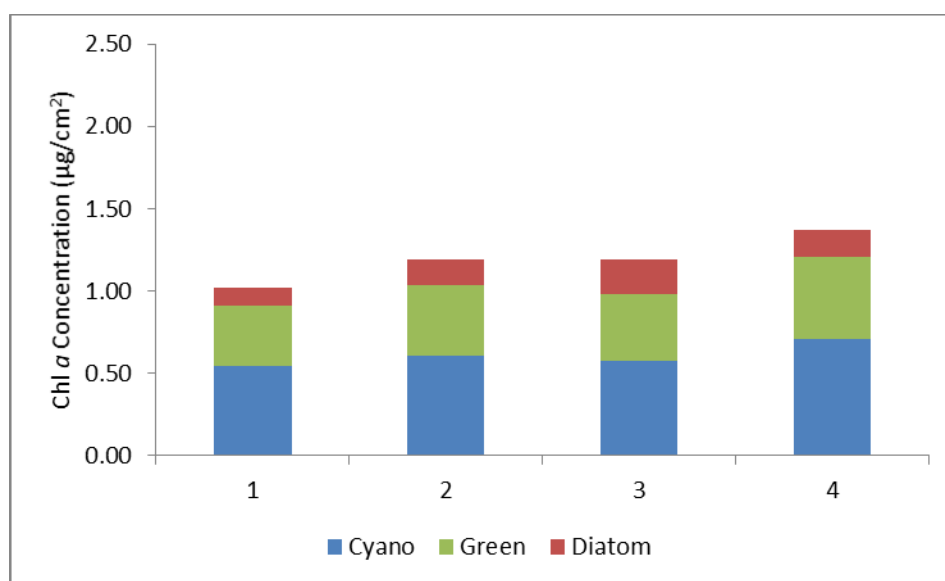


Figure 33: The average benthic algae concentrations of the three taxa in Puddle Pond of each sampling day.

3.1.11 Quantum efficiency of green algae in the top and bottom of the water column in Some Pond in 2013

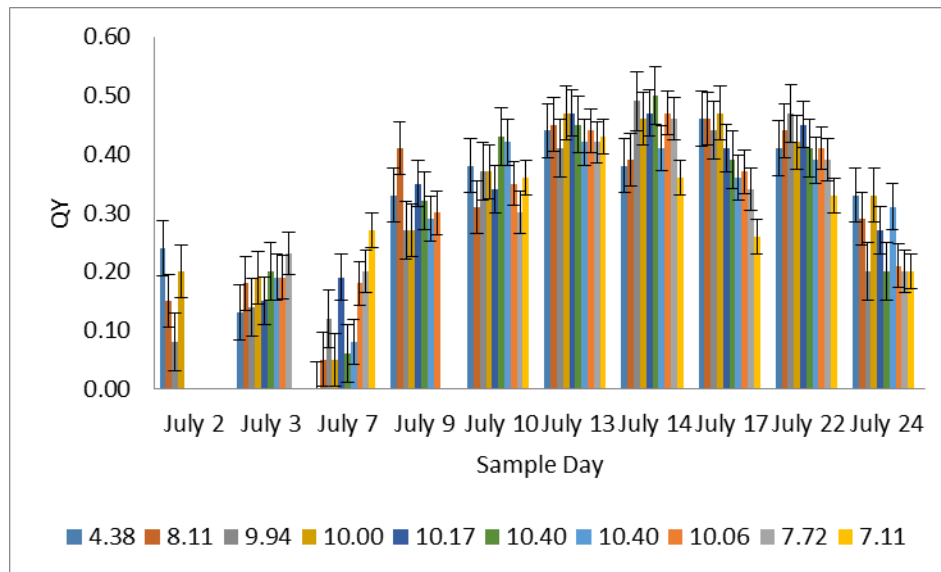


Figure 34: The temporal and spatial pattern of the quantum efficiency of the upper layer of the water column in Some Pond during the 2013 field season ( $n=91$ ). Each bar represents the sample location along the transect of Some Pond represented by the average depth at which the sample was taken of the top layer of the water column in cm. The error bars are the standard deviation of the average quantum efficiency measured.

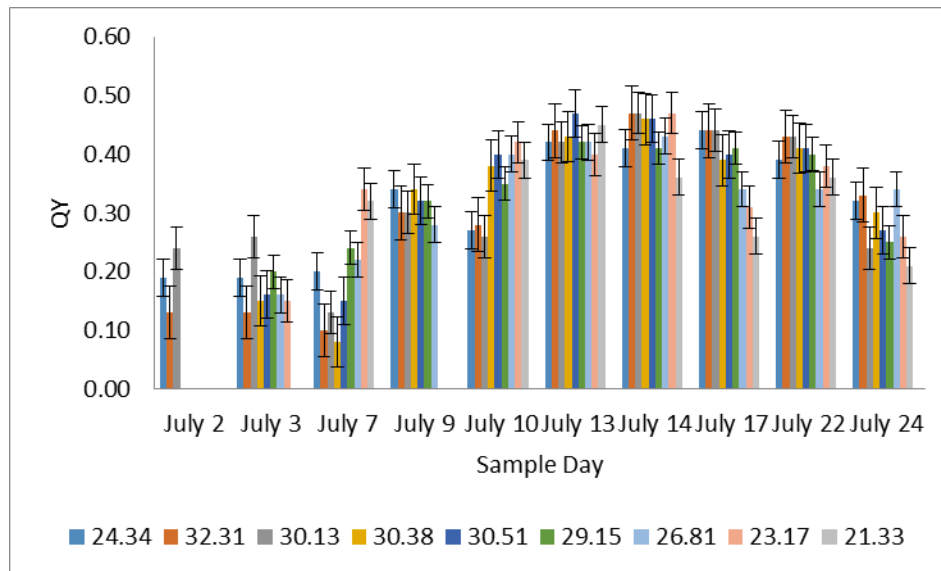


Figure 35: The temporal and spatial pattern of QY of the lower layer of the water column in Some Pond during the 2013 field season ( $n=81$ ). Each bar represents the sample location along the transect of Some Pond represented by the average depth at which the sample was taken of the bottom layer of the water column in cm. It is important to note that sample location 1 is omitted and defined as an upper layer due to very shallow depths. The error bars are the standard deviation of the average quantum efficiency measured.

There was an interesting development in the quantum efficiencies that were measured over the 10 sample days in July. The quantum efficiencies of the pelagic algae seem to peak mid-July, and drop off towards the end of the sampling week. Both the upper and bottom layers at each sample location experience a similar temporal pattern. In the first week of July, the quantum efficiency of the green pelagic algae did not surpass 0.40. Quantum efficiencies steadily increased later into the month of July. Both the quantum efficiencies of the upper and bottom layers of the water column in Some Pond experience an increasing trend surpassing the quantum efficiency of 0.40.

Quantum efficiency was an important indicator of how the phytoplankton in the water column of Some Pond responded to the intense sunlight in the Subarctic and how efficiently the phytoplankton converted carbon dioxide into oxygen through photosynthesis. Quantum efficiencies of cyanobacteria in the water column were too low for the Aqua Pen to measure, thus only measurements of green pelagic algae are available. The quantum efficiencies of the green pelagic algae in the upper layer of the water column (Figure 34) had no significant difference with the quantum efficiencies of the green pelagic algae in the bottom layer (Figure 35). Using ANOVA, there was a significant difference between the temporal changes of  $Q_y$  for both the top and bottom of the water column ( $p < 0.05$ ). The highest average  $Q_y$  values of the top of the water column is 0.44, measured on July 13 and July 14, 2013. The highest average  $Q_y$  measured of the bottom of the water column is 0.44, which was also measured on July 14, 2013.

#### 3.1.12 Limnological properties of Some Pond 2013 and 2014

In a mixed water column, there were no apparent changes in the pH levels measured at different depths and locations of the pond. In the sampling protocol, the water column of Some Pond was divided into an upper and bottom layers to identify if Some Pond had a hypolimnion or is well mixed by assessing the pH. Through the analysis of a Wilcoxon test, the mean pH of the upper part of the water column and the bottom of the water column (Figure 36) were not significantly different ( $p > 0.05$ ). Using a Kruskal-Wallis test identified that there was a significant difference between the day to day variations of the pH in both the upper and lower part of the water column ( $p < 0.05$ ). However, variations did not exist spatially ( $p > 0.05$ ). The upper and bottom layers experienced a difference in the seasonal average pH at each sample location. Each sample location experienced little deviation of pH amongst each sampling day in both layers of the water column. Sample location 1 had a shallow depth

and experienced significant wave action to differentiate a top layer and a bottom layer. Sample location 1 had a lower pH in comparison to the other sample locations.

Using Wilcoxon analysis had shown that the pH values at top and bottom layers of each sample location of Some Pond (Figure 37) were not significantly different ( $p > 0.05$ ). However, when comparing the average pH of the upper and bottom layers of Some Pond, the values of pH were not significantly different ( $p > 0.05$ ). Seasonal average of pH values in Some Pond differ from the spatial averages. Both the average pH of each sample day in the upper and bottom layers were significantly different with a  $p < 0.05$  (Figure 38). However, when comparing seasonal average of the upper and bottom layer of Some Pond, the pH values were not significantly different ( $p > 0.05$ ) The drop in pH on July 13, corresponds with precipitation events indicated in Figure 16.

DO concentrations were higher along the shore line, where predominant winds have the ability to mix the water with  $O_2$  from the atmosphere. Analysis had also shown that the pond averages of DO at each sample location of the upper and bottom layers of the water column were significantly different from one another with a  $p < 0.05$  (Figure 39). When comparing the pond averages of the upper and bottom layer of Some Pond as a whole, there were significant differences ( $p < 0.05$ ).

The DO concentration of each sampling day of the upper layer of the water column in Some Pond suggests that there was significant difference with a  $p < 0.05$  (Figure 40). However, the seasonal average DO concentration of the bottom layer of Some Pond suggests that there was a significant seasonal change ( $p < 0.05$ ). Comparing the seasonal averages of DO concentration values of the upper and bottom layer of Some Pond show that there was a significant difference between the upper and bottom layers ( $p < 0.05$ ). Consistency within the top layer of the water column in Some Pond indicated constant or an even amount of interaction with the atmosphere, whereas the variability within the bottom of the water column is an indicating of the interactions with the sediment and benthos.

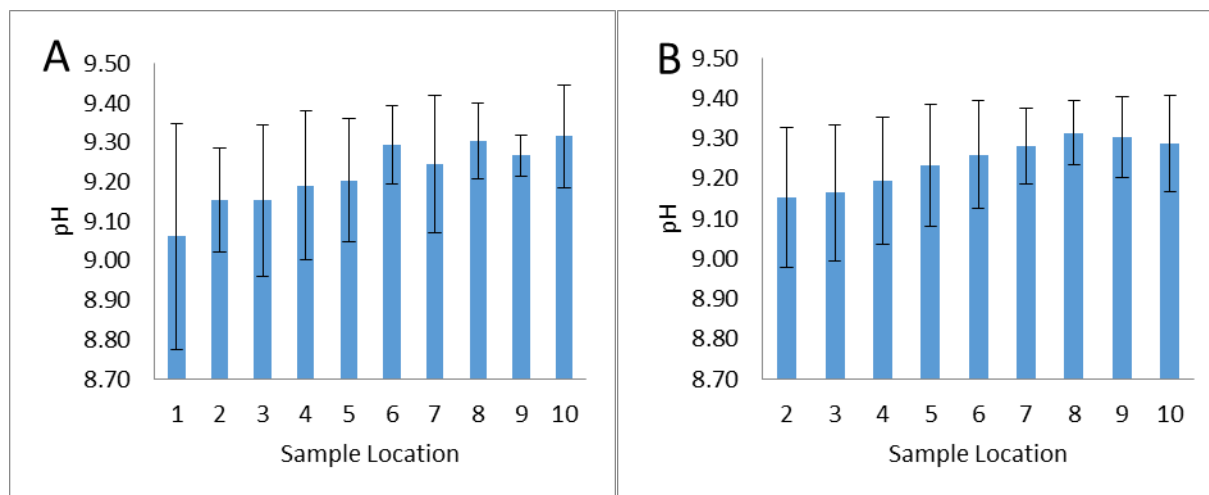


Figure 36: The seasonal average of pH of the upper (A) and bottom (B) layer of the water column in Some Pond during the 2013 summer field season. It is important to note that sample location 1 is omitted and represented as the top layer of the water column only.

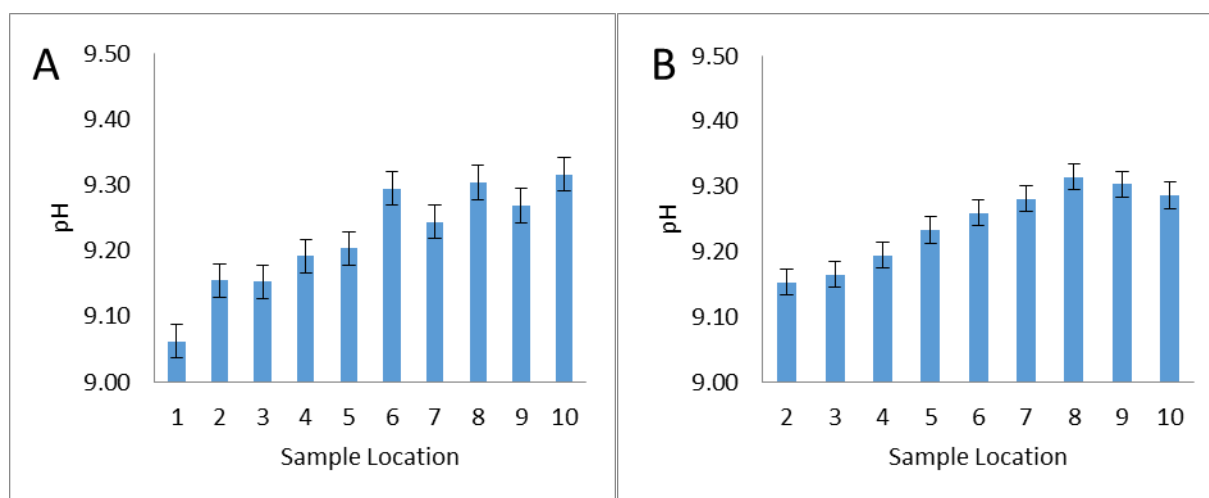


Figure 37: Spatial pattern of average pH levels of the top layer (A) and bottom layer (B) of the water column of each sampling location in Some Pond in 2014.



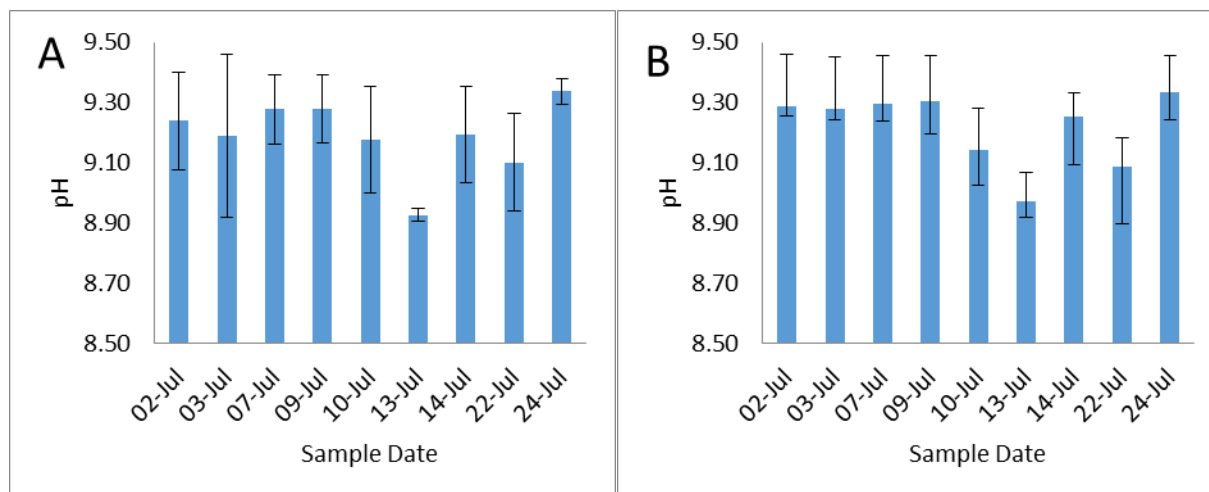


Figure 38: Temporal pattern of average pH levels of the top layer (A) and bottom layer (B) of the water column of each sampling location in Some Pond in 2014.

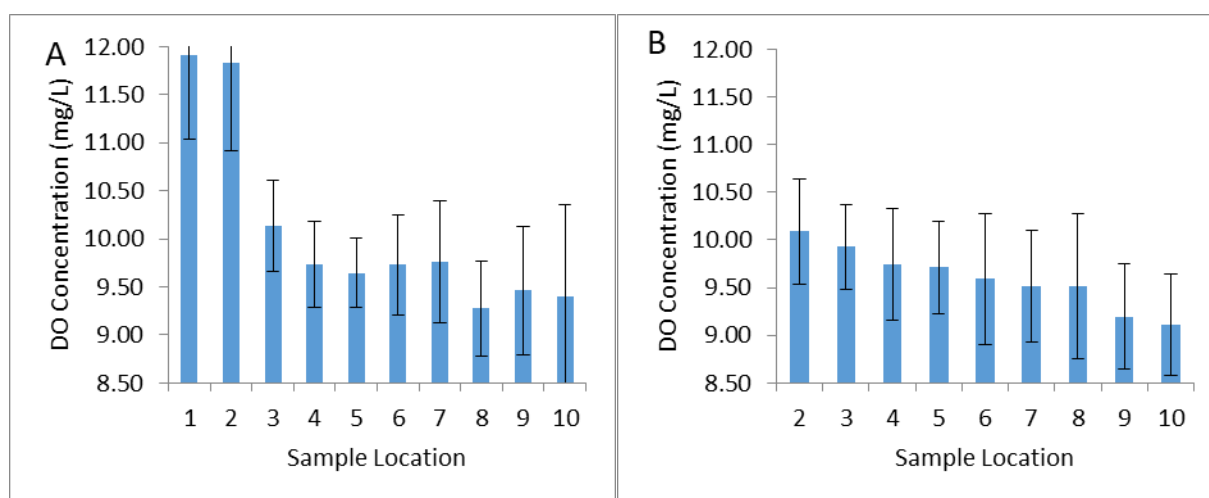


Figure 39: Spatial pattern of average dissolved oxygen concentrations of the top layer (A) and bottom layer (B) of the water column of each sampling location in Some Pond in 2014.

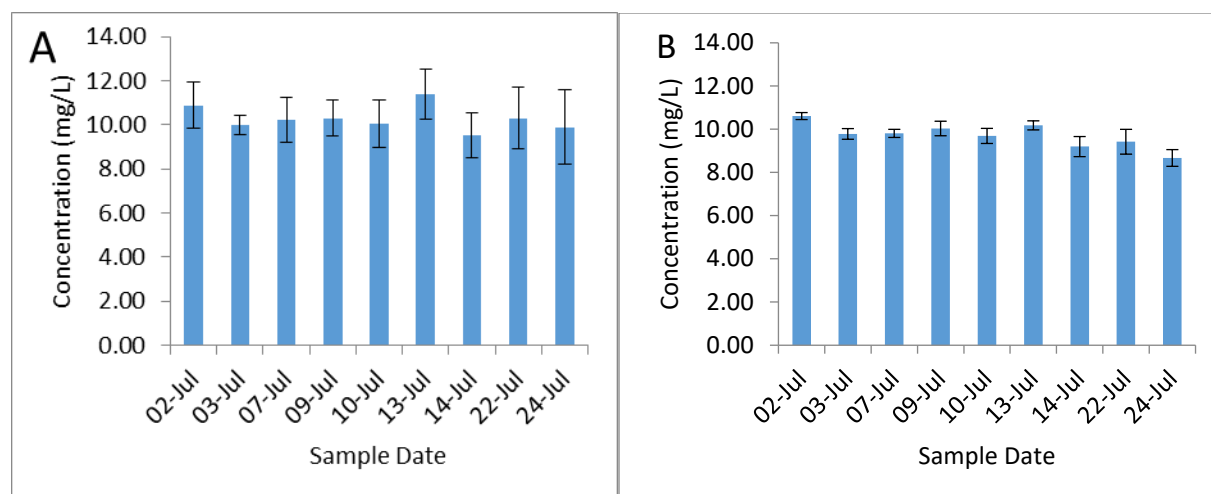


Figure 40: Temporal pattern of average DO concentrations of the top layer (A) and bottom layer (B) of the water column of each sampling location in Some Pond in 2014.

### 3.1.13 Measured abiotic variables of the ponds

Table 3: The average seasonal limnological and biological characteristics of the water column at each sample location of Some Pond in 2013.

Sample Location	Depth Avg	Depth stdev	pH Top	pH Bot	DO Top (mg/L)	DO Bot (mg/L)	SpCond Top ( $\mu\text{S}/\text{cm}$ )	SpCond Bot ( $\mu\text{S}/\text{cm}$ )	QY Top	QY Bot	OD Top Green Algae	OD Bot Green Algae
1	8.54	2.29	9.06		11.91		-		0.31		0.0000	0.0000
2	31.79	2.12	9.15	9.15	11.83	10.02	2.30	2.53	0.31	0.32	0.0000	0.0261
3	40.25	1.97	9.15	9.16	10.13	9.84	8.80	11.07	0.30	0.31	0.0036	0.0121
4	40.25	1.71	9.19	9.19	9.73	9.63	3.48	6.93	0.32	0.32	0.0019	0.0024
5	40.45	2.39	9.20	9.23	9.65	9.60	1.84	2.63	0.34	0.33	0.0000	0.0031
6	40.91	2.38	9.29	9.26	9.73	9.47	2.59	5.19	0.33	0.34	0.0009	0.0034
7	38.86	4.03	9.24	9.28	9.76	9.42	1.29		0.32	0.33	0.0183	0.0011
8	35.78	1.30	9.30	9.31	9.27	9.51	1.54	2.71	0.32	0.33	0.0017	0.0000
9	30.89	1.76	9.27	9.30	9.46	9.20	1.76	1.43	0.32	0.34	0.0038	0.0000
10	28.44	1.94	9.32	9.29	9.40	9.11	1.57	2.24	0.32	0.34	0.0011	0.0029
Average	33.62	2.19	9.22	9.24	10.09	9.53	2.8	6.69	0.32	0.33	0.0031	0.0057
STDEV	9.92	0.73	0.08	0.06	0.97	0.28	2.35	7.68	0.01	0.01	0.0055	0.0085

Table 4: The limnological and biological characteristics of the water column of each sample location in Strange Pond in the summer field season of 2014.

Sample Location	Depth Avg	Depth stdev	WMD	pH	DO (mg/L)	SpCond (uS/cm)	QY	OD Green Algae	OD Cyanobacteria
1	30.20	8.81		9.60	10.05	279.84	0.19	0.0020	0.0015
2	33.20	17.57		9.77	8.84	257.07	0.20	0.0001	0.0000
3	22.60	4.56		9.36	8.94	269.88	0.24	0.0000	0.0000
4	21.60	1.64		9.85	9.33	269.20	0.24	0.0000	0.0001
5	15.90	5.54		11.64	11.16	278.53	0.24	0.0021	0.0000
6	26.80	2.66		10.92	10.87	237.03	0.18	0.0031	0.0000
7	25.50	3.35		11.58	10.80	235.93	0.22	0.0006	0.0009
8	28.50	3.84		10.13	10.90	259.73	0.20	0.0000	0.0000
Pond Avg	25.54	6.00	0.17	10.36	10.11	260.90	0.21	0.0012	0.0003
STDEV	5.45	5.15		0.90	0.96	17.02	0.03	0.0010	0.0006

Table 5: The limnological and biological characteristics of the water column of each sample location in Left Pond in the summer field season of 2014.

Sample Location	Depth Avg	Depth stdev	WMD	pH	DO (mg/L)	SpCond (uS/cm)	QY	OD Green Algae	OD Cyanobacteria
1	11.70	2.91		9.64	11.41	NIL	0.12	0.0000	0.0004
2	19.50	2.29		NIL	11.04	188.78	0.16	0.0033	0.0041
3	30.70	2.95		9.57	10.97	336.80	0.16	0.0065	0.0000
4	23.30	4.38		8.90	10.89	216.33	0.14	0.0018	0.0034
Pond Avg	21.30		0.10	10.10	11.08	191.73	0.15	0.0029	0.0020
STDEV	7.91			1.51	0.23	128.40	0.02	0.0027	0.0021

Table 6: The limnological and biological characteristics of the water column of each sample location in Some Pond in the summer field season of 2014.

Sample Location	Depth Avg	Depth stdev	WMD	pH	DO (mg/L)	SpCond ( $\mu\text{S}/\text{cm}$ )	QY	OD Green Algae	OD Cyanobacteria
1	19.83	2.93		9.60	10.06	352.25	0.32	0.0000	0.0026
2	49.17	1.76		9.63	10.37	340.65	0.29	0.0063	0.0049
3	48.17	4.54		9.53	10.70	403.92	0.28	0.0000	0.0070
4	50.67	4.16		9.45	12.61	400.50	0.3	0.0005	0.0000
5	50.00	5.57		9.50	10.46	399.33	0.27	0.0000	0.0030
Pond Average	43.57	3.79	0.19	9.54	10.84	379.33	0.29	0.0014	0.0035
STDEV	13.30	1.48		0.07	1.02	30.34	0.02	0.0028	0.0026

Kruskal-Wallis statistical analysis showed that the limnological characteristics the specific conductivity, pH, and dissolved oxygen values in Strange Pond (Table 4) did not vary from sample location to sample location ( $p > 0.05$ ). Both the optical densities of green algae and cyanobacteria also had no significant difference ( $p > 0.05$ ). Strange Pond was the only pond studied that had a significant difference in the quantum efficiency from location to location with a 95% confidence level. From Table 5, the values for Left Pond suggest that there were no significant differences in both limnological and biological characteristics between sample locations all analyzed with a confidence level of 95%. Sample location 1 had a specific conductivity of  $25.00 \mu\text{S}/\text{cm}$ , much lower than the pond average of  $191.73 \mu\text{S}/\text{cm}$ . As a small pond, many of its limnological variables such as the pH and the dissolved oxygen are thoroughly mixed throughout the pond area.

Similar to the biological and limnological characteristics of Left Pond, there were no significant differences in the characteristics in the water column of each sample location in Some Pond (Table 6). This is with a confidence level of 95%. The mean pH and dissolved oxygen concentration throughout the water column had a standard deviation of  $\pm 0.07$  and  $\pm 1.02$  respectively, indicating that from a shallow depth of 19.0 cm to the middle of the pond, was well mixed. Even the low deviation on the specific conductivity of the water, which is a measure of total dissolved solids, suggests and well mixed water system.

### 3.1.14 Assessing the quantum efficiency of the pelagic algae in the summer field season of 2014

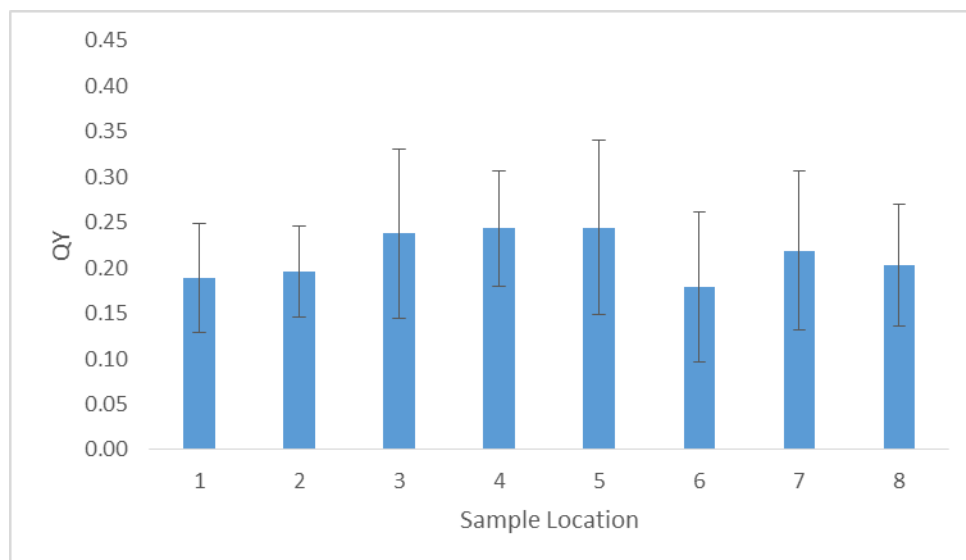


Figure 41: The temporal pattern of the measured quantum efficiency in Strange Pond in 2014.

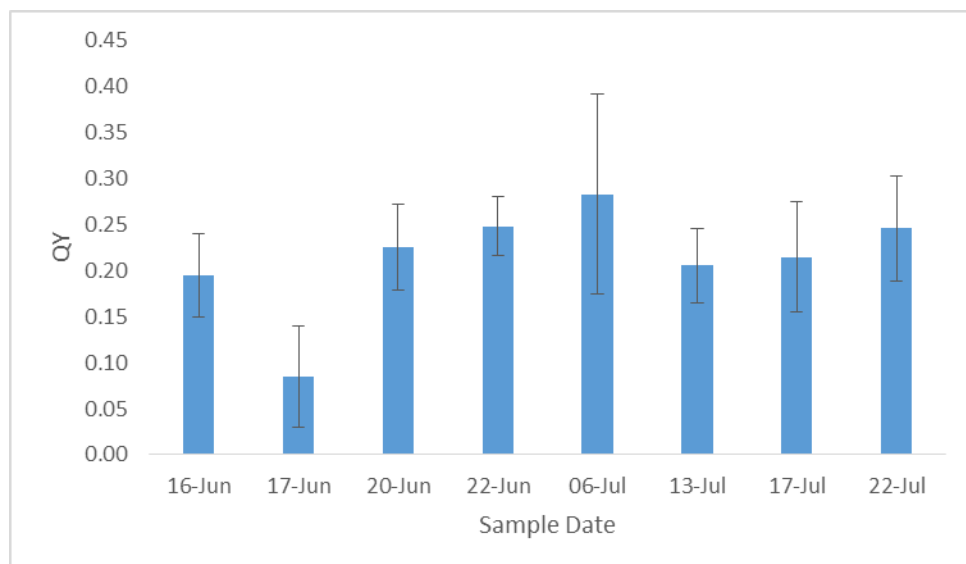


Figure 42: Spatial pattern of the quantum efficiency measured in Strange Pond in 2014.

The average spatial quantum efficiency (Figure 41), through Kruskal-Wallis testing, was significantly different ( $p < 0.05$ ) amongst sampling locations. When looking at Figure 42, an anomaly occurs on June 17, in which the average quantum efficiency is 0.08. The average quantum efficiency amongst the different sampling locations was not significantly different ( $p > 0.05$ ), also indicating that sampling conditions and location are important in understanding and studying algae in ponds. The range

of the measured average quantum efficiency in the 8 sample locations was between 0.18 and 0.24. Therefore, external and internal factors drive the daily quantum efficiencies. The overall weak nature of the pelagic algae in the water column may suggest that significant primary productivity occurred somewhere else within the ponds rather than in the water column.

The quantum efficiencies measured in Left Pond indicate that there was a significant difference in the temporal pattern of the green algae ( $p < 0.05$ ) (Figure 43). Similar to Strange Pond, on June 22, Left Pond experienced a decrease in the average  $Q_y$  with a value of 0.05. On the same day Strange Pond had an average  $Q_y$  of 0.25. The average quantum yields amongst the sampling locations did not significantly differ ( $p > 0.05$ ) (Figure 44). The range of the average  $Q_y$  value in Left Pond sampling locations is between 0.12-0.16. Reminiscent of the bell shaped curve that was measured in Some Pond in the 2013 field season (Figure 43), both Strange Pond and Left Pond have a similar shape, peaking between July 6 and July 9, 2014. In the 2013 field season, the  $Q_y$  values of the pelagic algae in the water column peaked between July 13 and July 14.

There was evidence of weak temporal variability ( $p > 0.05$ ) in the  $Q_y$  of the pelagic green algae in Some Pond (Figure 45). The average temporal quantum yields ranged between 0.27 and 0.31. These values are higher than that of Strange Pond and Left Pond. Unlike Some Pond in 2013, and Strange Pond and Left Pond in 2014, the quantum yields did not appear to follow a bell-shaped curve during the 2014 summer field season. In Figure 46, the average  $Q_y$  of the pelagic algae at each of the 5 sample locations in Some Pond were significantly different ( $p < 0.05$ ). Sample location 1 had a higher  $Q_y$  compared to the central locations of Some Pond. Statistically, when comparing the  $Q_y$  of the green algae present at each of the ponds, values are similar ( $p > 0.05$ ).

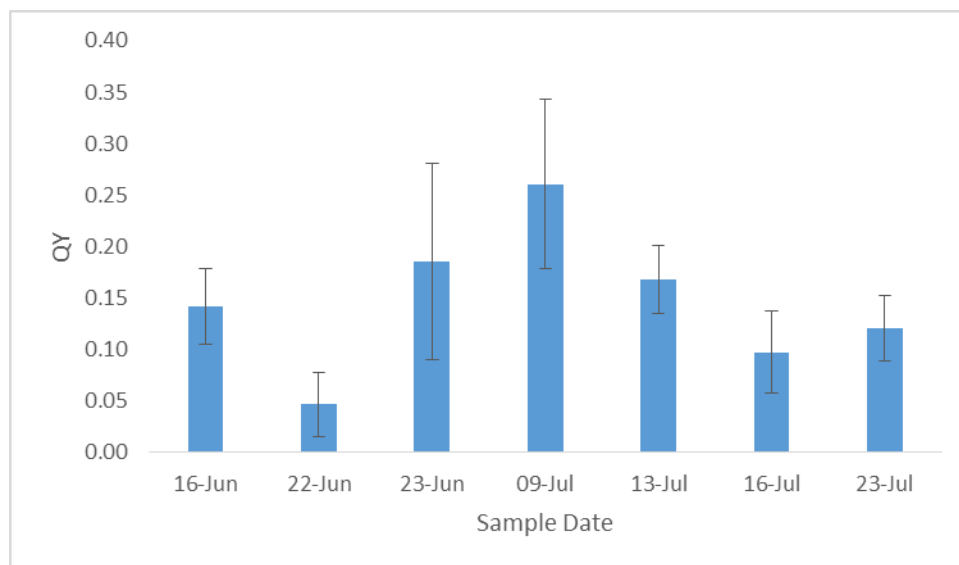


Figure 43: Temporal pattern of the quantum yield in Left Pond in 2014.

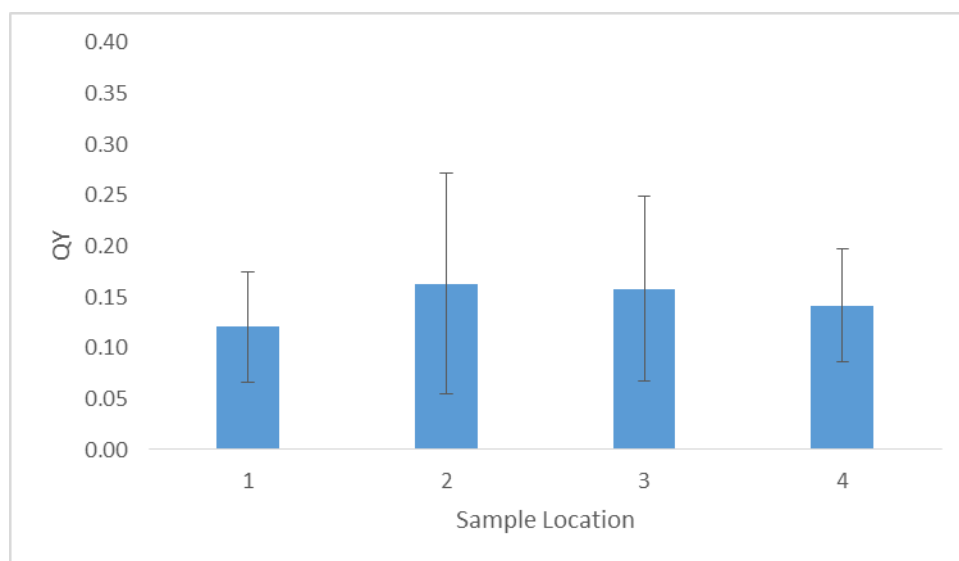


Figure 44: Spatial pattern of the quantum yield in Left Pond in 2014.

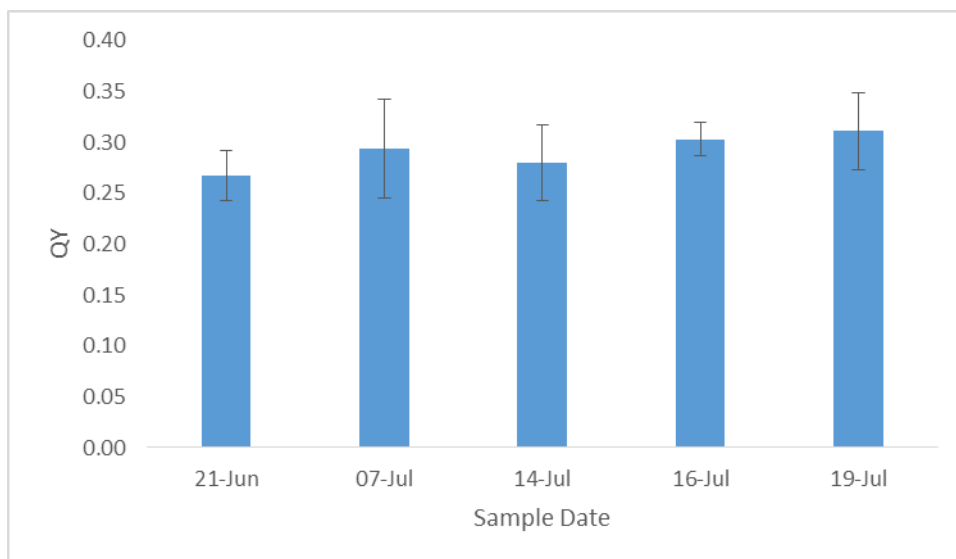


Figure 45: Temporal pattern of the measured quantum yield in Some Pond in 2014.

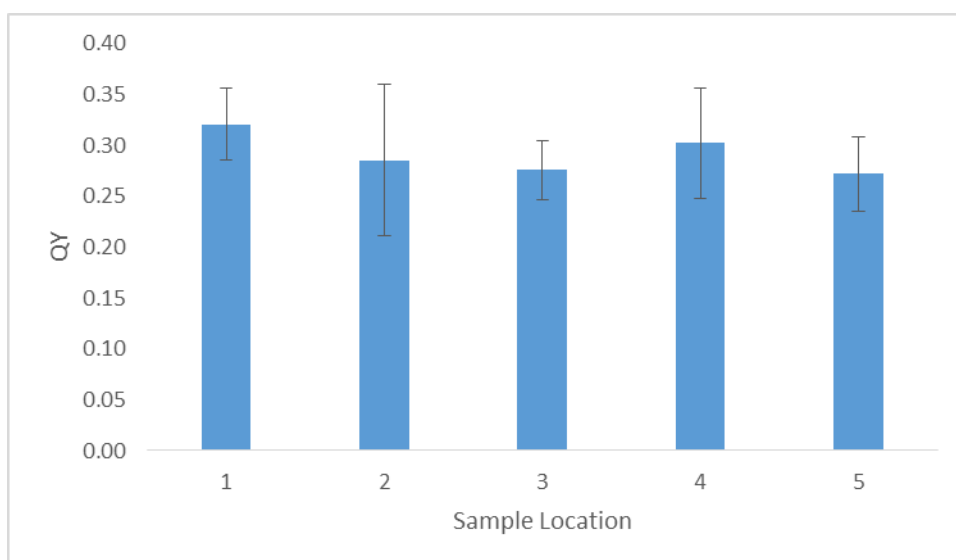


Figure 46: Spatial pattern of the quantum yield measured in Some Pond in 2014.



### 3.2.0 Discussion of within pond variability of the measured limnological variables

#### 3.2.1 How ambient atmospheric and weather conditions affect ponds

There was enough energy from the incoming solar radiation to uniformly heat up the water column in the ponds. The input of radiation from June 26, 2014 to July 25, 2014 cycles depending on the time of day. The variability in the fluctuations is due to variability in weather. Cloud cover is an effective medium that affects the amount of PAR and UV radiation that enters the pond ecosystem. The wave action, affected by the wind speed and fetch, also affects the attenuation coefficient of the water. On the majority of the days PAR was between 1200 and 1600  $\mu\text{mol}/\text{m}^2/\text{s}$ . During precipitation events and cloudy days, the PAR decreased to below 1200  $\mu\text{mol}/\text{m}^2/\text{s}$ , and in extreme circumstances below 400  $\mu\text{mol}/\text{m}^2/\text{s}$  during the day. In part due to the wind's ability to resuspend sediment and affect the extinction of PAR (Einem & Wilhelm, 2014). There are very low concentrations of pigments and DOC to inhibit high intense PAR and UV from stressing the biota in the water column (Hodgson et al., 2004). The average attenuation coefficient for Strange Pond is  $0.120 \pm 0.03 \text{ cm}^{-1}$  and for Some Pond is  $0.007 \pm 0.001 \text{ cm}^{-1}$ . This indicates how substantially clear the water column which similarly compares to Subarctic and Arctic ponds and lakes that range from 0.117 to  $0.207 \text{ cm}^{-1}$  (Vinebrooke & Leavitt, 1999).

Temperature of the water and sediment is directly and indirectly affected by the meteorological variables through the radiation and energy balance. The ponds are shallow enough that ambient air temperatures directly affect both the water column and sediment surface. There are instances where water temperatures are warmer than that of the air, due to the high heat capacity water, allowing the ponds to sustain warmer temperatures as the air gets cold overnight. Sediment temperatures were found to be cooler than that of the water and the air. The depth at which sediment temperature is measured is important to the study. Surface temperatures of the sediment was the warmest. The deepest sediment at 9.0 cm, was cooler. The temperature profile is due to the regulation of heat above the sediment from the surface from the water, and the cooler temperatures from the deeper layers are affected by the underlying permafrost, which remains frozen beneath the pond.

Weather patterns in the Hudson Bay Lowlands are highly variable. Observed data in Strange Pond indicate that the ponds experienced three stages of declining water levels, and two instances in which precipitation occurred. The shallow waters result in greater proportional changes in volume during precipitation. During the end of May and the beginning of June, ice and snow began to melt, bringing the pond to its maxima. Increasing temperatures and low precipitation during the month of

June forces water column loss through evaporation. Heavy rainfall events occurred during the end of June bringing the average pond depth above 15.0 cm. Water depth fell back to the pond minima in mid-July. In mid-July, Strange Pond experienced heavy rainfall in which the average depth of Strange Pond nearly reached its earlier spring maxima.

The year to year variability in water depths is largely due to the pond reliance on precipitation as the major source of water to compensate for evaporative losses. In 2013 field season, it was dry with 360 mm of precipitation. In 2014, it was wetter with a cumulative 600 mm of rain, of which approximately 340 mm of rain fell in one day; similar to the entire field season in 2013. These annual variations may affect light transmission, O<sub>2</sub>, and algal activity as suggested by Sutherland et al. (2015) but give opportunities for ponds to be highly productive during wet years (Voch et al., 2014; Macrae et al., 2004).

The variability of the changes in the water column may affect the fluctuations of temperature by water depth acting as a control mechanism. With less water to warm up in the pond, less energy is also required from the sun, allowing the pond to heat up more quickly within the day establishing peak primary productivity sooner in the day. Besides seasonal changes, year to year variability in water depths is large.

In these ponds the water columns were shallow enough that the wind mixed depth reached all the way to the bottom, making the ponds very well mixed. This causes temperature of the ponds to be homogenous. Predominant wind directions were also measured and analyzed to determine whether wind had an effect on the distribution of the benthic algae in the ponds. In 2013, winds came the north and the west, while in 2014, the wind were blowing from the north and the south east. Less wind was blowing from the west at Strange Pond during this field season due to shrubs and trees in the west, while winds measured at Some Pond in 2013 had open tundra and ponds to its west.

Dominant wind directions in the 2013 field season were northerly and westerly. The transect in Some Pond runs from west to east. The shallow ends on the leeward east side of the transect have higher concentrations compared to the western portion of the transect where turbulence was higher. The eastern side of Some Pond is likely protected from the westerly winds by the steep banks. The protection from the winds accommodates the accumulation of benthic algae in shallow areas on the eastern end of the pond, demonstrating that the direction of the wind may affect the distribution of benthic algae and especially cyanobacteria in the pond.

Regardless of the wind direction and potential inhibition from the riparian zone, modelled wind mixed depths are deep enough to promote circulation of the water column, and deep enough to cause burial events in the benthos. If the winds were dominant in one direction, burial or loss of chl *a* would be more prominent in the same windward direction. However, it was found that the benthic chl *a* concentration of cyanobacteria, green algae, and diatoms were distributed evenly through the ponds. If significant differences in benthic algae were to occur based on the wind direction, burial on the northern and south eastern locations would be more prominent, thus having a lower concentration of benthic algae. In the opposing directions, algae concentrations would be higher due to minimal sediment loss and the protection from the shoreline.

In the field season of 2014, the dominant winds came from the north and the south east. If the wind mixed depth was constantly deep enough to churn the benthic sediment, there would be a correlation with the wind direction and benthic algae concentrations. In the case of the studied ponds where the benthic algae concentrations were measured around the perimeter, there were no significant differences amongst the sample locations. This provided evidence that a continuous mat existed throughout the pond, and that any sampling point may be used to collect benthic and limnological data.

### 3.2.2 Benthic algae patterns in the shallow Subarctic ponds

The benthic algae concentrations and proportions measured using the BenthosTorch have displayed interesting results in the interactions with the ambient weather conditions and limnological characteristics. One pattern that stays consistent with Some Pond (Figure 24), Strange Pond (Figure 28), Left Pond (Figures 30), and even the desiccated Puddle Pond (Figure 33) is that cyanobacteria are the dominant algae and that algae concentrations are evenly distributed throughout the ponds. With that in mind, it is important to observe how the ponds change diurnally given that weather patterns and limnological characteristics of the ponds can change drastically due to their small size allowing them to be influenced easily. Therefore, the expectation was that benthic algae concentrations should remain evenly distributed but can fluctuate within the summer field seasons, especially for small ponds (Left Pond) and desiccated ponds (Puddle Pond). Benthic algae on the interface sediment were distributed evenly in the shallow ponds. Spatial distribution becomes insignificant in determining where to sample in a pond while temporal changes were important.

### 3.2.3 Benthic algae concentrations in Some Pond

Some Pond is one of the larger and deeper ponds in the study. It has been found that a gradient does exist along the transect. Concentrations in cyanobacteria, green algae, and diatoms were not significantly higher during the 2014 field season in comparison to the 2013 field season. The lack of difference could be the result of the water column acting as a buffer from the atmosphere, creating similar conditions in the water column despite being drought like years. Droughts lead to a lower inflow of nutrients originating from the surrounding basin, leaving the benthos to absorb the majority of the required nutrients from the sediments. Input of nutrients into the system would promote primary productivity and benthic algae growth.

The depth of Some Pond was lower in 2013 than in 2014, thus exposing the sediments to the atmosphere. Without a layer of water to protect the algae from high inputs of radiation and regulate temperature, ideal growing conditions for the algal species are not maintained. Wave action may also contribute to the lower concentration of algae at Location 1. Increased wave action in 2013 may have resulted in benthic algae being unable to colonize the zone due to high wave disturbance. Increased water levels in 2014 may have neutralized the wave action, as well as moderate shallow water temperature.

The statistical analysis of the temporal resolution of benthic algae in Some Pond suggests that the benthic algae proportions and concentrations of the three major taxa do not differ from each unique sampling day. However, when analyzing the spatial distribution of the benthic algae along the transect, there are spatial differences in both the proportions and concentrations. The sediment bottom of Some Pond ranges from 10 to 50.0 cm below the water surface, making the sediment surface flat. Ponds and lakes with variable depths have benthic concentration gradients (Cantonati & Lowe, 2013), which leads to the belief with the flat like morphology of ponds like Some Pond, would allow for the similar amount of PAR to reach the benthic bottom regardless of the depth. However even with a small gradient in depth, Some Pond still has shown to have an observed gradient in benthic algae concentrations. Towards the middle of Some Pond, benthic green algae concentrations are slightly higher in 2013 than in 2014. This moderate difference may be a result of water temperature and depth. Through this study, it has been determined that > 98% of photosynthetic active radiation and UV radiation reaches the pond bottom (Figures 13 & 14). However, the depth of the water, and volume of the Pond will determine the temperature regulation of the water column, and the response of benthic algae production.

Cyanobacteria concentrations are lower during the 2013 field season, when the water column is lower, and temperatures were higher during the daytime.

With > 98% of the measured PAR and potentially UVR reaching the pond bottoms, both radiation from the sun and temperature would have a profound affect the benthos and microbes on the sediment surface. The shallow depth of the water and volume of the pond causes these variables to effectively affect the pond's metabolism without any inhibition. From sample location 3 to 7 the total benthic algae concentrations are similar. The benthic algae concentration from sample locations 8 to 10 do not taper off while the water column decreases with depth. Benthic algae concentrations at sample location 1 due to the turbulence constant mixing of the water column, creating a difficult local habitat to reside. The total concentrations of each major taxa, especially cyanobacteria increase once the water column depth exceeds the average wind mixed depth of 0.19 m in Some Pond.

#### 3.2.4 Benthic algae concentrations in Strange Pond and Left Pond

Left Pond experienced similar patterns to what has been measured in Strange Pond despite their physical separation, differences in depth and differences in surrounding vegetation. In comparison to the other benthic communities in the other ponds, diatoms in Left Pond are adversely affected by the changes in the benthic communities within the pond and temperatures fluctuations. This ease of changes results from the small size of Left Pond. Especially with a smaller pond, it may be expected to have all the concentrations of the three types of algae to be uniform. The impact of the different variables on Diatoms may suggest its importance to climate change. This importance is valuable especially when even in a small pond, concentrations differ amongst the three algae types.

Diatoms in the ponds act as indicators for climate change. As a result, diatom assemblages are susceptible to changes in water depth, PAR, and temperature fluctuations in the shallowing system. The lack of changes in the diatom community may be a result of no severe changes in the conditions of their environment, or the temporal scale was too small to see significant changes in the diatom community other than the bloom found in Some Pond. The concentration changes of cyanobacteria differ in Strange Pond. In Left Pond, cyanobacteria concentrations differ significantly during the sampling periods versus Strange Pond where concentrations remained similar throughout the field season. When comparing Strange Pond and Left Pond, Left pond has a higher concentration of cyanobacteria than Strange Pond (Figures 28 and 30). With a higher concentration of cyanobacteria in Left Pond, the cyanobacteria

concentrations are less susceptible to change due to being more established, whereas lower concentrations of cyanobacteria experience more significant changes in concentrations, even though the changes are marginal.

### 3.2.5 Benthic summary

Akin to many Arctic and Subarctic aquatic systems, the ponds studied in Churchill, Manitoba are dominated by cyanobacteria with 50%, and upwards of 60 to 90% of the total proportion of benthic algae. The range is similar to that of lakes and ponds sampled on Bylot Island (Vézina & Vincent, 1996). However, a spatial pattern with the depth gradient was not found. This may be due to the combination of the high exposure of ultraviolet radiation and shallow depth throughout the pond that creates a lack of a depth gradient. As a mainstay in the benthic community, cyanobacteria are the dominant taxa in Some Pond. All three ponds were dominated by cyanobacteria, with a proportion between 55.9 and 59.3%. Higher concentrations of diatoms were found on the sample locations that have large pebbles and sheltered by large macrophytes in comparison to the fine sediments which has a significantly lower proportions of diatoms.

### 3.2.6 Benthic algae concentrations in Puddle Pond

Including an ephemeral pond into the sampling protocol may establish an understanding of how exposed benthos and sediment would change on a temporal and spatial scale without the influence of a water column. Cyanobacteria represent the highest overall concentration of chlorophyll *a* as it was statistically determined that cyanobacteria, green algae, and diatoms do not vary overtime and between sampling locations.

The lack of water column on the benthos will promote both the increase of respiration from decomposition and influx of invertebrates into the system. The temporal changes in the concentrations of cyanobacteria and green algae suggest that without a significant water column, the benthos is exposed to terrestrial insects and microorganisms that would feed upon the benthic algae. The stress of ultraviolet radiation can create a cycle of cyanobacterial dominance as well, where the peaks and minima suggest an alternating reproductive cycle of cyanobacteria and green algae. During the 2014 field season, cyanobacteria and green algae demonstrated significant changes, varying between

sampling days while diatom concentrations did not differ. Due to the lack of a water column, water runoff and precipitation can lead to pulses of nutrients and moisture into the dried sediment, changing the complex interactions of the benthos. Diatom concentrations remained stagnant, suggesting that microorganisms favour feeding on what is left of the cyanobacteria and green algae. Diatoms typically have low concentrations on the sediment surface due to their ability to reside within the first couple millimeters of the sediment (Michelutti et al., 2003).

Ponds can be hydrologically classified into three phases: the aquatic phase, transferal phase, and the dry phase (Gilbert et al., 2017). In the aquatic phase, traditional aquatic carbon cycling occurs with photosynthesis and respiration occurring both in the water column and the sediment bottom. Gross Primary Productivity (GPP) increases as the water column level decreases in the water column (Hornback et al., 2017), signalling that their ponds have a peak productivity phase and then decline once the evaporation of the water column causes the ponds to enter the dry phase. In the dry phase, the sediment is exposed converting the pond to a source of CO<sub>2</sub> and CH<sub>4</sub>. The exposed sediment becomes an ecosystem for both aquatic and terrestrial bacteria that directly becomes a greenhouse gas source to the atmosphere without a water column acting as barrier. In the dry phase, the pond then becomes terrestrialized as the exposed sediment bed is encroached by terrestrial vegetation. In this dry phase, vegetation easily manifests in the sediment due to the high nutrient and organic matter concentration. The pond potentially becomes a carbon sink due to the emergence of pioneer plants that are able to photosynthesize quickly under the right conditions.

### 3.2.7 Pelagic patterns within the ponds

The very low chl *a* concentrations of pelagic algae in the water columns of Some Pond, Strange Pond, and Left Pond are shown in Tables 4, 5 and 6. The low total concentration of all three types of pelagic algae is a testament to the nutrient poor water column found in all three ponds. A water column without sediment would benefit phytoplankton because sediment acts as a sponge that absorbs nutrients efficiently. Sediment beds in some of the ponds of the Hudson Bay Lowlands originate as thermokarst ponds, formed and filled in collapsed peat. Nutrients found in the sediment bed of the ponds allow benthic algae to be the dominant primary producers in the shallow ponds. The low concentration of pelagic algae is limited by the low nutrients, shallow water column, and benthic algae competition (Eichel et al., 2014). This is shown through an established benthos versus the lack of algae

in the pelagic zone. Concentrations of benthic algae are higher versus the concentration of pelagic algae when comparing results found in Figures 24, 28, 30, and 33. The  $Q_Y$  of the sampled pelagic algae in the water column also exhibit variability. In southern Spain ( $36^{\circ}13'N$   $5^{\circ}27'W$ ), the quantum efficiency in estuaries are between 40-45% in green pelagic algae, indicating that there likely is photo-inhibition. The pelagic algae in the shallow freshwater ponds near Churchill, Manitoba, experience similar stress levels. The seasonal patterns of the  $Q_Y$  found in the Some Pond in 2013 (Figure 34 and 35) indicate that the photosynthetic capabilities are dependent on seasonal variables.

### 3.2.8 pH patterns in the water column of the ponds

The high pH levels in the three may ponds favour cyanobacteria, as found by Schlichting (1974) and Wäckstrom et al. (1997), promoting its dominance in the benthos. In the sample locations of Some Pond, the water column was divided into an upper and lower layer to determine if the water column is well mixed or not. There is no difference between the pH of the upper and lower layers in Some Pond. This suggests that the wind mixed depth is deep enough to mix the water column uniformly. The pH of the water provides an indication of the concentration of  $CO_2$  in the water column. This characterizes Some Pond as one where aqueous gas transferred or lost from the atmosphere or benthos does not remove within one layer of the pond. The drastic decline of the pH such as the rain event on July 13, 2014 in Some Pond indicate that there was an increase in  $CO_2$  concentrations due to the decrease in primary productivity with increased cloud cover and lower temperatures.

### 3.2.9 Dissolved oxygen patterns in the water column of the ponds

In Some Pond, dissolved oxygen concentrations in the water column was at or near saturation. In shallow waters where wind-generated mechanical turbulence should extend to the bottom, the bottom layer of the water had a lower concentration than the upper water column (Figure 39), but by an insignificant amount ( $p$ -value  $> 0.05$ ). Similar to the other limnological characteristics being well mixed in the water column, dissolved oxygen concentrations collected at each sampling location within Some Pond in 2013 (Figure 40a & b) indicate that a strong horizontal  $O_2$  exists ( $p$ -value  $< 0.05$ ). The spatial pattern along the transect shows that dissolved oxygen concentrations increases as the water column gets deeper. Oxygen is added to the water column continually at the water surface from the atmosphere. The shallow water is subjected to churning in the benthos, affecting the ability of



cyanobacteria and green algae to establish mats near the shore, thereby limiting photosynthesis. The benthos is therefore a site of net  $O_2$  consumption and when the removal rate exceeds the rate of addition from above, the concentration will decrease. The deeper water columns not only have the capacity to dissolve more  $O_2$  but the benthos also suffers less disturbance, allowing for oxygen production (Tables 4, 5, and 6).

#### 3.2.10 Quantum Yield patterns in Some Pond in 2013

The quantum yield,  $Q_y$  (efficiency) of the pelagic algae ranges from medium to low and is not significantly different from the upper and lower layers of the water column. The quantum efficiency in Some Pond is uniform along the transect in both the upper and lower layers of the water column, indicating that the green algae was affected by stress no matter the location in the water column. Although there may be no spatial patterns within Some Pond, there is a significant difference in the temporal patterns in the quantum yield. The pattern suggests that  $Q_y$  of the green pelagic algae increases towards mid-summer, in Churchill, Manitoba as the sun's intensity is decreasing post-solstice. The peak that was observed in Some Pond is similar to that found by Sheath (1986) where pelagic algae experienced a similar peak in the mid-summer. Towards the end of July, the quantum efficiency decreases despite declining light intensities and this may reflect a response to some other stress related to temperature or nutrient availability.

#### 3.2.11 Quantum yields of the studied ponds

The daily input of PPFD reaches a peak between 12h and 14h CDT (Figure 13) corresponding to the peak extraterrestrial radiation at solar noon. This bell-shaped pattern of the PPFD can be an indication of a similar trend for the quantum yields. In Strange Pond, there is a significant difference in quantum efficiency values of pelagic algae in the water column at the eight different sampling locations. There is also evident change in the temporal patterns of the quantum efficiency values of Strange Pond (Figure 41). The statistically significant differences both spatially and temporally suggest the water column is in a dynamic state and a snapshot or point sample is not representative of what is occurring in a pond (Figure 42). Some Pond quantum yields behave similarly. (Figure 45 & 46).

Left Pond is a small sized pond in comparison to Strange Pond and Some Pond. Due to its small size, there is no significant difference in the quantum yield at each sample location (Figure 44), yet the average quantum efficiency values change significantly (Figure 43). The lack of difference in average quantum efficiency values at each sample location is due to the lack of variation within Left Pond that is defined by water column depth, shadowing effects from the riparian zone of the pond, and the well mixed water. Variability in quantum yields exists in the larger ponds studied.

### 3.2.12 Conclusion: Cyanobacteria dominance and where to collect samples

The shallow zones in ponds of the Hudson Bay Lowlands serve as excellent hosts for cyanobacteria to thrive. Water temperatures during the study period in both field seasons averaged  $16.00^{\circ}\text{C} \pm 3.07^{\circ}\text{C}$  in Some Pond and  $16.33^{\circ}\text{C} \pm 4.27^{\circ}\text{C}$  in Strange Pond. Diatoms would be able to thrive in similar conditions with the temperatures found in this system, but the high PAR observed in this study, and the low attenuation, allows the majority of the spectra to reach the bottom of the ponds. The pH of the water column in the ponds studied are not ideal for green algae, as green algae prefer the pH of water to be closer to 4.0 to be competitive against other types of algae. Thus, the ability of cyanobacteria to adapt to the long intense day light hours, and varying pH and temperatures (Beaulieu et al. 2013) make them an excellent driver in the photosynthesis of the ponds in the Hudson Bay Lowlands. With the cyanobacteria being dominant in the benthos, it leaves the potential for other pelagic algae species to dominate the water column. However, it is shown that pelagic cyanobacteria was undetectable, and green algae quantum yields are very low. It is clear that these systems are benthically dominated.

Benthic algae concentrations are found to be generally similar amongst the ponds measured, with each of the ponds' benthos being dominated by cyanobacteria. The temperature conditions of the water column and the sediment are highly correlated with ambient air temperature conditions. This provides the opportunity for future studies to see how ambient temperatures can be used as an indicator for limnological variables in the ponds. Stratification of the water column exists only weakly with temperature and dissolved oxygen, even with the shallow depths of the ponds.

For the limnological variables in the water column, and the benthic algae concentration, the variability of the system is dependent on the area of the pond. Variability exists for both limnological variables, and the benthic taxa over the field season. Homogeneity within the benthos exists due to the

dominance of the cyanobacteria in the system, which can be found throughout the pond bottom. This establishes that sampling can occur in one location within the pond, but the pond should be sampled multiple times within a field season to capture the temporal variability of the shallow system. The pond water column in the Canadian Arctic has been suggested by Laurion et al. (2011) to be stratified, however, findings in this study indicate that the water column is homogenous throughout the water column and therefore can be sampled at any location in the pond. With this in mind, the temperature or thermal gradient is best used to determine whether the water column of the ponds are stratified.

#### 4.0.0 Chapter 4: Benthic algae NEE and assimilated CO<sub>2</sub> and sediment respiration

##### 4.1.0 Results: Temperature versus respiration of sediment cores for Left Pond and Strange Pond

The in-lab incubations indicate that the temperature of the sediment highly influences respiration rates. The respiration flux was measured in triplicates using incubation like conditions to manipulate temperature. Under the same set of conditions, temperature manipulations from Left Pond and Strange Pond produce similar fluxes. Using the Kruskal-Wallis test, the relationship between the respiration flux and the core temperatures were statistically significant ( $p < 0.05$ ) with an  $R^2$  of 0.81 for Left Pond (Figure 47), and  $R^2$  of 0.90 in Strange Pond (Figure 48). With a strong correlation to temperature, it was determined that the exponential best fit equation of the correlation in Strange Pond can be used to model the respiration rate from the benthic algae and sediment using temperature of the water column and sediment.

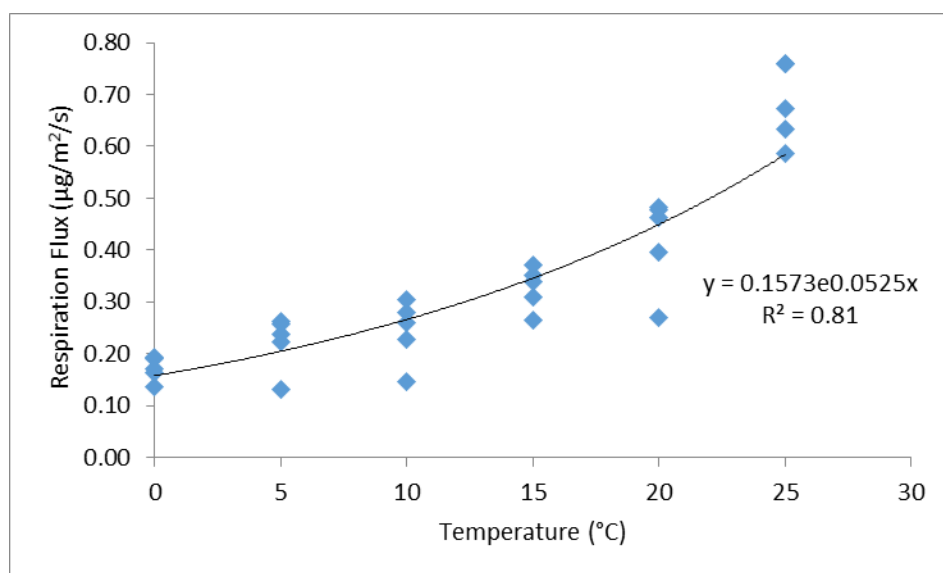


Figure 47: The exponential relationship and influence of temperature on the respiration flux of sediment cores from Left Pond ( $n=24$ ).

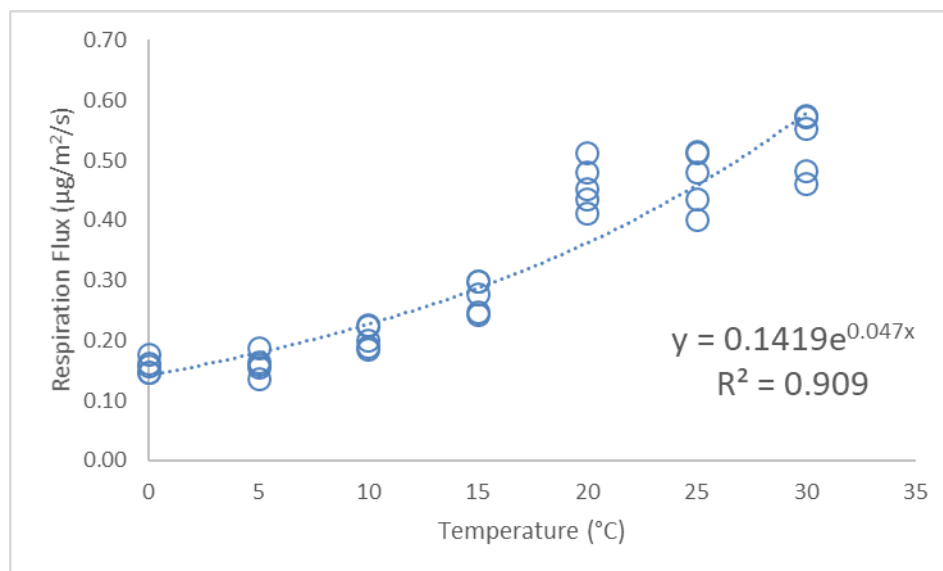


Figure 48: The exponential relationship and influence of temperature on the respiration flux of the sediment cores from Strange Pond ( $n=140$ ), with a calculated standard error of 0.074.

#### 4.1.1 Modelling respiration flux of Strange Pond

The modelled respiration flux of Strange Pond in June and July were derived from the empirical relationship of the in lab experiments using the LI-COR 8100,  $y = 0.1419e^{(0.047T)}$  (Figure 48). The x-variable was the in situ temperature of the sediment 1.0 cm below the surface of the sediment and the temperature of the water. The max temperature during the study is 24.56°C and the minimum was 5.58°C for the sediment 1.0 cm below the surface. The average temperature was 15.02°C. Using the sediment temperature, the maximum modelled respiration flux was 0.45  $\mu\text{mol}/\text{m}^2/\text{s}$  and the minimum was 0.18  $\mu\text{mol}/\text{m}^2/\text{s}$  (Figure 49). The average respiration flux was  $0.29 \pm 0.44 \mu\text{mol}/\text{m}^2/\text{s}$  in June and July based on the sediment temperature. The maximum temperature of the water during the summer field season was 28.26°C, and the minimum temperature was 5.52°C. The average respiration flux was  $0.31 \pm 0.06 \mu\text{mol}/\text{m}^2/\text{s}$ .

Within a 72-hour time frame (Figure 50), sediments in Strange Pond experienced fluctuations in respiration rates. This follows the peaks and valleys that represented the changes of increasing temperature during the day and decreasing temperatures in the evenings. For July 7 the maximum respiration flux based on the sediment temperature was 0.33  $\mu\text{mol}/\text{m}^2/\text{s}$ , and the flux based on the water temperature was 0.37  $\mu\text{mol}/\text{m}^2/\text{s}$ . The minimums were 0.23  $\mu\text{mol}/\text{m}^2/\text{s}$  and 0.25  $\mu\text{mol}/\text{m}^2/\text{s}$  respectively. The average respiration flux was 0.29  $\mu\text{mol}/\text{m}^2/\text{s}$ , and 0.31  $\mu\text{mol}/\text{m}^2/\text{s}$  derived from the

temperature of water. July 8 had a greater peak at  $0.35 \mu\text{mol}/\text{m}^2/\text{s}$  based on the temperature of the sediment and  $0.41 \mu\text{mol}/\text{m}^2/\text{s}$  based on the temperature of the water. The minimum respiration fluxes were  $0.26 \mu\text{mol}/\text{m}^2/\text{s}$  and  $0.28 \mu\text{mol}/\text{m}^2/\text{s}$ . The average respiration fluxes were  $0.30 \mu\text{mol}/\text{m}^2/\text{s}$  and  $0.34 \mu\text{mol}/\text{m}^2/\text{s}$  respectively. On July 9, based on the temperature of the sediment, the maximum respiration flux was  $0.34 \mu\text{mol}/\text{m}^2/\text{s}$ , the minimum was  $0.28 \mu\text{mol}/\text{m}^2/\text{s}$ , and the average respiration flux was  $0.31 \mu\text{mol}/\text{m}^2/\text{s}$ . Based on the temperature of the sediment the peak respiration flux was  $0.37 \mu\text{mol}/\text{m}^2/\text{s}$ , the minimum is  $0.28 \mu\text{mol}/\text{m}^2/\text{s}$ , and the average is  $0.32 \mu\text{mol}/\text{m}^2/\text{s}$ . From June 27 to July 25, Strange Pond had cumulatively respired  $716.44 \mu\text{mol}/\text{m}^2/\text{s}$  of carbon dioxide based on the model derived from the temperature of the sediment 1.0 cm below the surface of the sediment (Figure 51).

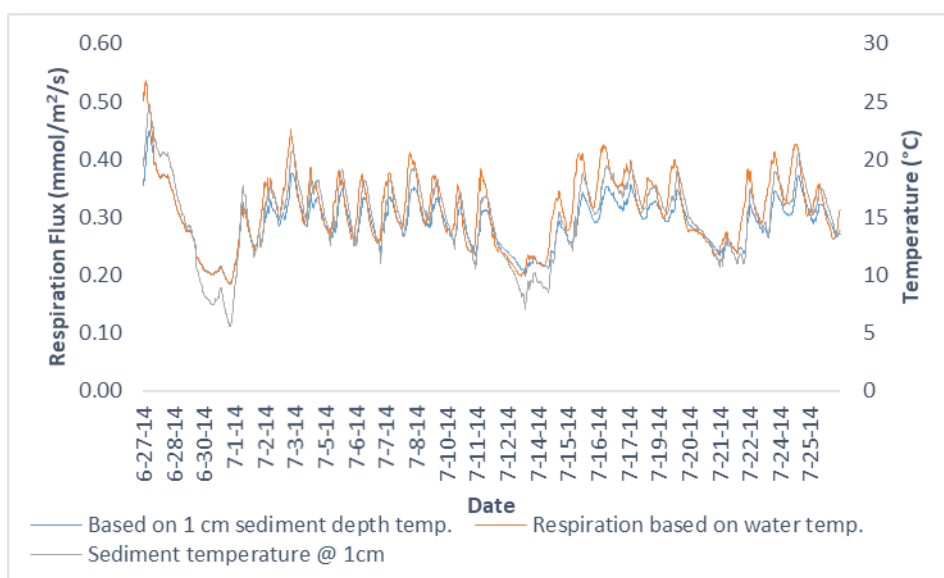


Figure 49: Based on the exponential relationship found from the sediment core respiration flux with temperature, respiration flux in Strange Pond was estimated using both the water temperature and sediment temperature at 1.0 cm below the sediment surface.

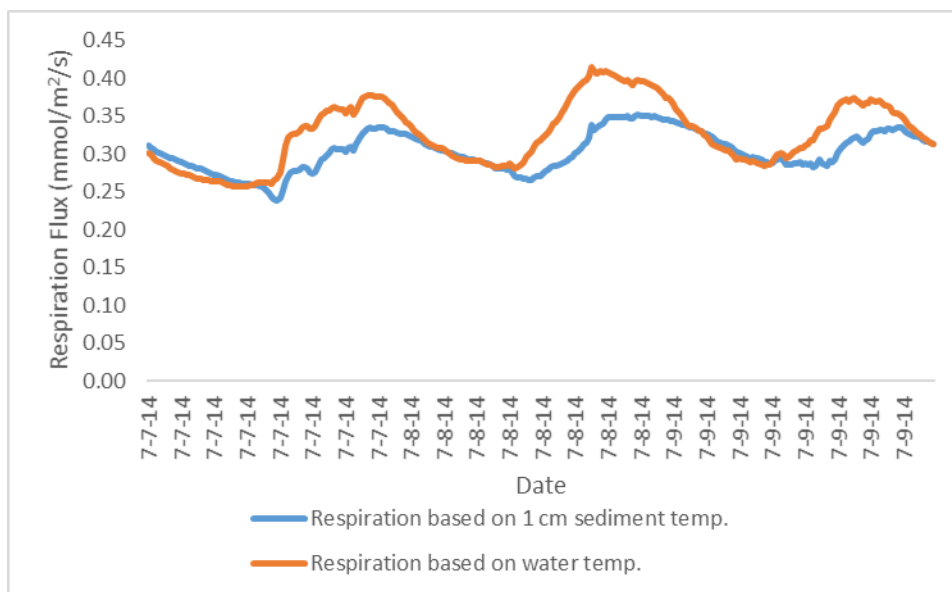


Figure 50: A 3-day period of the modelled respiration flux showing diurnal fluctuations.

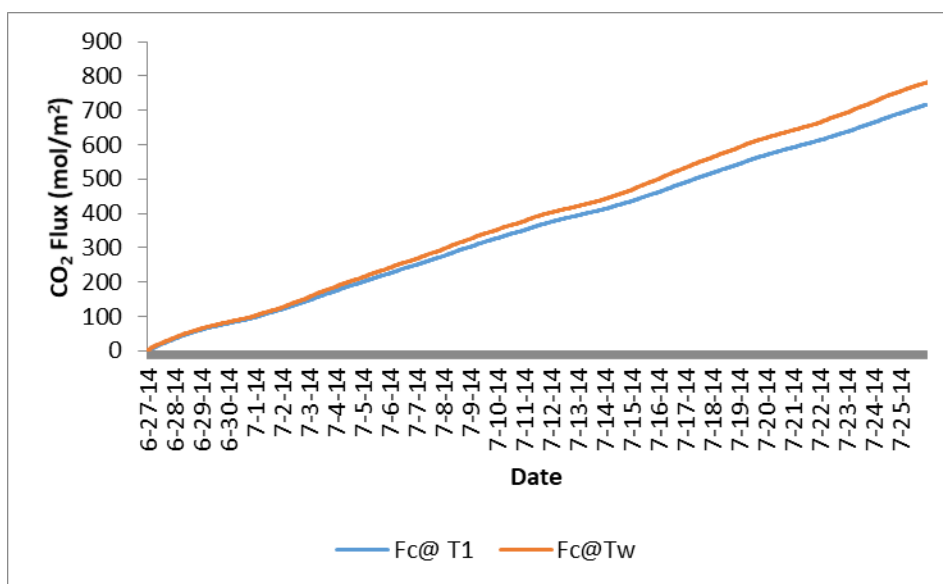


Figure 51: The cumulative benthic respiration from the beginning to the end of monitoring Strange Pond in the 2014 field season (June 27 to July 25, 2014).

#### 4.1.2 Modelling respiration and benthic cumulative respiration of Some Pond

The respiration model was used to estimate the benthic respiration flux and cumulative benthic respiration flux of Some Pond using measured temperature from 2013. The average flux was  $0.29 \pm 0.04$  mmol/m<sup>2</sup>/s, with a maximum of 0.42 mmol/m<sup>2</sup>/s and a minimum of 0.21 mmol/m<sup>2</sup>/s (Figure 52). Cumulatively, over a 28-day period (Figure 53), the sediment in Some Pond respired approximately 743.84 mmol/m<sup>2</sup>. In comparison, the sediment in Strange Pond over a period of 30 days, respired approximately 768.40 mmol/m<sup>2</sup> (Figure 51).

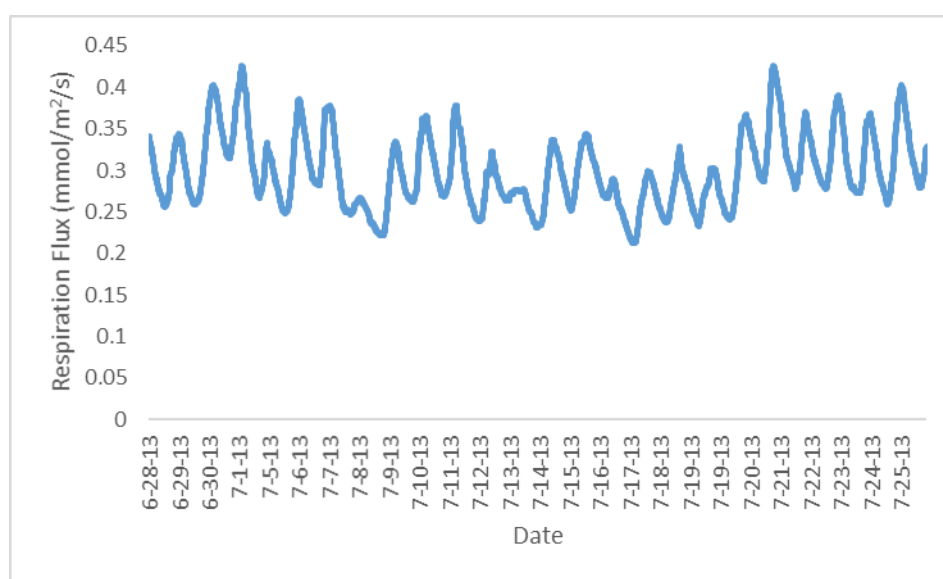


Figure 52: Modelled respiration of Some Pond.



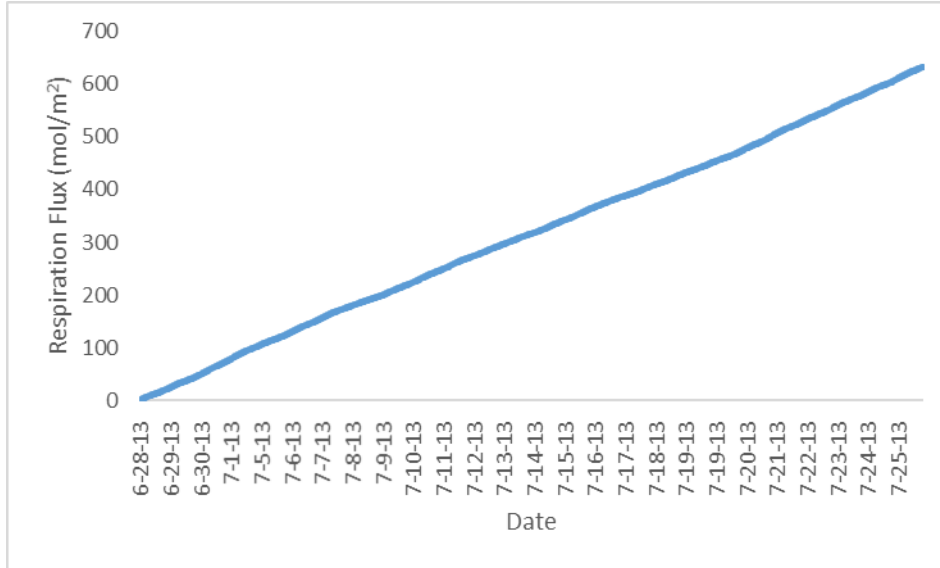


Figure 53: Modelled cumulative respiration of Some Pond during the 2013 field season from June 28 to July 25, 2013.

#### 4.1.3 Dissolved oxygen concentrations in the benthic chamber

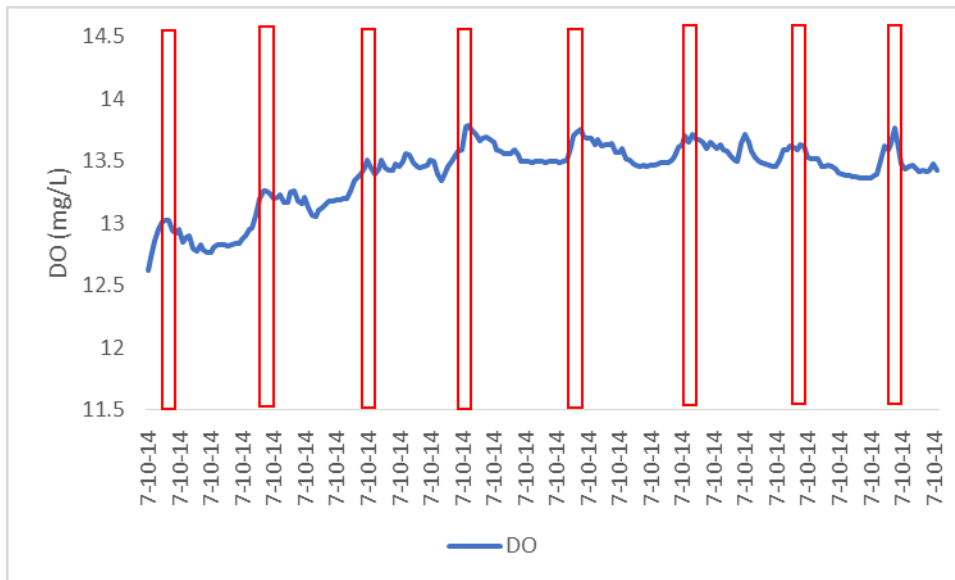


Figure 54: Observed DO concentrations on July 10, 2014, between the times of 2:30 p.m. and 6:10 p.m. This is a closer depiction of the fluctuations during each cycle, but also smaller fluxes occurring within the chamber. The highlighted areas show the peaks of O<sub>2</sub> produced from algal photosynthesis during the chamber's closed circulation phase. The remaining intervals of the graph indicate the equilibration of the gas chamber with ambient water within the pond during the chamber's open circulation phase.

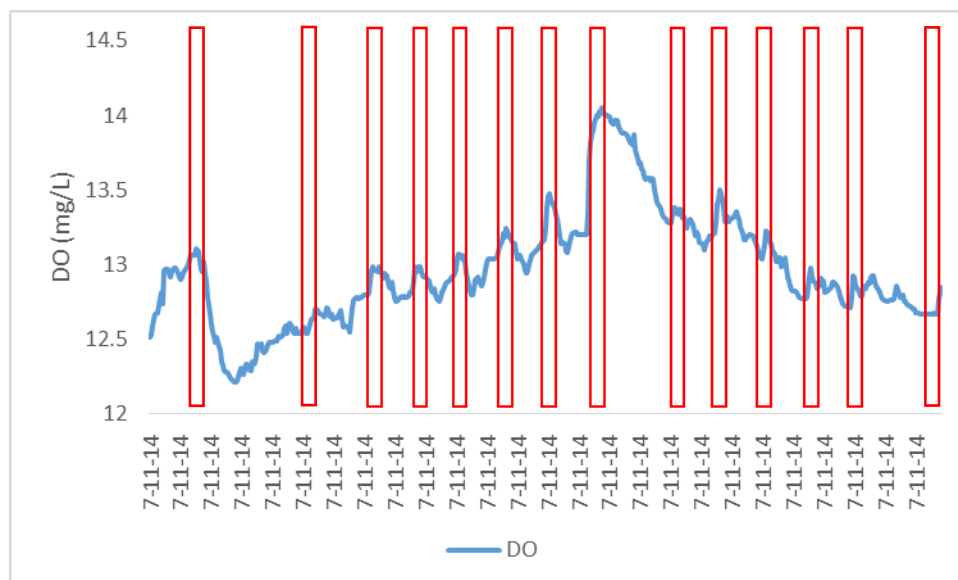
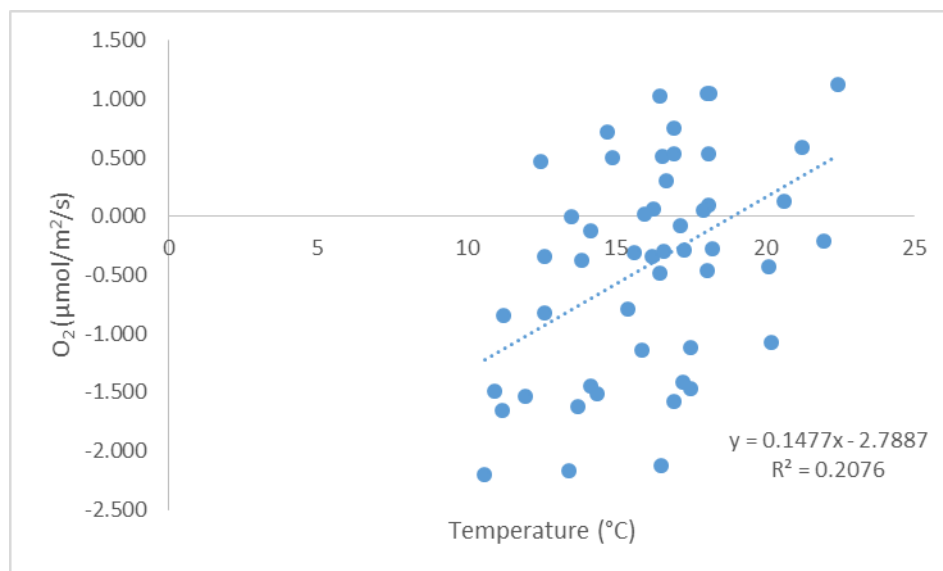


Figure 55: DO concentration fluctuations on July 11, 2014 between 9:30 a.m. and 4:15 p.m. The observed DO fluxes are not as consistent as seen on July 10, 2014. The highlighted areas denote the peaks of  $O_2$  produced from algal photosynthesis during the chamber's closed circulation phase. The troughs of the graph indicate the equilibration of the gas chamber with ambient water within the pond during the chamber's open circulation phase.

Dissolved oxygen concentrations were observed when the pumps were properly cycling water from the benthic chamber, SDGD, and the surrounding pond water. The average DO concentrations were similar on July 10 (Figure 54) and July 11 (Figure 55), with averages of  $13.39 \pm 0.26$  mg/L, with a range of 12.62-13.79 mg/L, and  $12.96 \pm 0.37$  mg/L with a range of 12.21-14.05 mg/L respectively. The peaks that are highlighted in the two graphs indicate the production of oxygen for the duration that the chamber was closed from the rest of the pond. The pattern in DO concentrations were similar for both days.

#### 4.1.4 Gas fluxes within the benthic chamber

The average net ecosystem exchange of  $O_2$  during the closed circulation phase of the benthic chamber was  $1.13 \pm 0.89$   $\mu\text{mol}/\text{m}^2/\text{s}$ . The average temperature was  $16.11 \pm 2.80$  °C. Temperature had a small effect on the production of  $O_2$  from the primary producers (Figure 56). The logarithmic regression ( $R^2 = 0.19$ ,  $p > 0.05$ ) may indicate that increasing temperature influences the photosynthetic efficiency of the algae within the chamber but it is not significant.



57Figure 56: Net ecosystem flux of O<sub>2</sub> during the closed circulation of the benthic chamber (for June 26, July 6, July 10, and July 11) regressed against temperature. Production of oxygen is indicated as positive values, and consumption of O<sub>2</sub> is indicated as negative values.

The consumption of O<sub>2</sub> was modelled as the inverse of the respiration flux (production of CO<sub>2</sub>) measured from the in lab incubation experiment. The modelled consumption of O<sub>2</sub> (Figure 57) was plotted as a function of measured temperature of the sediment at a depth of 1 cm. As the temperature increased in the sediment, the oxygen consumption and respiration rates increased as well. The average rate of consumption of O<sub>2</sub> was  $-0.30 \pm 0.04$  μmol/m<sup>2</sup>/s, with an average temperature of  $16.11 \pm 2.8$  °C.

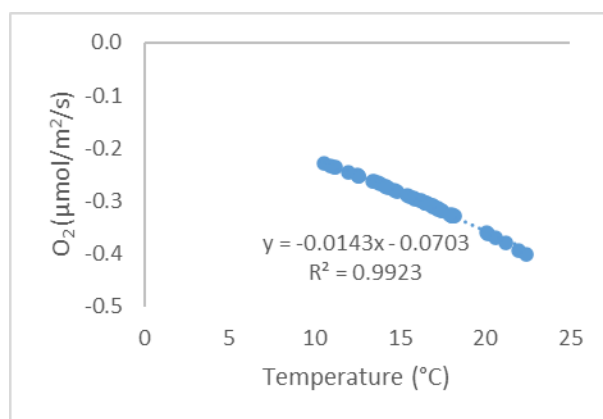


Figure 57: The modelled consumption of O<sub>2</sub> based on the temperature of the sediment at a depth of 1 cm. Increasingly negative values indicate higher consumption of O<sub>2</sub>.

Primary production of O<sub>2</sub> was isolated by subtracting the modelled respiration within the benthic chamber from the measured NEE (Equation 15). The average O<sub>2</sub> flux from the primary production was  $1.01 \pm 0.86 \mu\text{mol}/\text{m}^2/\text{s}$ . The positive values in the O<sub>2</sub> fluxes indicate (Figure 58) that primary production increased as incoming PPFD increased, though not significantly ( $R^2 = 0.11$ ,  $p > 0.05$ ). The overall pattern is somewhat linear which is not in keeping with expected light curves which show a levelling off of production as light levels increase above 300-500  $\mu\text{mol}/\text{m}^2/\text{s}$ . The scatter in the data is too large to detect such trends. Similarly, the negative correlation of primary production with temperature, indicates that temperature may also stress the primary production of the benthic algae, though not significantly ( $R^2 = 0.15$ ,  $p > 0.05$ ) (Figure 58 B).

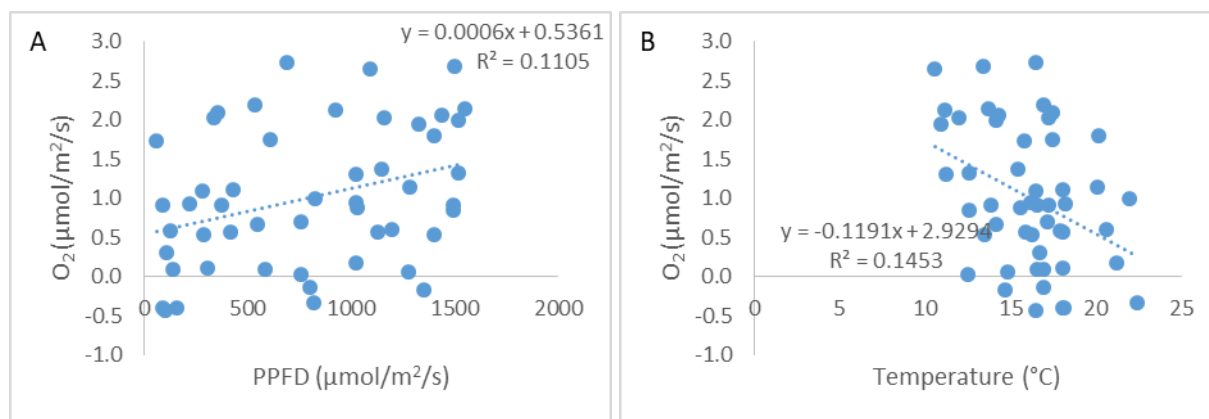


Figure 58: Dependence of primary production of O<sub>2</sub> on PPFD (A) and temperature (B) during the closed circulation of the benthic chamber (for June 26, July 6, July 10, and July 11). Production of oxygen is indicated as positive values, and the consumption of oxygen is indicated as negative values.

#### 4.1.5 Active surface sediment of Strange Pond

Cores of varying thickness had similar respirations rates. This indicates that microbial decomposition was prominent in the superficial layers of the cores and with minimal activity below this layer. The Bartlett test showed that the variances of the respiration fluxes were homogenous ( $p > 0.05$ ). At the same time, the ANOVA single factor test shows that the respiration flux of a 2.0 cm core is no different from the respiration flux of a thicker core ( $p > 0.05$ ), even though there was potentially more sediment to decompose. Biological processes and redox reactions that govern decomposition or mineralization may be occurring within the top surface layers of the sediment. Respiration requires oxygen which appears to be limiting below a critical depth of approximately 2 cm. The average benthic sediment respiration fluxes of each sediment layer from Strange Pond were compared. Both the 2 cm

and 4 cm thick cores had an average respiration flux of  $0.30 \mu\text{mol}/\text{m}^2/\text{s}$  (Figure 59). The 6.0 cm thick core had an average respiration flux of  $0.34 \mu\text{g}/\text{m}^2/\text{s}$  and the 8 cm cores have an average respiration flux of  $0.33 \mu\text{mol}/\text{m}^2/\text{s}$ . The thickest set of cores at 10 cm had an average respiration flux of  $0.35 \mu\text{mol}/\text{m}^2/\text{s}$ .

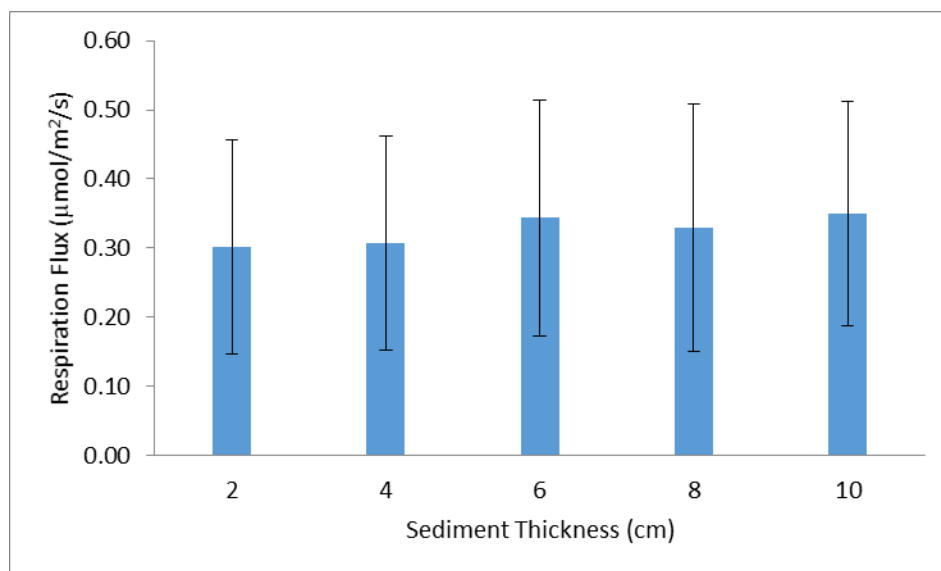


Figure 59: The average respiration flux of each of the 5 thicknesses of sediment cores.

#### 4.1.6 Organic carbon in Strange Pond

Table 7: Sediment characteristics in Strange Pond from the extracted sediment cores.

Sediment Depth (cm)	Bulk Density ( $\text{g}/\text{cm}^3$ )	Organic Fraction %	Carbon Content ( $\text{g C}/\text{cm}^3$ )
0-2	0.146	61.5	0.033
2-4	0.123	60.8	0.054
4-6	0.113	61.5	0.050
6-8	0.121	88.0	0.054

Sediment in Strange Pond (Table 7) had similar bulk density, organic fraction and carbon content. This indicated that the superficial sediment compares similarly to sediment between 4 and 6

cm depth. Sediment located within the 6 and 8 cm range has an average organic fraction of 88.0% compared to the 0 and 6 cm layer can be assumed to be uniform. Furthermore, the carbon content between the 2 to 4 cm range and the 6 and 8 cm depths are similar with an average carbon content of  $0.05 \text{ g C / cm}^3$ . In contrast, the top layer between 0 and 2 cm had an average carbon content of  $0.033 \text{ g C / cm}^3$ . A lower average carbon content in the top layer in comparison to the lower depths indicates a possibility of labile carbon being consumed through biotic processes. Compaction with increasing depth is not likely the cause as the upper layer is of similar or higher density than the lower layers.

#### 4.1.7 Pelagic algae chlorophyll a concentrations and cell counts in pond water column in 2014

The BenthosTorch was used to estimate pelagic algae in the water column. By filtering a known volume of water through a  $50 \mu\text{m}$  Whatman Filter it was possible to measure the concentration and identify the type of algae on the surface of the filter. Figure 60 illustrates the chlorophyll *a* concentrations of the three types of algae from the three ponds analyzed in this study. Green algae was the most dominant class of pelagic algae, and diatom had the lowest concentrations of algae in all three ponds. Some Pond has the highest concentration of cyanobacteria and Strange Pond had the highest concentration of green algae. Some Pond had the highest total concentration of algae at  $14.31 \mu\text{g/L}$ . The concentration of cyanobacteria in the water column of Some Pond is  $9.77 \mu\text{g/L}$ , and the concentration of green algae and diatoms are  $24.66 \mu\text{g/L}$  and  $0.63 \mu\text{g/L}$  respectively.

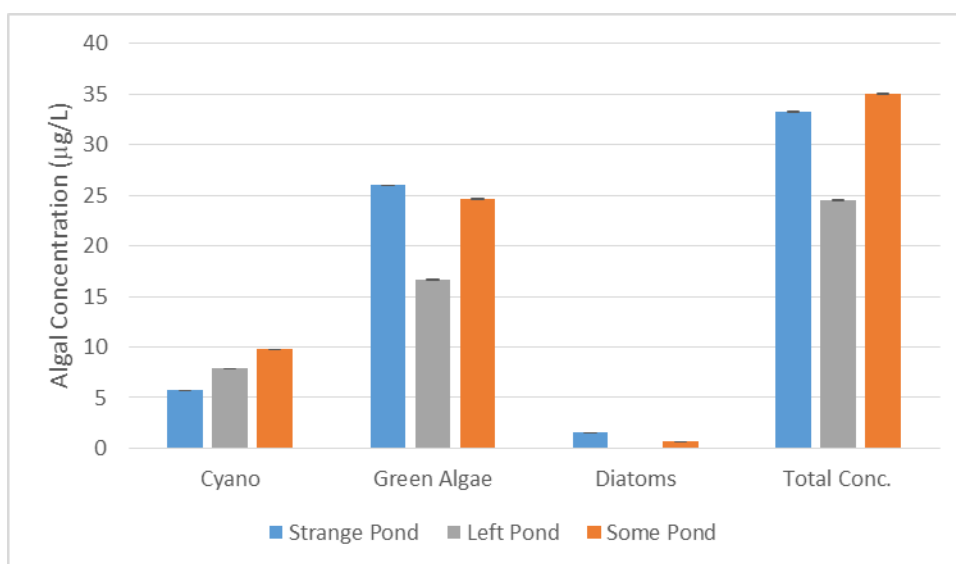


Figure 60: Pelagic algae chlorophyll *a* concentrations of each algae type in Strange, Left, and Some Pond. Concentrations of chl *a* for each of the three algae types are significantly different from each of the three ponds ( $p < 0.05$ ).

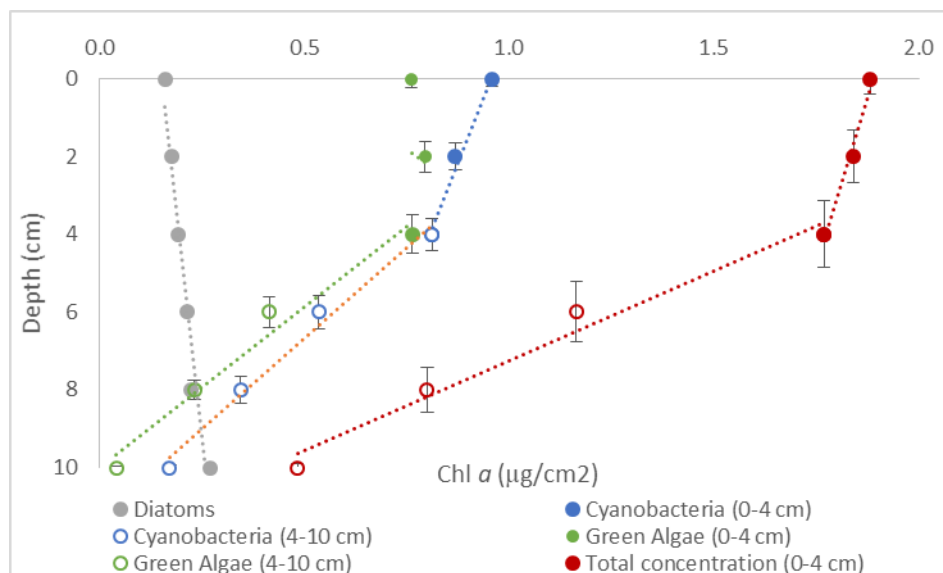


Figure 61: Chlorophyll *a* measurements taken with the BenthosTorch @ 2.0 cm increments. The linear equation of each chl *a* concentration can then be used to estimate the concentrations in a per mm increment or the entire core. The linear regression for total concentration for 0-4 cm ( $y = -34.582x + 65.503$ ,  $R^2 = 0.97$ ) and for 4-10.0 cm ( $y = -4.6213x + 11.872$ ,  $R^2 = 0.97$ ). For cyanobacteria the linear regression for 0-4 cm ( $y = -26.764x + 25.559$ ,  $R^2 = 0.98$ ) and for 4-10.0 cm ( $y = -9.3403 + 11.353$ ,  $R^2 = 0.99$ ). The linear regression for green algae at 0-4 cm is ( $y = 6.0233x - 2.6619$ ,  $R^2 = 0.0031$ ) and for 4-10.0 cm ( $y = -8.2711x + 10.003$ ,  $R^2 = 0.97$ ). The linear regression for diatoms is ( $y = 93351x - 14.242$ ,  $R^2 = 0.95$ ). Error bars indicate 1 standard deviation.

The vertical distribution of algae in a 10 cm core was analyzed to establish the availability of labile carbon and the distribution of potentially photosynthetically active algae. Figure 61 indicates green algae and cyanobacteria contain fairly consistent levels of chl *a* down to a depth of 4 cm which then rapidly declines to 10 cm. Conversely, diatoms have very low concentrations of chl *a* but increase slightly down to a depth of 10 cm.

In order to estimate the concentration of chl *a* in a 1.0 mm segment of the core, a model was used that was based on the regression linear equation of the total concentration of chl *a*. The linear equation of  $y = -34.582x + 65.503$  (Figure 63) was used to determine the total chl *a* concentration in 1 mm intervals between 0 to 4 cm and the linear equation of  $y = -4.6213x + 11.872$  was used to determine the concentration between the depths of 4 cm and 10 cm. The values of each depth were then summed to get total concentration of chl *a* of a core of any length and each of the layers (Table 7). This model was established to compare values found in Rautio et al. (2011), with measurements collected over the 2014 field season. As a result, the average benthic chl *a* total concentration was  $15.64 \mu\text{g}/\text{m}^2$  in the top 10 cm (Table 8).

Table 8: The average of chl *a* in each layer of the sediment bottom in Strange Pond up to 10.0 cm in depth.

Layer	Cyanobacteria ug/cm <sup>2</sup>	Green Algae ug/cm <sup>2</sup>	Diatom ug/cm <sup>2</sup>	Total Concentration ug/cm <sup>2</sup>
1	0.97	0.60	0.15	1.97
2	1.05	0.97	0.14	2.23
3	0.86	0.85	0.13	1.83
4	0.84	0.74	0.11	1.80
5	0.78	1.15	0.10	1.75
6	0.62	0.51	0.09	1.37
7	0.68	1.33	0.08	1.60
8	0.43	0.41	0.07	1.00
9	0.54	1.38	0.06	1.38
10	0.27	0.42	0.05	0.71
Sum	7.04	8.37	0.99	15.64

Table 9: Comparison of the chlorophyll concentration in benthic and pelagic algae in the studied ponds measured using the BenthosTorch. Value for Strange Pond for the 1 mm slab was calculated using the linear equation model estimating chl *a* concentrations at 0.1 mm intervals and summing the values for 2 cm thickness.

Churchill	Pelagic	Benthic @ sediment water interface	Average benthic chl <i>a</i> estimate to 2 cm slab	Average benthic chl <i>a</i> estimate to 10 cm slab
	Chl <i>a</i> (µg/L)	Chl <i>a</i> (mg/m <sup>2</sup> )	Chl <i>a</i> (mg/m <sup>2</sup> )	Chl <i>a</i> (mg/m <sup>2</sup> )
Strange	33.25	1.50	5.66	136.41
Left	24.52	1.41		
Some	35.06	1.49		
Puddle	N/A	1.19		
average w puddle	N/A	01.40		
average w/o puddle	30.94	1.47		
STDEV	0.03	0.01		



#### 4.1.8 Comparing regional pelagic and benthic algae concentrations

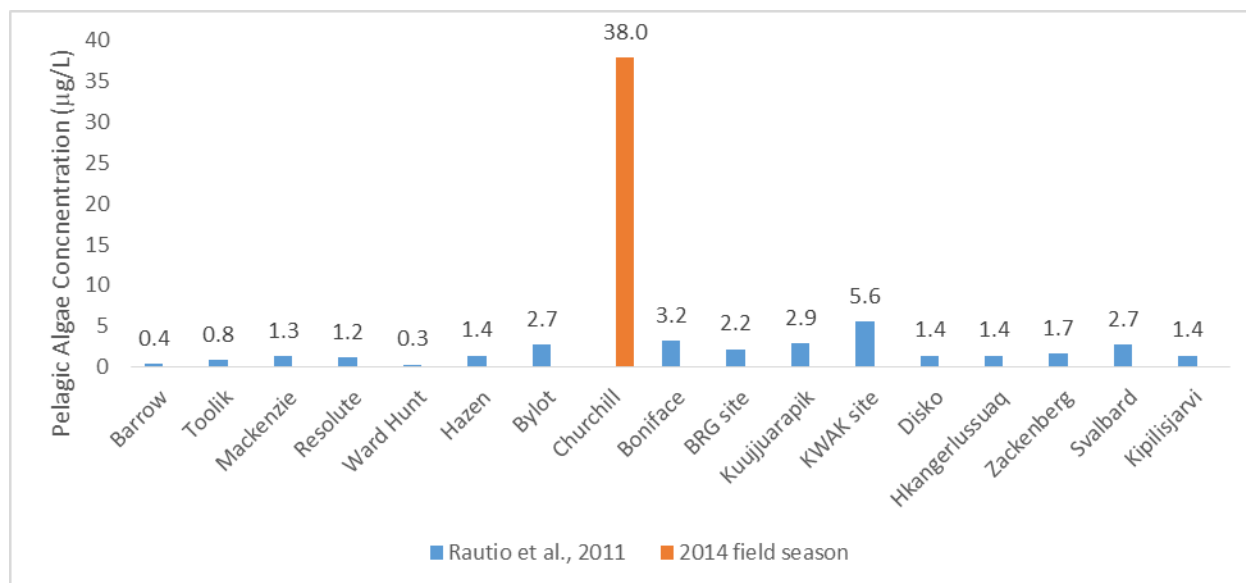


Figure 62: Comparison of the Churchill pelagic algae concentrations to Subarctic and Arctic freshwater ecosystems listed Rautio et al. (2011).

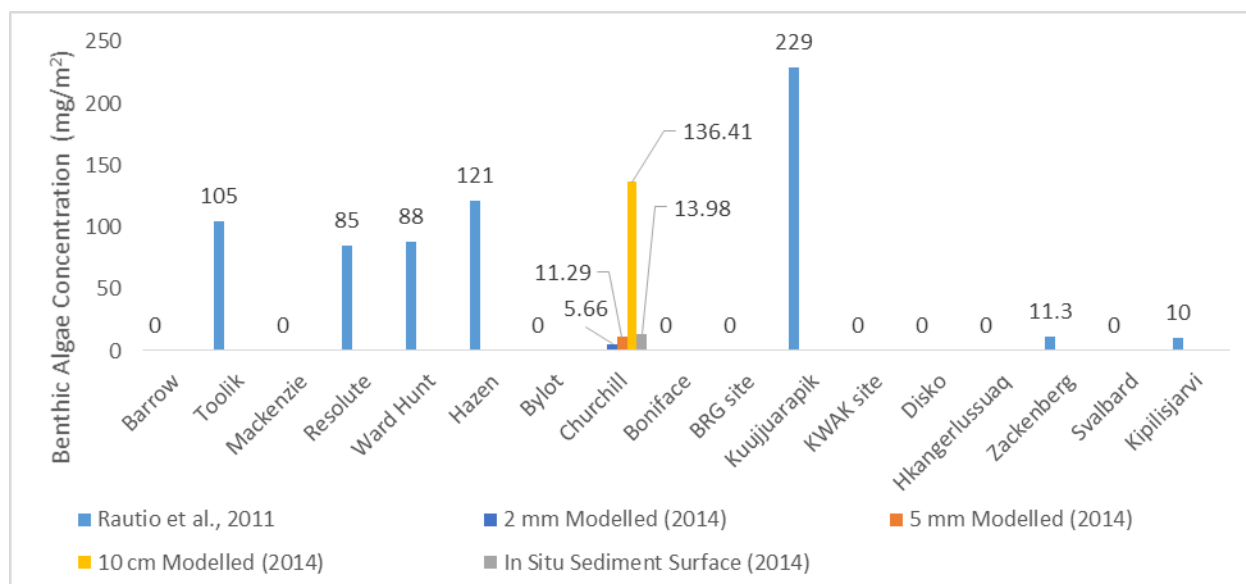


Figure 63: Comparison of the Churchill ponds to the different benthic algae concentrations studied in Rautio et al. (2011). The modelled concentrations are from Strange Pond cores, and the in-situ sediment surface measurements are from the survey of surface chl a on the 4 ponds studied.

Figure 62 shows that the average pelagic algae concentration of the three ponds studied in Churchill, Manitoba, was considerably higher (38 µg/L) in comparison to the ponds studied in other

regions in the Subarctic and Arctic. The KWAK site had one of the highest concentration of pelagic algae. On the lower end of the spectrum, ponds in Toolik, Barrow, Alaska and Ward Hunt had concentrations less than 1.0  $\mu\text{g/L}$ . The extremely high Churchill concentration is closer to eutrophic freshwater systems rather than the clear oligotrophic systems found in the Subarctic and Arctic.

Many of the sites studied in the Subarctic and Arctic regions contain little current data on the benthic concentrations in ponds. When comparing the benthic concentrations at Churchill, Manitoba to the concentration of algae in regions that have had samples collected, the average benthic algae concentration on the sediment surface of Strange Pond, Some Pond, Left Pond, and Puddle Pond with an average concentration of 13.98  $\text{mg/m}^2$  (Figure 65), are lower than the concentrations found in Kuujjuarapik (229.0  $\text{mg/m}^2$ ), Resolute (85.0  $\text{mg/m}^2$ ), and Ward Hunt (88.0  $\text{mg/m}^2$ ). Ponds located in Zackenberg and Kilisjarvi had values closer to the concentrations to Strange Pond (11.29  $\text{mg/m}^2$ ) when accounting for the additional layers in the sediment up to 5.0 mm. To be more consistent with the methodology used in the other regions, the concentrations were modelled to a depth of 2 mm, where Strange Pond exhibited a concentration of 5.66  $\text{mg/cm}^2$ . When totalling the chl *a* of the entire 10 cm core that was extracted, the concentration is 136.41  $\text{mg/m}^2$  which had the second highest concentration to only the ponds in Kuujjuarapik, Québec, located on the east shore of the Hudson Bay. This disparity may be due to the way that each location was sampled. The total thickness of the benthic mats or sediment may have been sampled and measured in comparison to using the BenthosTorch which only measured the superficial surface of the benthic mat or sediment from the chlorophyll fluorescence signal.

#### 4.1.9 Average algal distribution of the cores from Left Pond and Strange Pond

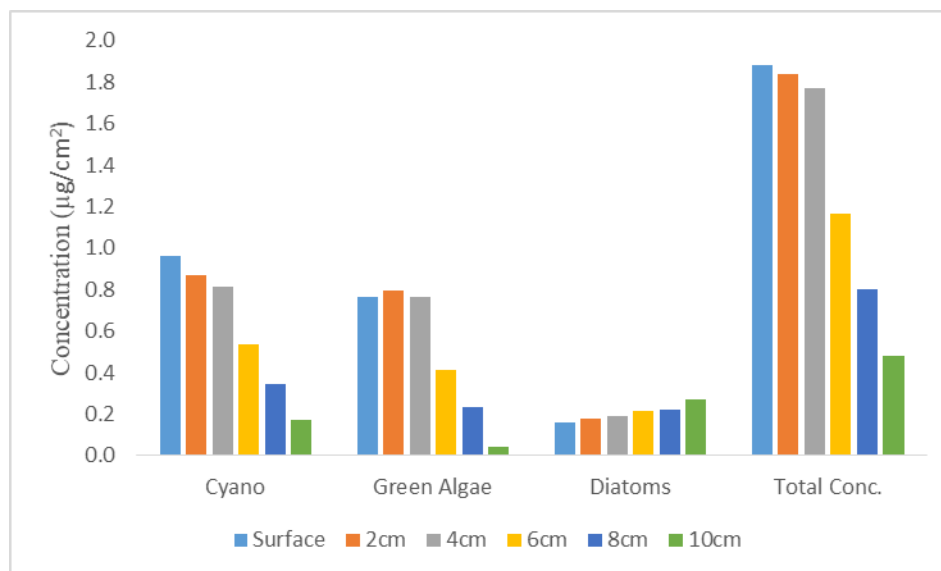


Figure 64: The average algal concentration or available organic carbon found in the sediment at surface of each sediment slab measured in 2.0 cm increment depths.

Chlorophyll *a* concentrations of the benthic and buried algae was used as an indicator of available labile carbon. Figure 64 illustrates the average algal concentration of the algae studied in 2 cm increment depths. The average concentration of algae at each depth measured is significantly different with a  $p < 0.05$ . For cyanobacteria the trend appeared to be higher concentration of cyanobacteria at the surface of the sediment with an average concentration of  $0.96 \mu\text{g}/\text{cm}^2$ , and as samples are taken deeper into the core, the concentration decreased with the lowest at 10 cm with a concentration of  $0.17 \mu\text{g}/\text{cm}^2$ . Green algae concentrations patterns were flat for the surface and first four centimeters with concentrations of  $0.76$  to  $0.80 \mu\text{g}/\text{cm}^2$ . Beyond 4.0 cm, the concentration drastically decreases. Diatoms showed a peculiar pattern in which concentrations marginally increases as depth increases from  $0.16 \mu\text{g}/\text{cm}^2$  at the surface to  $0.27 \mu\text{g}/\text{cm}^2$  at 10.0 cm.

#### 4.2.0 Discussion of benthic productivity and characteristics of pond sediments

##### 4.2.1 Temperature and respiration of sediment cores for Left Pond and Strange Pond

Temperatures in the water column and sediment can be used as a variable or indicator to estimate sediment respiration rates due to how closely they track one another. Through the in-lab incubation respiration experiment using the LI-COR LI-8100, temperature has a strong exponential correlation with the respiration flux from the sediment cores shown in Figures 47 and 48, similar to the findings in Comer-Warner et al. (2018). Also, from the same study, it has been determined that sediment characteristics such as pore size and grain size also play a large role as well in respiration rates. Using one set of cores from Left Pond, and four set of cores from Strange Pond, a benthic sediment respiration model using the surface sediment or water temperature is used to generate CO<sub>2</sub> fluxes from the pond bottoms. These findings are distinctive in producing seasonal fluxes that generally comply with literature stating that temperature significantly affects the respiration of benthic algae and grazers living on the sediment (Dodds et al., 1999; Guðmundsdóttir, 2012; Fujita et al., 2014).

The respiration flux does not differ from a 2 cm core of benthic sediment to a 10 cm core. The insignificant difference suggests that the benthic and sediment biological activity occurs within the first 2 cm of the sediment, known as the biological zone (Figure 65). Similarly, this biological zone had also been found by Stanley (1976) and Cantonati & Lowe (2013). Biological activity in another study was determined to occur in the *first upper layers* of the sediment (Whalen, 2013). Between the active layers with depths reaching all the way to 0.15 to 0.55 mm in shallow Arctic ponds, the sediment is anoxic, indicating that the estimated 2 cm active layer found in Strange Pond is thicker. To further understand the sediment interface, processes involving invertebrates need to be studied. With biological activity occurring within the first 2 cm of the sediment, the water or sediment temperature in the middle of the biological zone of the pond sediment can be used to determine the respiration flux and photosynthetic activity during daylight hours.

##### 4.2.2 Benthic algae on the surface layer and the 2-4 cm layer

It is evident that on the superficial layer of the sediment in Strange Pond and Left Pond that there is a significant difference in the concentration of the cyanobacteria and green algae. This demonstrates that the surface of the sediment in both ponds are not homogenous especially with the combination of the concentrations of the benthic algae at the different sampling locations which

supports the heterogeneous makeup of the pond bottoms. The chlorophyll fluorescence in the 2 to 4 cm layer suggests that algae are dormant while buried in the sediment. When modelling the concentrations of chl *a* within the sediment core, it was found in Figure 62 that two regimes exist. The first regime is the biological zone within the 0 to 4 cm layer. Within this layer more chl *a* exists, indicating a more labile layer. Below the 4.0 cm depth, the chl *a* decreases with depth to 10 cm. The prolonged duration that algae can survive in the absence of light and what mechanisms are involved deserves future consideration. The differences in chlorophyll *a* concentration of cyanobacteria and green algae could be affected by the effective wave mixing or grazing as suggested by Stanley (1976). Algae of both cyanobacteria and green algae were found within the top layer of the sediment due to the ability of light penetration into the surface couple of centimetres (Cantonati & Lowe, 2013).

With the linear models of chl *a* concentration with depth, we have the ability to model the concentration of chl *a* for every 1.0 mm layer in Strange Pond for a more accurate depiction of the total concentration per unit area. This provides a comparison of Strange Pond with different shallow systems in the Subarctic and Arctic. Benthic chl *a* concentrations of Strange Pond are similar to that of the concentrations found in Zackenberg and Kilisjarvi (Rautio et al., 2011).

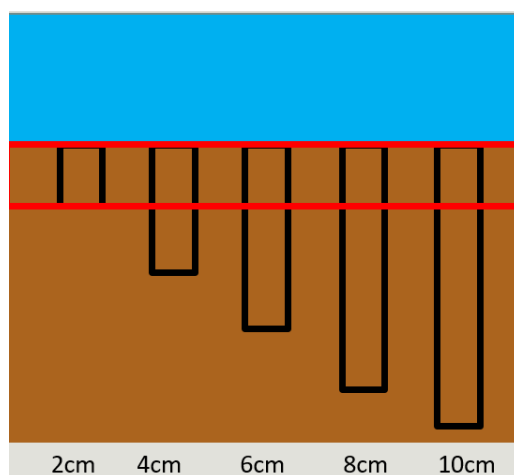


Figure 65: The biological zone (highlighted in red), establishing the same zonal thickness despite the different depths of the sediment cores that would be extracted from Left Pond and Strange Pond.

#### 4.2.3 Critique of the BenthosTorch chlorophyll *a* measurements

It is important to consider that chl *a* concentrations using the BenthosTorch are determined differently than methods traditionally used and may have relevance to the comparisons with the work of Rautio et al. (2011) in their synthesis. Echénique-Subiabre et al. (2016) estimate that the BenthosTorch underestimated the concentrations of chl *a* of cyanobacteria mats, biofilms, and sediment > 2.0 mm, while maintaining more accurate readings with biofilms of cyanobacteria that are < 2.0 mm thick. They also suggest diatom chl *a* concentrations are over estimated. Furthermore, if cyanobacteria contains phycoerythrin that helps give the mats the orange brown hue in the ponds, the readings will be undervalued to a greater extent. However, if cyanobacteria proportions exceeded 50% of the total biomass, the accuracy of the measurements is high ( $p < 0.001$ ).

Even though the confounding results between *in situ* and in lab measurements exist, it is suggested by Harris & Graham (2015) that the BenthosTorch can be used as a simple and time saving method to determine the relative periphyton biomass overtime. This results from the BenthosTorch measured chl *a* concentrations were statistically similar to in lab measurements on all the sampling dates. Furthermore, the maximum chl *a* concentrations were the same at all sampling dates as well. Therefore, despite the potential inaccuracies of the BenthosTorch, it serves as a means to establish spatial and temporal variations of the benthic algal community within an aquatic system.

In the study by Harris & Graham (2015), there is a positive correlations of laboratory measured and BenthosTorch measured chl *a* concentrations ( $p < 0.01$ ,  $R^2 = 0.47$ ). Similar to the findings of Echénique-Subiabre et al. (2016), the relationship are strongest when the BenthosTorch chl *a* concentrations were  $< 4 \mu\text{g}/\text{cm}^2$  ( $p < 0.01$ ,  $R^2 = 0.50$ ), and weakest when concentrations were  $> 4 \mu\text{g}/\text{cm}^2$ . Furthermore, through this study, correlations are strongest when the variability on a within site scale was relatively small. Essentially, BenthosTorch enabled the measurement of the abundance and density of the biofilms (Piano 2015). The findings of Harris & Graham (2015) findings also suggest that the BenthosTorch underestimates the relative abundance of green algae, and diatoms. The BenthosTorch capabilities are limited because it does not account for the variability in the size of cells of the algae (Kahlert & McKie, 2014). Based on the findings by Kahlert & McKie (2014), the BenthosTorch is capable to accurately measure the density of the benthic algae, but the output for the estimate of the algal distribution should be used with caution. In sampling locations where in lab measurements indicate that no benthic cyanobacteria community exist, the BenthosTorch still outputs a measurement of cyanobacteria concentrations and relative abundance.

In situ measurements taken by the BenthosTorch in Churchill are smaller than what is reported using in-lab measurements done on biofilms. With this in mind, it was important to model chl *a* concentrations within the sediment cores to produce a more accurate assessment of the algal taxa in the ponds. The BenthosTorch is calibrated to be accurate within the natural environment where algae are more naturally distributed. This distribution onto coarse or fine sediments would allow penetration of the wavelengths used to measure chl *a* concentrations within the benthos and sediment. In the in-lab setting where chl *a* concentration were much higher, the biofilms may have been much more densely populated, not allowing for wavelengths to scatter appropriately. From the BenthosTorch critique literature, it appears necessary for bbe-Moldaenke to use a wider spectrum of wavelengths to measure different pigments corresponding to each type of algae. It is important to note, despite the critique, the BenthosTorch still gives a good indication of patterns and proportions within the system and has been shown recently to provide meaningful correlations with hyperspectral signatures of benthic algae in Churchill ponds (Ghunowa et al., 2019).

#### 4.2.4 Pond productivity in Strange Pond

Since biological activity occurs within the top layer of the benthos and sediment, the temperature located at 1 cm of biological zone in Strange Pond can be used to predict the respiration flux of the benthic sediment during day-light hours. In situ temperature measured over the summer is used to calculate the respiration flux of Strange Pond over the entire field season. Figure 49 illustrates similar trends for both modelled respirations calculated from the temperature of the sediment at 1 cm and the water column above the sediment. Over the study period, the average respiration flux is 0.31  $\mu\text{g}/\text{m}^2/\text{s}$ , indicating an overall low respiration rate. The peaks of the respiration flux occurs during the day, and the low points of the respiration flux is during the short evening between 12:00 a.m. and 4:00 a.m. On days such as July 14 and July 22, cooler weather and the lack of PAR from storm events limits the productivity of benthic algae and microorganisms in Strange Pond.

Pond productivity is measured in situ in Strange Pond using a combination of the benthic chamber with the pulsed YSI oxygen probe and modelled sediment respiration. Data collected from 4 days over the sampling period were compiled to analyze the primary productivity of Strange Pond. The 4 days chosen for analysis were June 26, July 6, July 10, and July 11. These dates were chosen because the system measuring the productivity of the pond was running optimally. Other days have had instances

where battery did not charge to optimum capacity, or the water pumps that were circulating the water to and from the acrylic chamber were not running.

The oxygen flux produced through photosynthesis is correlated with PPFD but varied depending on in situ conditions in Strange Pond (Figure 58). Literature supports that the efficiency of the photosynthesis of algae is highly dependent on the amount of incoming photosynthetic active radiation and ultraviolet radiation (Frolking et al., 1998; Dodds et al., 1999; Vopel & Hawes, 2006). Furthermore, the modelled consumption of O<sub>2</sub> (Figure 57) in Strange Pond indicates temperature dependence as well. Opposing this is respiration and release of CO<sub>2</sub>. Both incoming PPFD<sub>A</sub> and temperature have strong effects on the carbon dynamics of the ponds. Stanley (1976) claims that PAR does not have an effect on the oxygen production within the ponds. This claim may be due to the long duration and availability of incoming PPFD during the day varying with cloud cover, precipitation events, and attenuation within the water column. This may suggest that the carbon dynamics is governed by the PPFD dependence of primary production to uptake CO<sub>2</sub> (produce O<sub>2</sub>) during the day, and by temperature during the evening during respiratory events. Furthermore, photosynthesis is affected by the mixing and burial of algae due to the loose sediments found in the ponds (Moss, 1977).

The average net ecosystem exchange flux is positive for all 4 sampling days (only July 10 and July 11 are shown) indicating Strange Pond is a sink of carbon, thus absorbing more CO<sub>2</sub> through photosynthetic activity rather than consuming O<sub>2</sub> through respiration. As long as the NEE within the chamber is positive (producing oxygen), this is an indication that the system is sequestering carbon. The average net ecosystem flux for the 4 sampling days was 0.54 μmol/m<sup>2</sup>/s, with an average respiration flux of -0.39 μmol/m<sup>2</sup>/s, and a benthic photosynthetic flux of 0.39 μmol/m<sup>2</sup>/s. The average sequestered carbon from Strange Pond (0.56 g C /m<sup>2</sup>/d) is comparable to values from similar bodies of water in different peatland types found by McLaughlin et al. 2014 (Table 10). When comparing these values to the values illustrated in Table 10 the average daily sequestration of CO<sub>2</sub> in Strange Pond is similar to the ponds studied in Quebec keeping in mind that the values here are for only a few selected summer days. Although the ponds studied are the same ponds studied by Macrae et al. (2004), the annual changes in pond dynamics and characteristics can create annual variability to the sequestration of carbon dioxide from the atmosphere and into the water column and the sediments. The potential is there for ponds to slow down the respiration process from the peatlands, however when comparing the scale and rate at which the ponds need to sequester the CO<sub>2</sub> from the melting permafrost, there may be no feasible way in which the ponds alone can mitigate the release of greenhouse gases from terrestrial ecosystems.



Table 10: CO<sub>2</sub> sequestration rates of peatland type and features in the Hudson Bay Lowlands in Manitoba, Ontario and Quebec, + sign indicating uptake, and - sign indicating CO<sub>2</sub> release (McLaughlin et al., 2014).

Peatland type/feature	Location	CO <sub>2</sub> sequestration (g C /m <sup>2</sup> /d)	Reference
Bogs	Ontario	-1.7 to 0.5	(Roulet et al., 1992)
	Quebec	-0.2	(McEnroe et al., 2009)
Fens	Ontario	-1.0 to -0.4	(Roulet et al., 1992,1994; Bubier, 1995)
	Quebec	-0.6 to 0.2	(Moore et al., 1994; Pelletier et al., 2007)
	Manitoba	-0.9 to 0.7	(Boubier et al., 1995; Joiner et al., 1999)
Thermokarast	Manitoba	0.54	(Bellisario et al., 1999)
Ponds	Ontario	3.0 to 3.1	(Roulet et al., 1994)
	Quebec	0.22	(McEnroe et al., 2009)
	Manitoba	1.1 to 4.5	(Macrae et al., 2004)

Although environmental variables may be poor indicators, temperature is a significant indicator when determining respiration as suggested by Cobelas & Rojo (1994) and Comer-Warner et al. (2018). Thus, ambient air temperature could be used in models to determine respiration from sediments and photosynthetic fluxes of the benthic algae. With calculations of NEE, it appears that Strange Pond is a carbon sink at the sediment-water interface where algae (mainly cyanobacteria) is photosynthesizing. Smol et al. (2014) determined that Arctic and Subarctic ponds in the northern latitudes are more productive as the climate warms. With the low capabilities found in Strange Pond for the pelagic zone, the productivity is driven by the dominant cyanobacteria similar to the aquatic systems studied by Pasternak et al. (2009) and Glud et al. (2009). Competition between the pelagic and benthic community of algae may also be driven by the oligotrophic water column. A pelagic community would be unable to sustain itself due to the lack of available nutrients, whereas the benthic community derives their plentiful nutrient source from the sediments (Pasternak et al., 2009) while cyanobacteria can also acquire dissolved nitrogen from the water column.

#### 4.2.5 Pelagic algae in the studied ponds

Chlorophyll *a* concentrations are supposed to be an indicator for both pelagic and benthic algae to determine if the water column or the benthos in the ponds were drivers for the primary productivity.

Despite the varying area, and depth of Strange, Some and Left Ponds, the average total concentration of chlorophyll *a* is higher in comparison to the different freshwater ecosystems in different regions of the Arctic and around the world (Table 10). The BenthosTorch derived values for pelagic concentrations are inconclusive, both because of limitations of the instrument and the fact that they are in opposition to the chlorophyll fluorescence determinations of pelagic optical densities which are all near zero.

Despite the higher than average concentration of chl *a*, the BenthosTorch measurements from the water column at least show that the concentration of each the three algae types are significantly different ( $p < 0.05$ ) between ponds (Figure 60). The concentration of green algae has the highest concentration of the major taxa of pelagic algae. Sample location may be a factor in the varying concentrations of the major taxa of the pelagic algae. Water samples are taken on the surface of the water column where only algae may be available. Cyanobacteria and diatoms have the ability to move lower into the water column in the attempt to avoid the high UV radiation. In turn, green algae lack motility, thus remaining at the surface of the water column. The low concentration of pelagic algae in the water column is suggested to be a combination of stress variables such as UV radiation, PAR, temperature, and competition with the benthos (Rautio et al., 2011). When comparing the measured pelagic algae using the BenthosTorch to the pelagic concentrations of pelagic algae listed in Rautio et al. (2011), concentrations are significantly greater than that of the ponds studied near Churchill, Manitoba (Figure 62).

The average benthic algae concentration of all three major taxa on the surface of core is  $1.46 \mu\text{g}/\text{m}^2$  for the three ponds which is comparable the measured concentrations listed in Rautio et al. (2011) (Figure 63). However, when the different layers of sediment is considered, the concentration within the first 2.0 mm is  $2.65 \mu\text{g}/\text{m}^2$  in Strange Pond, and  $15.64 \mu\text{g}/\text{m}^2$  to 10.0 cm in the sediment. This comparison of chl *a* concentrations from other Arctic and Subarctic regions provides insight to where Strange Pond is situated. With the chl *a* values being similar to that of the other regions, we hope that the BenthosTorch provides an accurate assessment of the taxa that exists on and within the sediments. In situ benthic algae concentrations were collected using the BenthosTorch, a new in field technique as opposed to the traditional methodology of measuring concentration in the lab using spectrophotometry.

#### 4.2.6 Organic carbon and the vertical distribution of algae in the sediments

Stanley (1976) approaches the two regimes by categorizing the algae as surface algae and buried algae, in which the surface algae was able to photosynthesize, whereas the buried algae remain dormant. However, Stanley (1976) was unable to measure the surface and buried algal biomass due to the loose pond sediments. With the Strange Pond cores, the chl *a* concentrations were measured and quantified, giving a more detailed perspective of the regimes that Stanley describes. This has implications to the carbon dynamics of the ponds in the Hudson Bay Lowlands where primary productivity and respiration is affected by the depth at which photosynthesis occurs and where organic matter is decomposed.

Protocol for the regional values of the other researchers have cores of different diameters extracted from their ponds with a core depth from 1 to 5.0 mm (Bonilla, 2005; 2009; Laurion et al., 2010; Roiha et al., 2012; Rautio et al., 2009). Due to the different protocols from each author, it may be difficult to accurately assess and compare the total concentration of chl *a* in the pond sediments amongst the different regions. As a result, concentrations of chl *a* at different thicknesses (surface, 2 mm, 5 mm, and 10 cm) were compared from Strange Pond. This might give a better assessment of the active chl *a* that is available within the core and gives a better representation of the concentration of active algae within the biological zone, as well as labile carbon throughout the core.

Within the tundra ponds in Alaska, similar profiles have been measured (Round, 1964) in comparison to the vertical distribution of the chl *a* concentrations of the three types of algae measured in Strange Pond (Figure 59). Availability of organic matter within the first 6.0 cm was similar (Table 9) and increased below the same depth from 60 to 88%. Labile carbon is available on and within the sediment as benthic algae. Cyanobacteria exhibits the peculiar pattern in which concentrations decreased as depth increases. Green algae maintained similar concentrations within the first 4.0 cm indicating that green algae is able to regain productivity despite the lack of light penetrating the sediment. The increase in diatoms with depth is indicative to the physiology of species in which enable some of the diatoms to rest or remain dormant. With activity occurring within the first 2.0 cm of the sediment layer it can be determined that concentrations of labile carbon beneath the active layer is not degraded through organic decomposition in oxic conditions but from microorganisms that can function in anoxic conditions.

When looking at a shallow aquatic system as a whole, the gross primary production is temperature sensitive, and the respiration that is occurring in the water column and sediment bottom is temperature dependent. This is true across a wide range of aquatic ecosystems (Yvon-Duroche et al., 2010; 2012; Comer-Warner et al., 2018). Microbial activity in the sediments is an important aspect to the cycling of carbon in the ponds. The activity of the microbes for decomposition and respiration is dependent on many variables such as the lability of sediment and the temperature of the sediment-water interface. There are also microbes within the sediment interface that undergo methanogenesis, in which the microbes produce  $\text{CH}_4$  rather than  $\text{CO}_2$  in anoxic environments. Essentially, by collecting samples of the sediment, a survey can be done on the species of microbes that are living within the sediment interface. Through the measurement of the fluxes of dissolved oxygen, the metabolism of primary producers and bacteria can be estimated. In the nutrient limited systems near Churchill, Manitoba, the mineralization of the first 2 cm of the sediment is providing nutrients for benthic algae to continue to grow. The slow down of decomposition slows the availability of nutrients for growth. These two systems are linked, and therefore if one system is temperature dependent, then the other system is then too via the supply of available nutrients.

#### 4.2.8 Implications from studying the net ecosystem flux of Strange Pond

The productivity of Strange Pond, and despite the low concentrations of pelagic and high concentrations of benthic algae illustrates that implication of a stressed but non-stagnant system in the field season of 2014. Minimal wind mixing and a slow rate of release of  $\text{CO}_2$  into the atmosphere make Strange Pond a slow sequester of  $\text{CO}_2$ . Increasing temperatures in the Subarctic, compounded with the low concentrations of pelagic and benthic algae makes climate change a worrying trend for shallow Subarctic ponds with shallow ponds tend to be benthically driven, theorized to have increased productivity as temperatures increase (Smol et al., 2004), however at least for Strange Pond, this may not be the case. Rain events that can potentially provide nutrients like dissolved  $\text{CO}_2$  to the benthos from the runoff, showed no increase of benthic algae on the sediment such as in a desiccated pond like Puddle Pond, which is indicative to no change in photosynthetic production. Despite the quality of the surrounding environment, Strange Pond, and potentially the other ponds, have the ability to be sequesters of  $\text{CO}_2$  depending on the daily and annual conditions in the Hudson Bay Lowlands. As productive as the benthic algae are in up taking  $\text{CO}_2$  through strong photosynthesis, bottom sediments

with the high availability of labile carbon can be as sources of CH<sub>4</sub> while the ponds act as up takes of CO<sub>2</sub>.

#### 4.2.9 Concluding remarks on shallow Subarctic ponds in the Hudson Bay Lowlands

Despite the uncertainties associated with the BenthosTorch, it is suggested that primary production in the ponds are benthically driven, as indicated with the low levels of measured  $Q_Y$  from the pelagic algae in the water column. With the respiration and net ecosystem exchange modelling in Strange Pond, it can be concluded that the shallow ponds in the Hudson Bay Lowlands have the potential to be sinks during the productive stages of the benthic algae. While the benthos is productive, respiration within the top 2.0 cm of the sediment in Strange Pond releases CO<sub>2</sub> to the water. The ponds studied reflect the potential that even in low productive states that the cyanobacteria were measured in, Strange Pond is still a carbon sink during the day owing to the primary productivity on the pond bottom being greater than respiration. The productivity and potential of the ponds as a net sink for carbon is dependent on PAR availability during the day for uptake of carbon, and temperature during the evenings when respiration is dominant for the release of carbon.

For future studies, it is recommended to study both biogeochemistry of both the water column and the benthos in order to have a complete assessment of the productivity and activity that is occurring within the system. With this in mind, stronger evidence that these ponds are benthically driven and are carbon sinks can be collected. A longer time series may be needed to determine the processes and fluxes within the ponds to provide stronger evidence that the ponds are carbon sinks for the majority of the summer season. As suggested from this thesis, temperature is a strong determinant for respiration. Measurements of temperature from numerous ponds can be taken using in situ methods, drones or satellite imagery to model and assess the respiration rates from the sediment of the ponds in the Hudson Bay Lowlands on a large scale.

From the calculations of the net ecosystem exchange and oxygen production from the benthos of Strange Pond, the shallow Subarctic ponds that are found in the Hudson Bay Lowlands near Churchill, Manitoba have the potential to be carbon sinks. The study found weak correlations with an increase in primary production with increased PPFD, and temperature induced stress. To have more conclusive results however, future studies should include a larger sample size by extending the data set over a larger period of time in order to measure gross primary production. Extending the data will also increase

the confidence in respiration results. However, with a small sample size the study has shown that even with the relatively low activity of the benthic cyanobacteria mats, and the non-detectable values and low  $Q_Y$  of algae in the water column, Strange Pond is productive enough during day light hours to be a sink. Benthic chl *a* concentration amongst the ponds studied showed similarity within the sediment, and even the comparison between Some Pond in 2013 and 2014 showed very little variability in the taxa.

Chlorophyll *a* concentrations in Strange Pond are similar to that of ponds and shallow lakes in the Arctic and Subarctic. If the minimum productivity rates of Arctic and Subarctic ponds are similar to that of Strange Pond, then there is potential that many of these ponds are carbon sinks during daylight hours. If the NEE, primary production, and respiration rates were scaled to all the ponds located within the Hudson Bay Lowlands, the rates of the processes may be more profound. Future studies would be needed to assess the capabilities of the ponds to the fullest extent. With this in mind, there is hope that ponds with even higher concentrations of benthic algae in the Hudson Bay Lowlands and shallow systems in the northern latitudes would be more productive, thus becoming more effective sinks. This opens up the avenue for research to study ponds of various size and depths on a larger scale to assess the effectiveness and potential for these Subarctic ponds.

### 5.0.0 Conclusion

The objective of chapter 3 was to determine whether the HBL ponds experience temporal and spatial variability in the benthic algal composition and limnological variables. The benthic community and limnological variables were affected by both temporal and spatial affects. Spatial variability of the benthic community existed in ponds with a smaller area. Therefore, sampling location on the ponds is of major importance depending on the area of the pond, especially when the depth of the ponds do not differ significantly, as relatively uniform light penetration prevails. Variability in both the benthic composition and limnological variables exist when looking at the temporal change within the four ponds. Benthic community composition and concentration differ in both wet and dry ponds. This could result from the benthic community being affected by bacterial decomposition and scavenging.

Over a period of time the benthic community can change depending on the grazing population, and the impact of light/UV stress, and temperature fluctuations. Limnological variability follows a similar trend to the benthic composition of the ponds. Limnological variables are similar throughout the depth of the water column due to its shallow nature of being well mixed. With the water well mixed, even large ponds such as Some Pond experience very little variability along the length of the pond. Temporal activity exists for both benthic composition and limnological variables. Therefore, it is important to pay attention to when sampling occurs during the field season rather than the location within the pond. When comparing the benthic and pelagic composition of the Churchill ponds to other ponds in the Subarctic and Arctic regions, it was determined that Churchill ponds have low concentrations of pelagic algae.

The objective of chapter 4 was to determine whether the benthos in the HBL ponds processed and stored autochthonous carbon. Productivity and the net ecosystem exchange of oxygen was determined to be low. Based on this work, longer sampling duration, and proper maintenance and reliability of the pumps, chamber, and LI-COR, can yield more definitive results on the productivity of the ponds. The collection of sediment cores of different lengths, and the measurement of CO<sub>2</sub> flux emitted at different temperatures allowed for the modelling of respiration rates based on sediment temperature and identified the layer of sediment contributing to respiration. In tandem with the DO concentrations measured by the YSI probe, the NEE was calculated and compared to previously published values.

### 6.0.0 Bibliography

Aguilera, J., Dummermuth, A., Karsten, U., Schriek, R., & Wiencke, C. (2002). Enzymatic defences against photooxidative stress induced by ultraviolet radiation in Arctic marine macroalgae. *Polar Biology*, 25(6), 432–441.

Algesten, G., Sobek, S., Bergström, A.K., Jonsson, A., Tranvik, L. J., & Jansson, M. (2005). Contribution of sediment respiration to summer CO<sub>2</sub> emission from low productive Boreal and Subarctic Lakes. *Microbial Ecology*, 50(4), 529–535.

Antoniades, D., Douglas, M., & Smol, J. P. (2004). Diatom species-environment relationships and inference models from Isachsen, Ellef Ringnes Island, Canadian High Arctic. *Hydrobiologia*, 529(1), 1–18.

Antoniades, D., Douglas, M. S., & Smol, J. P. (2005). Benthic diatom autecology and inference model development from the Canadian High Arctic Archipelago. *Journal of Phycology*, 41(1), 30–45.

Barker, A. H. (1935). Photosynthesis in diatoms. *Archiv Für Mikrobiologie*, 6(1–5), 141–156.

Beaulieu, M., Pick, F., & Gregory-Eaves, I. (2013). Nutrients and water temperature are significant predictors of cyanobacterial biomass in a 1147 lakes data set. *Limnology and Oceanography*, 58(5), 1736–1746.

Bellido, J., Peltomaa, E., & Ojala, A. (2011). An urban boreal lake basin as a source of CO<sub>2</sub> and CH<sub>4</sub>. *Environmental Pollution*, 159(6), 1649–1659.

Bellisario, L., Bubier, J., Moore, T., & Chanton, J. (1999). Controls on CH<sub>4</sub> emissions from a northern peatland. *Global Biogeochemical Cycles*, 13(1), 81–91.

Billett, M., & Moore, T. (2008). Supersaturation and evasion of CO<sub>2</sub> and CH<sub>4</sub> in surface waters at Mer Bleue peatland, Canada. *Hydrological Processes*, 22(12), 2044–2054.

Bonilla, S., Villeneuve, V., & Vincent, W. F. (2005). Benthic and planktonic algal communities in a high Arctic lake: pigment structure and contrasting responses to nutrient enrichment. *Journal of Phycology*, 41(6), 1120–1130.

Bouchard, F., Francus, P., Pienitz, R., & Laurion, I. (2011). Sedimentology and geochemistry of thermokarst ponds in discontinuous permafrost, subarctic Quebec, Canada. *Journal of Geophysical Research: Biogeosciences (2005–2012)*, 116(G2).

Boulay, C., Abasova, L., Six, C., Vass, I., & Kirilovsky, D. (2008). Occurrence and function of the orange carotenoid protein in photoprotective mechanisms in various cyanobacteria. *Biochimica et Biophysica Acta (BBA) - Bioenergetics*, 1777(10), 1344–1354.

Bowden, W. B. (2010). Climate change in the Arctic – permafrost, thermokarst, and why they matter to the non-Arctic world. *Geography Compass*, 4(10), 1553–1566.



Bubier, J. L., Moore, T. R., Bellisario, L., Comer, N. T., & Crill, P. M. (1995). Ecological controls on methane emissions from a Northern Peatland Complex in the zone of discontinuous permafrost, Manitoba, Canada. *Global Biogeochemical Cycles*, 9(4), 455–470.

Cantonati, M., & Lowe, R. L. (2014). Lake benthic algae: toward an understanding of their ecology. *Freshwater Science*, 33(2), 475–486.

Cobelas, A. M., & Rojo, C. (1994). Spatial, seasonal and long-term variability of phytoplankton photosynthesis in lakes. *Journal of Plankton Research*, 16(12), 1691–1716.

Coulombe, O., Bouchard, F., & Pienitz, R. (2016). Coupling of sedimentological and limnological dynamics in subarctic thermokarst ponds in Northern Québec (Canada) on an interannual basis. *Sedimentary Geology*, 340, 15–24.

Dinsmore, K. J., Billett, M. F., & Moore, T. R. (2009). Transfer of carbon dioxide and methane through the soil-water-atmosphere system at Mer Bleue peatland, Canada. *Hydrological Processes*, 23(2), 330–341.

Dodds, W. K., Biggs, B. J., & Lowe, R. L. (1999). Photosynthesis-irradiance patterns in benthic microalgae: variations as a function of assemblage thickness and community. *Journal of Phycology*, 35(1), 42–53.

Echenique-Subiabre, I., Dalle, C., Duval, C., Heath, M. W., Couté, A., Wood, S. A., Humbert, J.-F., and Quiblier, C., 2016, Application of a spectrofluorimetric tool (bbe BenthosTorch) for monitoring potentially toxic benthic cyanobacteria in rivers: *Water Research*, v. 101, p. 341–350.

Erikson, R. (1998). Algal respiration and the regulation of phytoplankton biomass in a polymictic tropical lake (Lake Xolotlán, Nicaragua). *Hydrobiologia*, 382(1/3), 17–25.

Fee, E., Hecky, R., Kasian, S., & Cruikshank, D. (1996). Effects of lake size, water clarity, and climatic variability on mixing depths in Canadian Shield lakes. *Limnology and Oceanography*, 41(5), 912–920.

Figuerola, F. L., Conde-Álvarez, R., & Gómez, I. (2003). Relations between electron transport rates determined by pulse amplitude modulated chlorophyll fluorescence and oxygen evolution in macroalgae under different light conditions. *Photosynthesis Research*, 75(3), 259–275.

Frolking, S., Bubier, J., Moore, T., Ball, T., Bellisario, M., ... Whiting, G. (1998). Relationship between ecosystem productivity and photosynthetically active radiation for northern peatlands. *Global Biogeochem Cycles*. 12. 115-126.

Fujita, K., Okai, T., & Hosono, T. (2014). Oxygen Metabolic Responses of Three Species of Large Benthic Foraminifers with Algal Symbionts to Temperature Stress. *PLoS ONE*, 9(3), e90304.

Glud, R. N., Woelfel, J., Karsten, U., Kühl, M., & Rysgaard, S. (2009). Benthic microalgal production in the Arctic: applied methods and status of the current database. *Botanica Marina*, 52(6), 559–571.

Griffiths, M.S., Gallon, J.R., & Chaplin, A.E. (1987). The diurnal pattern of dinitrogen fixation by cyanobacteria in situ. *New Phytologist*, 107(4), 649–657.

Ghunowa, K., AS Medeiros, and R. Bello 2019 Hyperspectral analysis of algal biomass in northern lakes, Churchill, MB, Canada. Arctic Science doi.org/10.1139/as-2018-0030

Guðmundsdóttir, R. (2012). Primary producers in sub-Arctic streams and the effects of temperature and nutrient enrichment on succession.

Häder, D.-P., Kumar, H., Smith, R., & Worrest, R. (2007). Effects of solar UV radiation on aquatic ecosystems and interactions with climate change. *Photochemical & Photobiological Sciences*, 6(3), 267–285.

Harris, T. D., and Graham, J. L., 2015, Preliminary evaluation of an in vivo fluorometer to quantify algal periphyton biomass and community composition: Lake and Reservoir Management, v. 31, p. 127–133.

Hinkel, K. M., Lenters, J. D., Sheng, Y., Lyons, E. A., Beck, R. A., Eisner, W. R., ... Potter, B. L. (2012). Thermokarst Lakes on the Arctic Coastal Plain of Alaska: spatial and temporal variability in summer water temperature. *Permafrost and Periglacial Processes*, 23(3), 207–217.

Hobbie, J. E. (1980). Limnology of tundra ponds, Barrow, Alaska.

Jäger, C. G., Diehl, S., & Emans, M. (2010). Physical determinants of phytoplankton production, algal stoichiometry, and vertical nutrient fluxes. *The American Naturalist*, 175(4), E91–E104.

Jeppesen, E., Sondergaard, M., Jensen, J., Havens, K.E., Anneville, O., Carvalho, L., ...Winder, M. (2005). Lake responses to reduced nutrient loading – an analysis of contemporary long-term data from 35 case studies. *Freshwater Biology*, 50(10), 1747–1771.

Joiner, D. W., Lafleur, P. M., McCaughey, H. J., & Bartlett, P. A. (1999). Interannual variability in carbon dioxide exchanges at a boreal wetland in the BOREAS northern study area. *Journal of Geophysical Research: Atmospheres* (1984–2012), 104(D22), 27663–27672.

Jones, B., Grosse, G., Arp, C., Jones, M., Anthony, W. K., & Romanovsky, V. (2011). Modern thermokarst lake dynamics in the continuous permafrost zone, northern Seward Peninsula, Alaska. *Journal of Geophysical Research: Biogeosciences* (2005–2012), 116(G2), 1-13.

Kahlert, M., and McKie, B. G., 2014, Comparing new and conventional methods to estimate benthic algal biomass and composition in freshwaters: Environmental Science: Processes & Impacts, v. 16, p. 2627–2634.

Kling, G. W., O'Brien, J. W., Miller, M. C., & Hershey, A. E. (1992). The biogeochemistry and zoogeography of lakes and rivers in arctic Alaska. *Springer*, 1–14.

Kosek, K., Polkowska, Ż., Żyszka, B., & Lipok, J. (2016). Phytoplankton communities of polar regions– Diversity depending on environmental conditions and chemical anthropopressure. *Journal of Environmental Management*, 171, 243–259.

Kosten, S., Huszar, V. L., Bécares, E., Costa, L. S., Donk, E., Hansson, L., ... Scheffer, M. (2012). Warmer climates boost cyanobacterial dominance in shallow lakes. *Global Change Biology*, 18(1), 118–126.

Laurion, I., & Mladenov, N. (2013). Dissolved organic matter photolysis in Canadian arctic thaw ponds.

*Environmental Research Letters*, 8(3), 1-12.

Lin, C., & Wu, J. (2014). Tolerance of soil algae and cyanobacteria to drought stress. *Journal of Phycology*, 50(1), 131–139.

Low-Décarie, E., Fusann, G.F., & Bell, G. (2011). The effect of elevated CO<sub>2</sub> on growth and competition in experimental phytoplankton communities. *Global Change Biology*, 17(8), 2525–2535.

Macrae, M., Bello, R., & Molot, L. (2004). Long-term carbon storage and hydrological control of CO<sub>2</sub> exchange in tundra ponds in the Hudson Bay Lowland. *Hydrological Processes*, 18(11), 2051–2069.

Markager, S., Vincent, W. F., & Tang, E. (1999). Carbon fixation by phytoplankton in high Arctic lakes: Implications of low temperature for photosynthesis. *Limnology and Oceanography*, 44(3), 597–607.

Masini, R., & McComb, A. J. (2001). Production by microphytobenthos in the Swan–Canning Estuary. *Hydrological Processes*, 15(13), 2519–2535.

McEnroe, N., Roulet, N., Moore, T., & Garneau, M. (2009). Do pool surface area and depth control CO<sub>2</sub> and CH<sub>4</sub> fluxes from an ombrotrophic raised bog, James Bay, Canada? *Journal of Geophysical Research: Biogeosciences (2005–2012)*, 114.

McLaughlin, J., & Webster, K. (2014). Effects of climate change on peatlands in the far north of Ontario, Canada: A synthesis. *Arctic, Antarctic, and Alpine Research*, 46(2), 84–102.

Michelutti, N., Holtham, A. J., Douglas, M. S., & Smol, J. P. (2003). Periphytic diatom assemblages from ultra-oligotrophic and UV transparent lakes and ponds on Victoria Island and comparisons with other diatom surveys in the Canadian Arctic. *Journal of Phycology*, 39(3), 465–480.

Moon, Y.-J., Kim, S., & Chung, Y.-H. (2012). Sensing and responding to UV-A in cyanobacteria. *International Journal of Molecular Sciences*, 13(12), 16303–16332.

Moore, K. E., Fitzjarrald, D. R., Wofsy, S. C., Daube, B. C., Munger, W. J., Bakwin, P. S., & Crill, P. (1994). A season of heat, water vapor, total hydrocarbon, and ozone fluxes at a subarctic fen. *Journal of Geophysical Research: Atmospheres*, 99(D1), 1937–1952.

Moss, B. (1977). Adaptations of epipellic and epipsammic freshwater algae. *Oecologia*, 28(1), 103–108.

Overnell, J., Edwards, A., Grantham, B. E., Harvey, S. M., Jones, K. J., Leftley, J. W., & Smallman, D. J. (1995). Sediment-water Column coupling and the fate of the spring phytoplankton bloom in Loch Linnhe, a Scottish Fjordic Sea-loch. Sediment processes and sediment-water fluxes. *Estuarine, Coastal and Shelf Science*, 41(1), 1–19.

Pasternak, A., Hillebrand, H., & Flöder, S. (2009). Competition between benthic and pelagic microalgae for phosphorus and light – long-term experiments using artificial substrates. *Aquatic Sciences*, 71(2), 238–249.

- Piano, E., Bona, F., Falasco, E., Morgia, L. V., Badino, G., and Isaia, M., 2015, Environmental drivers of phototrophic biofilms in an Alpine show cave (SW-Italian Alps): *Science of The Total Environment*, v. 536, p. 1007–1018.
- Pelletier, L., Moore, T., Roulet, N., Garneau, M., & Beaulieu-Audy, V. (2007). Methane fluxes from three peatlands in the La Grande Rivière watershed, James Bay lowland, Canada. *Journal of Geophysical Research: Biogeosciences (2005–2012)*, 112.
- Perga, M., Maberly, S. C., Jenny, J., Alric, B., Pignol, C., & Naffrechoux, E. (2016). A century of human-driven changes in the carbon dioxide concentration of lakes. *Global Biogeochemical Cycles*, 30(2), 93–104.
- Pessoa, M. (2012). Harmful effects of UV radiation in algae and aquatic macrophytes – A review. *Emirates Journal of Food and Agriculture*, 24(6), 510-526.
- Pierangelini, M., Stojkovic, S., Orr, P. T., & Beardall, J. (2014). Elevated CO<sub>2</sub> causes changes in the photosynthetic apparatus of a toxic cyanobacterium, *Cylindrospermopsis raciborskii*. *Journal of Plant Physiology*, 171(12), 1091–1098.
- Prescott, G. (1963). Ecology of Alaskan Freshwater Algae II. Introduction: General Considerations. *Transactions of the American Microscopical Society*, 82(1), 83.
- Oke, T.R. (1987) Boundary layer climates. 2<sup>nd</sup> Edition, Methuen, London.
- Rautio, M., Dufresne, F., Laurion, I., Bonilla, S., Vincent, W. F., & Christoffersen, K. S. (2011). Shallow Freshwater Ecosystems of the Circumpolar Arctic. *Ecoscience*, 20(4), 204–222.
- Riordan, B., Verbyla, D., & McGuire, D. A. (2006). Shrinking ponds in subarctic Alaska based on 1950–2002 remotely sensed images. *Journal of Geophysical Research: Biogeosciences (2005–2012)*, 111(G4).
- Rõõm, E.-I., Nõges, P., Feldmann, T., Tuvikene, L., Kisand, A., Teearu, H., & Nõges, T. (2014). Years are not brothers: Two-year comparison of greenhouse gas fluxes in large shallow Lake Võrtsjärv, Estonia. *Journal of Hydrology*, 519, 1594–1606.
- Roulet, N., Moore, T., Bubier, J., & LaFleur, P. (1992). Northern fens: methane flux and climatic change. *Tellus B*, 44(2), 100–105.
- Roulet, N. T., Jano, A., Kelly, C., Klinger, L., Moore, T., Protz, R., ... Rouse, W. (1994). Role of the Hudson Bay lowland as a source of atmospheric methane. *Journal of Geophysical Research: Atmospheres*, 99(D1), 1439–1454
- Rouse, W., Oswald, C., & ..., B. J. (2005). The role of northern lakes in a regional energy balance. *Journal of Hydrometeorology* 6(3), 291-305.
- Rouse, W. R., Douglas, M.S., Hecky, R. E., Heshey, A.E., Kling, G.W., Lesack, L., ... John P. (1997). Effects of climate change on the freshwaters of Arctic and Subarctic North America. *Hydrological Processes*, 11(8), 873–902

Rühland, K. M., Paterson, A. M., & Smol, J. P. (2015). Lake diatom responses to warming: reviewing the evidence. *Journal of Paleolimnology*, *54*(1), 1–35.

Rühland, K., & Smol, J. P. (2005). Diatom shifts as evidence for recent Subarctic warming in a remote tundra lake, NWT, Canada. *Palaeogeography, Palaeoclimatology, Palaeoecology*, *226*(1–2), 1–16.

Sabbe, K., Hodgson, D. A., Verleyen, E., Taton, A., Wilmotte, A., Vanhoutte, K., & Vyverman, W. (2004). Salinity, depth and the structure and composition of microbial mats in continental Antarctic lakes. *Freshwater Biology*, *49*(3), 296–319.

Sakshaug, E., Bricaud, A., Dandonneau, Y., Falkowski, P., Kiefer, D., Legendre, L., ... Takahashi, M. (1997). Parameters of photosynthesis: definitions, theory and interpretation of results. *Journal of Plankton Research*, *19*(11), 1637–1670.

Saulnier-Talbot, É., Pienitz, R., & Vincent, W. F. (2003). Holocene lake succession and palaeo-optics of a Subarctic lake, northern Québec, Canada. *The Holocene*, *13*(4), 517–526.

Schlichting, H. E. (1974). Survival of some freshwater algae under extreme environmental conditions. *Transactions of the American Microscopical Society*, *93*(4), 610-3.

Singh, S. P., Häder, D.-P., & Sinha, R. P. (2010). Cyanobacteria and ultraviolet radiation (UVR) stress: Mitigation strategies. *Ageing Research Reviews*, *9*(2), 79–90.

Smol, J. P., Wolfe, A. P., Birks, J. H., Douglas, M. S., Jones, V. J., Korhola, A., ... Weckström, J. (2005). Climate-driven regime shifts in the biological communities of arctic lakes. *Proceedings of the National Academy of Sciences of the United States of America*, *102*(12), 4397–4402.

Sospedra, J., Falco, S., Morata, T., Gadea, I., & Rodilla, M. (2015). Benthic fluxes of oxygen and nutrients in sublittoral fine sands in a north-western Mediterranean coastal area. *Continental Shelf Research*, *97*, 32–42.

Stanley, D. (1976). A Carbon Flow Model of Epipelagic Algal Productivity in Alaskan Tundra Ponds. *Ecology*, *57*(5), 1034-1042.

Tang, E. P., Tremblay, R., & Vincent, W. F. (1997). Cyanobacterial dominance of polar freshwater ecosystems: Are high-latitude mat-formers adapted to low temperatures?

Tang, M., & Kristensen, E. (2007). Impact of microphytobenthos and macroinfauna on temporal variation of benthic metabolism in shallow coastal sediments. *Journal of Experimental Marine Biology and Ecology*, *349*(1), 99–112.

Taranu, Z. E., Gregory-Eaves, I., Leavitt, P. R., Bunting, L., Buchaca, T., Catalan, J., ... Vinebrooke, R. D. (2015). Acceleration of cyanobacterial dominance in north temperate-subarctic lakes during the Anthropocene. *Ecology Letters*, *18*(4), 375–384.

Verleyen, E., Hodgson, D. A., Gibson, J., Imura, S., Kaup, E., Kudoh, S., ... Vyverman, W. (2012). Chemical

limnology in coastal East Antarctic lakes: monitoring future climate change in centres of endemism and biodiversity. *Antarctic Science*, 24(1), 23–33.

Vézina, S., & Vincent, W. (1997). Arctic cyanobacteria and limnological properties of their environment: Bylot Island, Northwest Territories, Canada (73°N, 80°W). *Polar Biology*, 17(6), 523–534.

Vinebrooke, R. D., & Leavitt, P. R. (1999). Differential responses of littoral communities of to ultraviolet radiation in an alpine. *Ecology*, 80(1), 223–237.

von Einem, J., & Granéli, W. (2010). Effects of fetch and dissolved organic carbon on epilimnion depth and light climate in small forest lakes in southern Sweden. *Limnology and Oceanography*, 55(2), 920–930.

Vopel, Kay & Hawes, Ian. (2006). Photosynthetic Performance of Benthic Microbial Mats in Lake Hoare, Antarctica. *Limnology and Oceanography*. 51. 1801-1812.

Wannikhof, R. (1988). Quantification of air-sea fluxes of gaseous compounds using deliberate tracers. *Applied Geochemistry*, 3(1), 104.

Weckström, J., Korhola, A., & Blom, T. (1997). Diatoms as quantitative indicators of pH and water temperature in subarctic Fennoscandian lakes. *Hydrobiologia*, 347(1/3), 171–184.

Whalen, S. C., Lofton, D. D., McGowan, G. E., & Strohm, A. (2013). Microphytobenthos in Shallow Arctic Lakes: fine-scale depth distribution of chlorophyll a, radiocarbon sssimilation, irradiance, and dissolved O<sub>2</sub>. *Arctic, Antarctic, and Alpine Research*, 46(2), 285–295.

Wolfe, A. P., Hobbs, W. O., Birks, H. H., Briner, J. P., Holmgren, S. U., Ingólfsson, Ó., ... Vinebrooke, R. D. (2013). Stratigraphic expressions of the Holocene–Anthropocene transition revealed in sediments from remote lakes. *Earth-Science Reviews*, 116, 17–34.

Wolfe, B. B., Light, E. M., Macrae, M. L., Hall, R. I., Eichel, K., Jasechko, S., ... Edwards, T. W. (2011). Divergent hydrological responses to 20th century climate change in shallow tundra ponds, western Hudson Bay Lowlands. *Geophysical Research Letters*, 38(23).

Yang, R., Chen, B., Liu, H., Liu, Z., & Yan, H. (2015). Carbon sequestration and decreased CO<sub>2</sub> emission caused by terrestrial aquatic photosynthesis: Insights from diel hydrochemical variations in an epikarst spring and two spring-fed ponds in different seasons. *Applied Geochemistry*, 63, 248–260.

Zona, D., Oechel, W., Peterson, K., Clements, R., K., P. T., & Ustin, S. (2010). Characterization of the carbon fluxes of a vegetated drained lake basin chronosequence on the Alaskan Arctic Coastal Plain. *Global Change Biology*, 16(6), 1870–1882.